NOTE TO USERS

Characterization of a temperature-sensitive mutation that impairs the function of yeast tRNA nucleotidyltransferase

Xunying Shan

A Thesis

in

The Department

of

Chemistry and Biochemistry

Presented in partial Fulfillment of the Requirements

for the Degree of Master of Science at

Concordia University

Montreal, Quebec, Canada

September, 2005

Your file Votre référence
ISBN: 0-494-10209-8
Our file Notre référence
ISBN: 0-494-10209-8

ABSTRACT

Characterization of a temperature-sensitive mutation that impairs the function of yeast tRNA nucleotidyltransferase

XunYing Shan

Mature tRNAs require a 3'-terminal cytidine-cytidine-adenosine sequence to function in protein synthesis. The addition of these nucleotides into tRNAs with incomplete 3'-termini is catalyzed by the enzyme tRNA nucleotidyltransferase. Genetic studies have resulted in the isolation of the gene coding for tRNA nucleotidyltransferase in yeast and *in vivo* studies identified a temperature-sensitive yeast strain with a mutant *CCA1* gene, which can survive at room temperature, but not at 37°C. Gene sequencing revealed that the temperature-sensitive phenotype came from a single nucleotide substitution in the *CCA1* gene, which led to the substitution of a glutamate residue by a lysine in the protein (D. Kushner, personal communication).

In this work, enzymatic characterization showed that this lysine variant had approximately 5% of the activity of the wild-type enzyme and a tertiary structural change as detected by fluorescence spectroscopy at the permissive temperature. Thermal stability monitored by circular dichroism showed that the lysine variant is less thermally stable than the wild-type enzyme with an approximately 6°C lower transitional temperature. Intrinsic fluorescence titration with tRNA suggests that this variant enzyme interacts less well with tRNA than does the native enzyme. Taken together all of these features are consistent with the temperature-sensitive phenotype seen *in vivo* for this variant enzyme.

To further probe the role of the amino acid at position 172 in the yeast enzyme, site-directed mutagenesis was used to generate variant proteins with glutamine, histidine or phenylalanine instead of the glutamate found in the wild-type enzyme. Enzymatic assays at the permissive and non-permissive temperatures were carried out to compare enzyme activities. The substitution of Glu172 with glutamine or histidine led to a 50% or 93% loss of activity respectively, while the substitution of Glu172 with phenylalanine had the same effect as the lysine substitution resulting in a 95-96% loss of activity.

Biophysical studies of these new variants support the hypothesis that a change from a glutamate at this position alters the structure of the protein even at the permissive temperature and that the structural change is more significant at the non-permissive temperature. Thermostability monitored by CD spectroscopy showed that substitution of Glu172 with phenylalanine led to a similar level of reduced thermostability as seen with the lysine variant while substitution of Glu172 with glutamine or histidine had almost no effect on the thermostability of the enzyme. Again these results are consistent with the temperature-sensitive phenotype seen *in vivo*. These results also suggest that the size of the amino acid at position 172 is more important in affecting enzyme stability and activity that is the charge of this amino acid.

ACKNOWLEDGEMENTS

To begin, I would like to express a very appreciative thanks to my research supervisor Dr. Paul B. M. Joyce for his patient guidance, reliability and availability, for his invaluable advice which kept me on track and allowed me the freedom to work and make decisions on my own, for his utmost care and countless hours on this manuscript. I feel fortunate to have such an excellent and tireless critic as a supervisor. I would like to gratefully thank my examining committee members Dr. Ann English and Dr. Judith Kornblatt for their valuable time. A special thank you to Dr. Joanne Turnbull for her assistance and excellent and helpful suggestions.

I also want to thank Dr. Pam Hanic-Joyce for her sage advice on some experimental skills, my colleagues and peers Azat, Wen Tzu, Sheehab and Kwang Bo who made my learning an enjoyable and fruitful experience.

Most of all, I would like to thank my family for their love, support and encouragement, and my friends in Montreal who made my life more enjoyable.

TABLE OF CONTENTS

LIST OF FIGURES

LIST OF TABLES

ABBREVIATIONS

Bp	Base pair
BSA	Bovine serum albumin
CCA	Cytidine,cytidine,adenosine
cpm	Counts per minute
EDTA	Ethylenediaminetetraacetic acid
GST	Glutathione S-transferase
IPTG	Isopropyl-(β-D-thiogalactopyranoside)
Kbp	Kilo base pairs
KDa	Kilo Daltons
Nm	Nanometers
OD	Optical density
PAGE	Polyacrylamide gel electrophoresis
PCR	Polymease chain reaction
PMSF	Phenylmethylsulfonyl fluoride
pfu	pfu DNA polymerase
rpm	Revolutions per minute
SDS	Sodium dodecyl sulphate
tRNA	Transfer ribonucleic acid
tRNA nucleotidyltransferase	ATP(CTP):tRNA-specific tRNA nucleotidyltransferase

1. INTRODUCTION

1.1 Transfer RNA and its maturation

Transfer RNAs are relatively small (containing about 76 nucleotides) and well-characterized RNA molecules arranged in a clover-leaf secondary structure with an acceptor stem and anticodon, D and TΨC stems and loops and a variable loop (Fig.1-1).

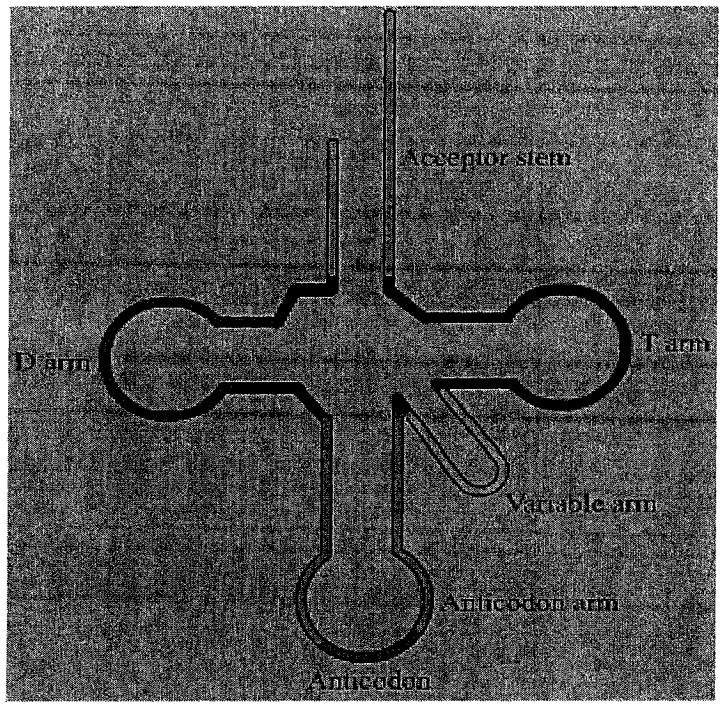

Fig. 1-1. The secondary structure of a tRNA molecule
(http://en.wikipedia.org/wiki/Transfer_RNA).

The three dimensional structure of yeast $tRNA^{Phe}$ was resolved from X-ray crystallographic studies (Fig. 1-2) (Hingerty *et al.*, 1978) and is typical of the L-shaped tertiary structure of most tRNAs which is held together by hydrogen bonds that result from intramolecular base pairing.

The major role of tRNAs is to translate messenger RNA (mRNA) sequences into amino acid sequences during protein synthesis (Voet and Voet, 1995). Transfer RNAs

carry amino acids to the ribosome for polymerization into a polypeptide. Each tRNA adds a specific amino acid to a growing polypeptide chain as defined by the nucleotide sequence of the mRNA being translated. The anticodon loop contains three bases (the anticodon) complementary to the codon in the mRNA while the acceptor stem is where the amino acid is covalently attached to the tRNA.

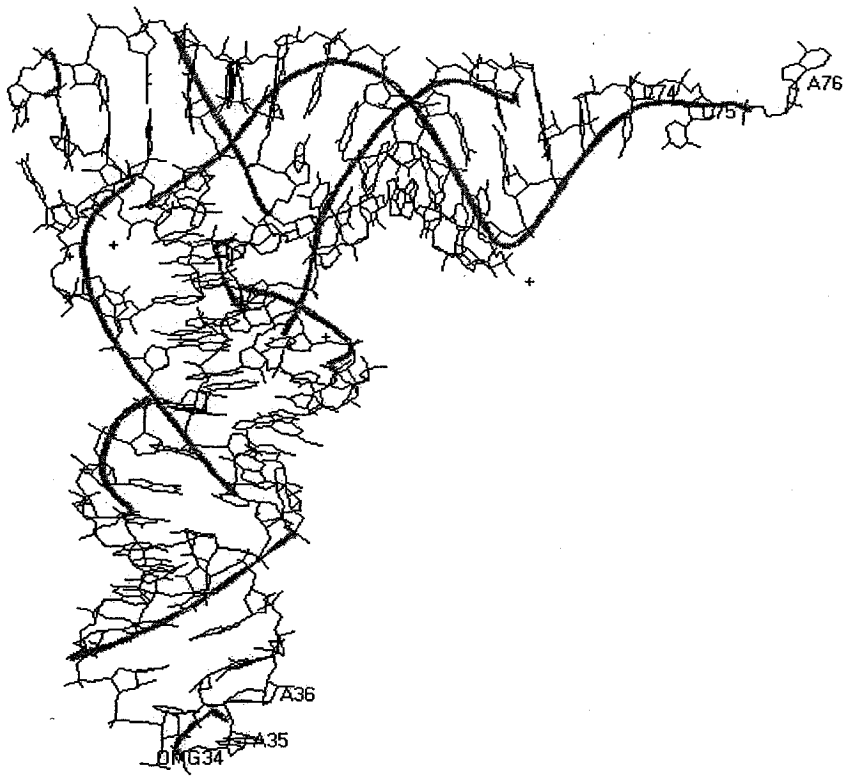

Fig. 1-2. Three dimensional L-shaped structure of yeast phenylalanine tRNA (4TNA in PDB database http://www.rcsb.org/pdb) (Hingerty *et al.*, 1978). The anticodon and 3'-end CCA are labeled.

Amino acid attachment to the tRNA requires a 3' terminal cytidine, cytidine, adenosine (CCA) sequence (present in Fig. 1-1 and Fig. 1-2). Transcription from tRNA genes generates tRNA precursors that do not function in protein synthesis (Bjork *et al.*, 1987). Precursor tRNAs contain the complete tRNA primary sequence as well as additional residues at both the 5' and 3' ends. The process of maturation involves

removal of these additional 5' and 3' sequences and any introns as well as specific base modifications and addition of the 3'- terminal cytidine, cytidine, adenosine (CCA) sequence, if it is not already present, by tRNA nucleotidyltransferase (CCA-adding enzyme) (Chen and Martin, 1988) (Fig. 1-3).

$$\textbf{tRNA + ATP + 2 CTP} \rightleftarrows \textbf{tRNA-CCA + 3 PP}_i$$

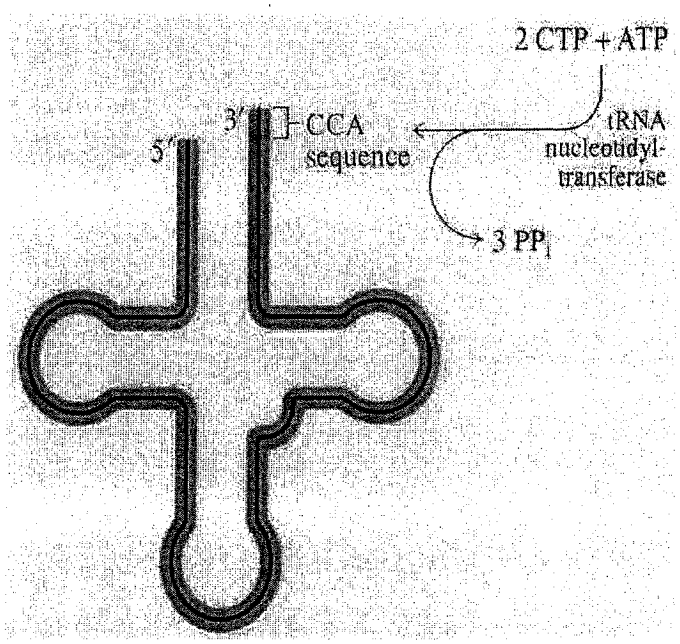

Fig. 1-3. The function of tRNA nucleotidyltransferase (modified from Moran *et al.*, 1994).

As a CCA sequence is required for aminoacylation, this enzyme activity is essential in all eukaryotes and archaea and in certain eubacteria where some or all tRNA genes do not encode the CCA sequence and the CCA has to be added post-transcriptionally (Maizels *et al*, 1999). In some prokaryotes like *E. coli*, the 3' CCA sequence is encoded

by the tRNA genes themselves and tRNA nucleotidyltransferase functions in repairing damaged tRNAs with incomplete CCA sequences (Yue *et al.*, 1998).

1.2 Transfer RNA nucleotidyltransferase superfamily

The enzyme ATP (CTP): tRNA nucleotidyltransferase (CCA-adding enzyme) has been identified in eubacteria, eukaryotes and archaea (Yue *et al.*, 1996). All CCA-adding enzymes belong to the nucleotidyltransferase (NT) family, which includes enzymes such as terminal deoxynucleotidyltransferase, DNA polymerase β, poly (A) polymerase, glutamine synthase, adenylytransferase and streptomycin and kanamycin nucleotidyltransferases (Holm and Sander, 1995). Based on sequence similarity, the nucleotidyltransferase superfamily can be divided into two classes (Yue *et al.*, 1996). Class I contains the archaeal CCA-adding enzymes, eukaryotic poly (A) polymerases, DNA polymerase β and kanamycin nucleotidyltransferase while class II contains eubacterial and eukaryotic CCA-adding enzymes and eubacterial poly (A) polymerases. Although all of the CCA-adding enzymes share local sequence similarity surrounding the active sites (with conserved DXD and RRD motifs, underlined in Fig. 1-4), class I enzymes do not show significant overall similarity to each other or to class II enzymes. However, class II enzymes show strong similarity at their N-termini and diversity in their C-termini (Yue *et al.*, 1998).

Multiple sequence alignments of the amino terminal regions of class II CCA-adding enzymes (Fig. 1-4) show several highly conserved motifs. Motif A containing the two carboxylates (DXD) is conserved in all members of the NT superfamily while the rest of the motifs are unique to the class II enzymes. Motif B is responsible for ribose

recognition and motif C connects the head and neck domain (Li *et al.*, 2002). Motif D functions as a nonspecific protein template for the incoming nucleotide and binds the triphosphate moiety. Motif E may function in the interaction with the tRNA (Li *et al.*, 2002). Those motifs involved in the selection of the correct nucleoside triphosphate (NTP) and the binding of the substrate tRNA are highly conserved in class II enzymes suggesting that the class II enzymes have similar NTP selection strategies for template-independent polymerization (Li *et al.*, 2002).

```
SC  ----------------------------MTNSN-----------------------------   5
CG  ----------------------------MFKAIRRVFT----------------------   10
KL  ----------------------------MFKMV-----------------------------   5
LA  MRLSFKTVTNVVVVLPRGRTRSIINFTLFPTITSNLVLHP-----LLRTPKTPS----FH   51
AT  MRLSSLPIN-TLINLP--KSLFLISPFRFRNLNRSLTVASRISSTLLRVSGVSSRPCGYW   57
BS  ------------------------------------------------------------
EC  ------------------------------------------------------------
AA  ------------------------------------------------------------
HS  ---MHHHHHHSSGLVPRGSGMKETAAAKFERQHMDSPDLG--------------------   37

SC  -------------------FVLNAPKITLTKVEQNICNLLNDYTDLYNQKYHNKPEPLTL   46
CG  ----------------------MIPRIQLTEKETRICNLLKDYTAHYNSLHYGQ-EPLTL   47
KL  ----------------------ASKIQLNKVESEICTLVKEFCSHYNKANAET-EPLVA   41
LA  SSLSSPMS-----------SHKVRDNIQLSDVEKRIFDRLLATLRFFN-------LQTHL   93
AT  FSTNAAMTNVGEEDKQSIPSIELKENIELTDKERKIFDRLLSTLRYCN-------LDTQL  110
BS  ----------------------------MKPPFQEALGIIQQLKQHG----------YDA   22
EC  ------------------------------------------------------MKI    3
AA  ----------------------------------MVGQIAKEMG-----------LRA   13
HS  -----------------TDDDDKMKLQSPEFQSLFTEGLKSLTELFVKEN------HEL   73

            motif A
SC  RITGGWVRDKLLGQGSHDLDIAINVMSGEQFATGLNEYLQQHYAKYGAKPHNIHKIDKNP  106
CG  RITGGWVRDKLLGQGSHDLDIAINIMSGEEFATGLNGYLLEHFDKYGVKPHSIHKIDKNP  107
KL  RITGGWVRDKLLGNDSNDLDIAINNMTGEQFAEKLCAFLQDR----GLETHSLHTIDKNP   97
LA  RVAGGWVRDKLLGKECYDIDIALDKMMGTEFVDKVREYLLSI----GEEAQGVCVIESNP  149
AT  RVAGGWVRDKLLGKESDDIDIAIDNMSGSEFLDKFKEYLSSR----DEEVQGDTVIERNP  166
BS  YFVGGAVRDLLLGRPIGDVDIATSALPEDVMAIFP------------------KTIDVGS   64
EC  YLVGGAVRDALLGLPVKDRDWVVVGSTPQEMLDAG------------------YQQVGR   44
AA  YIVGGVVRDILLGKEVWDVDFVVEGNAIELAKELAR-----------------RHGVNV   55
HS  RIAGGAVRDLLNGVKPQDIDFATTATPTQMKEMFQS-----------------AGIRMIN  116

                                                      motif B
SC  EKSKHLETATTKLFGVEVDFVNLRSEKYTELSRIPKVC-FGTPEEDALRRDATLNALFYN  165
CG  EKSKHLETATTKLFDVEVDFVNLRSEEYTEDSRIPTTQ-FGTPEEDALRRDATLNALFYN  166
KL  SKSKHLETCTTKLFDVPVDFVNLRSEEYTMESRIPKVE-FGTPYDDAMRRDATLNAMFYN  156
LA  DQSKHLETARMRLFDMWIDFVNLRSEEYTDNSRIPSMQRFGTPEEDAYRRDLTINSLFYN  209
AT  DQSKHLETAKLRIYDQWIDFVNLRSEEYTENSRIPTMK-FGTAKDDAFRRDLTINSLFYN  225
BS  KHGTVVVVHKGKAYEVTTFKTDGDYEDYRRPESVTFVR---SLEEDLKRRDFTMNAIAMD  121
EC  DFPVFLHPQTHEEYALARTERKSGS-GYTGFTCYAAPD--VTLEDDLKRRDLTINALAQD  101
AA  HPFPEFGTAHLKIGKLKLEFATARRETYPRPGAYPKVE-PASLKEDLIRRDFTINAMAIS  114
```

```
HS  NRGEKHGTITARLHEENFEITTLRIDVTTDG-RHAEVEFTTDWQKDAERRDLTINSMFLG 175
                .          .        .        .*  *** *:*::   .

                motif C                          motif D
SC  I----HKGEVEDFTKRGLQDLKDGVLRTPLPAKQTFLDDPLRVLRLIRFASRFNFT--ID 219
CG  I----QQDAVEDFTKRGWQDLQDGVLRTPLPARQTFLDDPLRVLRLIRFASRFNFN--IE 220
KL  I----TEDKIEDFTKKGFQDLNDGILRTPLPPRQTFIDDPLRVLRLIRFASRFNFQ--ID 210
LA  I----NTDSVEDFTKRGISDLKSGKIVTPLPPKATFLDDPLRVVRAIRFGARFEFT--LD 263
AT  I----NSGAVEDLTERGIDDLKSGKIVTPLPAKATFLDDPLRVLRAVRFGARFGFT--LD 279
BS  E----YGTIIDPF--GGREAIRRRIIRTVGEAEKRFREDALRMMRAVRFVSELGFA--LA 173
EC  D----NGEIIDPYNGLG--DLQNRLLRHVSP---AFGEDPLRVLRVARFAARYAHLGFRI 152
AA  VNLEDYGTLIDYF--GGLRDLKDKVIRVLHP--VSFIEDPVRILRALRFAGRLNFK---L 167
HS  F----DGTLFDYFN--GYEDLKNKKVRFVGHAKQRIQEDYLRILRYFRFYGRIVDK--PG 227
             .:     * . :.   :     .   : :* :*::*  ** ..

                          motif E
SC  PEVMAEMGDPQINVAFNSKISRERVGVEMEKILVGPTPLLALQLIQRAHLENVIFFWH-- 277
CG  AGVLKEMHDPEINEAFNNKISRERIGVEMEKILVGPNPILGLKLIQRTHLENVIFLWH-- 278
KL  PQTYQAMRDPGIHQSFNHKISKGRVYTEMHKTLTSANPFYALDLIQGAHLSRVIFTTN-- 268
LA  EDLKQAAACDEVKDALAAKISRERIGTEIDLMISGNQPVKAMTYICDLTIFWIVFSLPPT 323
AT  EELKEAASSEEVRVALGEKISRERIGNEIDLMISGNGPVSAVTYLSDLKLFSVVFALPSS 339
BS  PDTEQAIVQN---APLLAHISVERMTMEMEKLLGGPFAARALPLLAETGLN--------- 221
EC  ADETLALMREMTHAGELEHLTPERVWKETESALTTRNPQVFFQVLRDCGALRVLFP---- 208
AA  SRSTEKLLKQAVNLGLLKEAPRGRLINEIKLALREDRFLEILELYRKYRVLEEIIEG--- 224
HS  DHDPETLEAIAENAKGLAGISGERIWVELKKILVGNHVNHLIHLIYDLDVAPYIGLP--- 284
                        .  *:  * .  :        .

SC  NDSSVVKFNEENCQDMDKINHVYNDNILNSHLKSFIELYPMFLEKLPILREKIG-RSPGF 336
CG  GDQSVIEYNRKNWPQTKDVEDIYKKGIFNHHLKNFIHHYKDFLSRYLKLRQAIETKDKSF 338
KL  ESS------------PEIESIYEN--LDQHLKSVVETIPKLLKSHTTFASVFP----GM 309
LA  FEPAISDGCERLCISQLDISWNLIHLLGKTTFTDEQRRLTLYAAMFLPLRNTIYREKKAK 383
AT  AEPSPPENCGSLSQSYLEAMWSLLKTPRPGKFSGEQRRLALYAAMFLPFRKTVYKDTKGK 399
BS  -------------------------AYLPGLAGKEKQLRLAAAYRWPWLAARE------ 249
EC  ------------------------EIDALFGVPAPAKWHPEIDTGIHTLMTLSMAAMLSP 244
AA  --------------------------FQWNEKVLQKLYALRKVVDWHALEFSEERIDYG 257
HS  -------------------------ANASLEEFDKVSKNVDGFSP------------- 304
     . :  .       .  .                  .

SC  QQNFILSAILSPMANLQIIGNPKKKINNLVSVTESIVKEGLKLSKNDAAVIAKTVDSICS 396
CG  QQNFLLASILIPMADLKIIALPKKKLNNTLPVSESIVREGLKFNKASSIVVARCVENIAA 398
KL  QEPLILSLVLSGFKGLK--GPDPAKPKNSIPLAGVITKEGLNFPNTQVDNVIACVESEDS 367
LA  KVPVVNYIFRESLKRKAKDPETVLDLHRASNKFLSLIPCLVSNEDVQIVGHDWMTELID- 442
AT  SIPVVNHIFKFSMKRKTSDAETVMNIHQTTERFRSLIPSLEVKKDVELDELTWAADILEH 459
BS  -ERWALLCHALGVQESRPFLRAWKLPNKVVDEAGAILTALADIPRP------------- 294
EC  QVDVRFATLCHDLGKGLTPPELWPRHHGHGPAGVKLVEQLCQRLRVPNEIRDLAR----- 299
AA  WLYLLILISNLDYERGKHFLEEMSAPSWVRETYKFMKFKLGSLKEELK----------- 305
HS  -KPVTLLASLFKVQDDVTKLDLRLKIAKEEKNLGLFIVKNRK---------------- 345
                                          :              .

SC  YEEILAK--FADRSQLKKSEIGIFLRNFNGEWETAHFASLSDAFLKIPKLETKKIEL--- 451
CG  YNSMVEK--YLQSGDLKRSEVGTFLRELRGDWEIVHYVSLMDQYLKYISRKDNVVN---- 452
KL  YHNLVK-----NGKSMKRSELGFALRKLGKNWQMVHFYNLCLDYLRHGDEP--------- 413
LA  ----------VPVSSRVRVLTGFLLRELRDFWRVALLISILLHP-ID-VNDTEDE---SS 487
AT  WKSITLNDPVIPATSKIRVLTGFLLRDIKDFWRVSLLTSLLLSATVDGSNDHQDIGQLDF 519
BS  -----------EAWTNEQLFSAGLERALSVETVRAAFTGAPPGP--------------- 327
EC  -----------LVAEFHDLIHTFPMLNPKTIVKLFDSIDAWRKP--------------- 332
AA  ------------KAKENYEVYRLLKPLHTSVLLLLMLEEELKEK-------------- 337
HS  ------------DLIKATDSSDPLKPYQDFIIDSREPDATTRVC------------- 377
     .   .                                          .

SC  ----LFQNYNEFYSYIFDNNLNNCHELKPIVDGKQMAKLLQMKPGP-WLGKINNEAIRWQ 506
CG  ----IIDKYDRFWNYIQEQNLQDSDKMVPIIDGKRMVKILETKPGP-WLGKINDEVILWQ 507
KL  -----IPHYDEFYKHVHDCKLDDVYTLKHIINGKELAKLLDRKPGI-WMGETLDRILIWQ 467
```

```
LA  QLSKRRDLFNTVENSVIKLGLEKVWDVKQLINGKDVMSVLQLKGGP-MVKEWLDKAMACN 546
AT  QLERMRETYLTVEATIHELGLDKIWDAKPLVNGREIMQIAELKGGSRLIREWQQKLLTWQ 579
BS  -------WHEKLRRRFASLPIKTKG--ELAVNGKDVIEWVGKPAGP-WVKEALDAIWRAV 377
EC  -----QRVEQLALTSEADVRGRTGFESADYPQGRWLREAWEVAQSVPTKAVVEAGFKGVE 387
AA  -----IKLYLEKLRKVKLPKEKIEELKKQGLKGKELGERIEELKREIMNKIKLAAALE-- 390
HS  -------ELLKYQGEHCLLKEMQQWSIPPFPVSGHDIRKVGISSGKEIGALLQQLREQWK 430

SC  FDNPTGTDQELITHLKAILPKYL---- 529
CG  FDHPQGTEQELISFIKSILPNYLQ--- 531
KL  LDNPDISKETFIENLNDIVHLP----- 489
LA  LPIP-------QELQRNVLIG------ 560
AT  LAYPNGTAEECKEWMRDIKAKRQRIE- 605
BS  VNGEVENEKERIYAWLMERNRTREKNC 404
EC  IREELTRRRIAAVASWKEQRCPKPE-- 412
AA  --------------------------
HS  KSGYQMEKDELLSYIKKT--------- 448
```

Fig. 1-4. Sequence alignment of some class II CCA-adding enzymes. Sequence alignment of class II CCA-adding enzymes generated using CLUSTALW (Barton, 1993). SC, *Saccharomyces cerevisiae*; CG, *Candida glabrata*; KL, *Kluyveromyces lactis*; LA, *Lupinus albus*; AT, *Arabidopsis thaliana*; BS *Bacillus stearothermophilus*; EC, *E. coli*; AA, *Aquifex aeolicus*; HS, *Homo sapiens*. Numbers indicate amino acid positions within the proteins, (*) Indicates an amino acid conserved in all sequences, (:) indicates similar amino acids and (.) weakly similar amino acids. The amino acid corresponding to *S. cerevisiae* Glu172 is in bold. The conserved motifs A to E (Li *et al.*, 2002) are in italics. Active site signature residues are underlined.

1.3 The resolved crystal structures of CCA-adding enzymes

Up to now, four crystal structures of CCA-adding enzymes have been resolved. Of these, three are class II: human (Augustin *et al.*, 2003), *Bacillus stearothermophilus* (Li *et al.*, 2002) and *Aquifex aeolicus* (Tomita *et al.*, 2004) and one is class I: *Archaeoglobus fulgidus* (Okabe *et al.*, 2003; Xiong and Steitz, 2004; Xiong *et al.*, 2003). The CCA-adding enzymes for which the structures have been resolved have similar tertiary structures that can be subdivided into head, neck, body and tail domains (Fig. 1-5). The head domain (catalytic domain) is conserved in all of the known template-independent DNA and RNA polymerases (Okabe *et al.*, 2003). The head domain and neck domain form a U shaped structure for the accommodation of the 3' end of the tRNA (Augustin *et*

al., 2003). The body domain is in contact with the T stem and acceptor stem of the tRNA and the tail domain also may function in interactions with the tRNA (Augustin *et al.*, 2003; Tomita *et al.*, 2004; Xiong *et al.*, 2003).

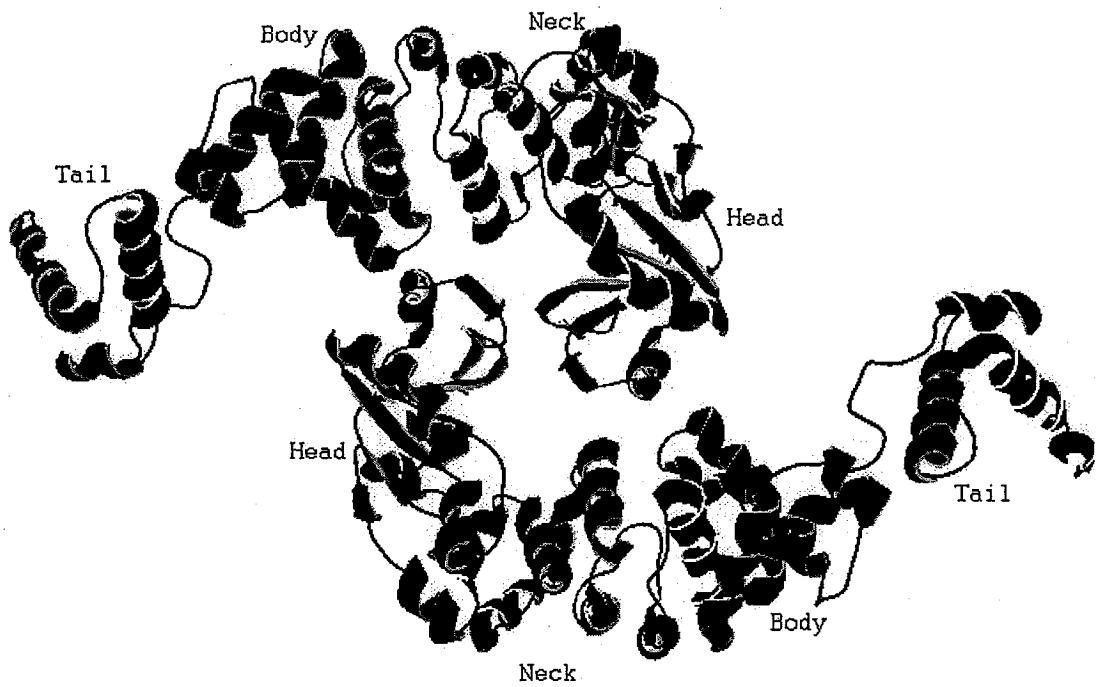

Fig. 1-5. The ribbon structure of the class II CCA-adding enzyme of *Bacillus stearothermophilus*. The crystal structure can be divided into head, neck, body and tail domains and is dimerized through head to head interaction (Li *et al.*, 2002).

Although the tertiary structures of class II CCA-adding enzymes are similar, their quaternary structures are quite different. While the crystal structures have shown CCA-adding enzymes as dimers (Li *et al.*, 2002; Augustin *et al.*, 2003; Xiong *et al.*, 2003; Xiong and Steitz, 2004), how the monomers interact is different for each different enzyme. The human enzyme is dimerized through body domain to body domain contact (Augustin *et al.*, 2003) while the *B. stearothermophilus* CCA-adding enzyme (Li *et al.*, 2002) is dimerized through head to head interaction (Fig.1-5) and the *A. aeolicus* enzyme

is dimerized through its head and neck domains (Tomita *et al.*, 2004). The class I *A. fulgidus* CCA-adding enzyme is dimerized through its body and tail domains (Okabe *et al.*, 2003). The tail domain of one subunit closely interacts with the neck, body and tail domains of another subunit resulting in a large interface area (2500Å^2) (Okabe *et al.*, 2003).

1.3.1 Catalytic domain

In spite of the overall conservation of the higher order structures of these enzymes they show limited conservation of primary sequence (see Fig. 1-4). The primary sequence conservation that does exist is confined mainly to the head domain (catalytic domain) of both classes. The catalytic domains contain the active site signature for the NT family with two conserved acidic residues (*e.g.*, Asp48 and Asp50 in the human CCA-adding enzyme) (underlined in Fig. 1-4). These conserved carboxylates are located closely to coordinate the catalytic Mg^{2+} ions. In all members of the nucleotidyltansferase superfamily, the catalytic domains contain at least two α helices and five β strands, which contribute to the binding of the incoming NTP (Xiong *et al.*, 2003). For example, two members of the NT family, *A. fulgidus* (class I) and *B. stearothermophilus* (class II) CCA-adding enzymes, show a similar arrangement in space of the catalytic domains (Okabe *et al.*, 2003) (Fig. 1-6).

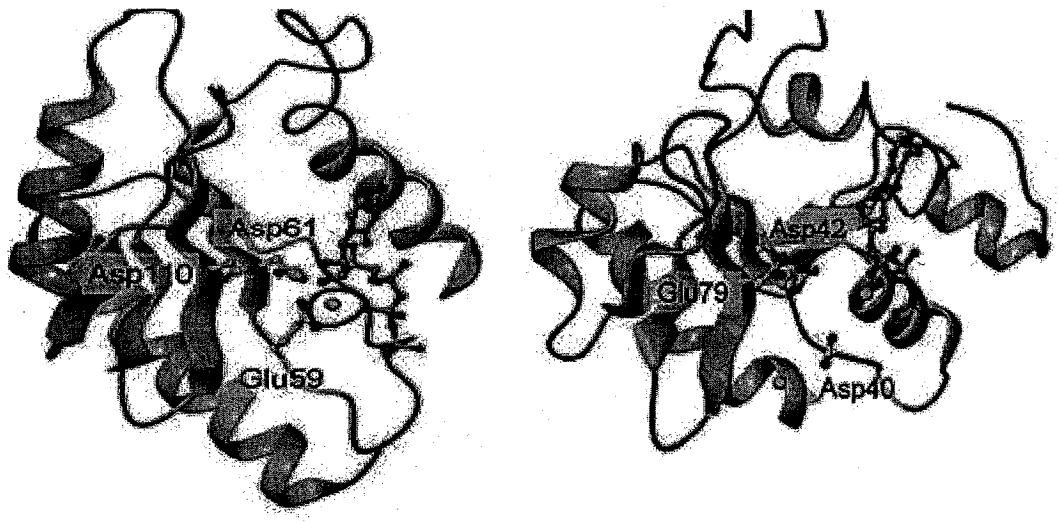

A B

Fig. 1-6 The arrangement of the catalytic domains of two members of the tRNA nucleotidyltransferase family. (A) Catalytic domain of class I CCA-adding enzyme of *A. fulgidus*. **(B)** Catalytic domain of class II CCA-adding enzyme of *B. stearothermophilus*. The conserved carboxylates are labeled and the metal ions are shown (Okabe *et al.*, 2003).

Among the DNA and RNA polymerases, CCA-adding enzymes are unique because they are able to add a specific nucleotide sequence (CCA) without a nucleic acid template. While DNA polymerases add deoxyadenosine, deoxycytidine, deoxyguanosine and deoxythymidine (dA, dC, dG and dT) residues in a specific sequence, this sequence is based on an available DNA template. Poly (A) polymerases do not require a template, but they add only A residues to a nucleic acid chain. In contrast, CCA-adding enzymes add a specific nucleotide sequence (CCA) in a non-template driven manner. How these enzymes distinguish ATP and CTP from one another and from GTP and UTP, and all

four of those from the corresponding deoxyribonucleotides (dNTPs) and add them in a specific order to the 3'-end of a tRNA is a challenge to understand.

Hydrogen bonding between the incoming bases and specific amino acids of the enzyme is used to distinguish ATP and CTP from UTP and GTP (Cho *et al.*, 2003). ATP is distinguished from CTP based on the size difference between pyrimidine and purine bases (Xiong and Steitz, 2004) because the size of the binding pocket changes during the addition of the nucleotide to accommodate the appropriate incoming NTP (Xiong and Steitz, 2004). A conserved RRD sequence in the catalytic domain (underlined in Fig. 1-4) is involved in the interaction with the 2'-hydroxyl of the ribose ring and this interaction is used to select NTPs and differentiate against dNTPs (Okabe *et al.*, 2003). The neck domain of the CCA-adding enzyme of *B. stearothermophilus* also provides a protein template to distinguish ATP from CTP and to differentiate them from the other nucleotides (Li *et al.*, 2002). The observation that the class I *A. fulgidus* CCA-adding enzyme cannot distinguish between correct and incorrect NTPs in the absence of tRNA, suggests that the 3' end of the tRNA also may be involved in the selection of the correct NTP (Xiong *et al.*, 2003). In summary, using a dynamic protein template, ribose reorganization, and purine-specific base stacking between conserved amino acids and ATP all are strategies that CCA-adding enzymes can use in nucleotide selection and addition (Li *et al.*, 2002; Xiong and Steitz, 2004; Tomita *et al.*, 2004).

1.3.2 Interaction of tRNAs with CCA-adding enzymes

A common structural feature of both classes of CCA-adding enzymes is the "deep cleft"(Augustin *et al.*, 2003; Okabe *et al.*, 2003; Xiong *et al.*, 2003; Tomita *et al.*, 2004).

In class I enzymes, the cleft is formed by the head, neck and body domains while it is formed by the head and neck domains in class II enzymes. The surface electrostatic potential of the *A. fulgidus* CCA-adding enzyme exhibits a strip of positive electrostatic potential on the body and tail domains (Xiong *et al.*, 2003). On the surface of the human CCA-adding enzyme, a similar positively charged cleft was found between the head and neck domains (Augustin *et al.*, 2003). The positively charged surface is likely to be the binding site of tRNA. A model of tRNA bound to *A. fulgidus* or human CCA-adding enzymes was built to accommodate the potential charge and architecture of the molecules. The tRNA acceptor stem and TΨC stem and loop are inserted into the cleft such that the 3'-terminus is orientated at the active site of the head domain (Okabe *et al.*, 2003; Xiong *et al.*, 2003). The body and tail domains are mainly involved in binding with the rest of the tRNA. The deletion of the tail domain of the *A. fulgidus* enzyme leads to less affinity toward tRNA and deletion of the tail domain of the *E. coli* enzyme results in the loss of the ability to incorporate CCA (Xiong *et al.*, 2003). Although the catalytic domains in class I and class II CCA adding enzymes are homologous, the remaining domains and oligomerization are quite different, suggesting that the orientation of the tRNA relative to the enzyme may be different between the two classes. This has been shown by the recently resolved crystal structures of class I and class II CCA-adding enzymes complexed with substrate tRNA (Okabe *et al.*, 2003; Tomita *et al.*, 2004). The crystal structures of the *A. fulgidus* CCA-adding enzyme complexed with tRNA (Xiong and Steitz, 2004) and *A. aeolicus* enzyme complexed with tRNA-CC and the ATP analogue AMPcPP (α, β-methyleneadenosine 5'-triphosphate) (Tomita *et al.*, 2004) show that the orientation of the tRNAs approaching the monomers of the enzymes is distinct between

the two enzymes. The resolved structure of the protein–tRNA complex helped to explain the interaction of protein and tRNA and elucidate the mechanism of CCA addition to some extent.

1.4 Proposed mechanism of CCA-addition

Even with all of the available information about CCA-adding enzymes, the mechanism for the specific incorporation of CCA by the enzyme is not well understood. Several models (Li *et al.*, 2000; Seth *et al.*, 2002; Tomita and Weiner, 2002; Cho and Weiner, 2004; Xiong and Steitz, 2004) have been proposed based on the resolved crystal structures and other types of experimental results. A two-binding site model was first proposed in which there existed two nucleotide binding sites, one for CTP and another for ATP (Deutscher, 1972b; Deutscher, 1982). This model was discarded because site-directed mutagenesis of either of the conserved acidic residues led to the loss of addition of both CTP and ATP indicating only one nucleotide-binding site in the enzyme (Yue *et al.*, 1998). More recently the resolved crystal structures of both class I and class II enzymes showed a single nucleotide-binding site (Li *et al.*, 2002; Augustin *et al.*, 2003; Xiong *et al.*, 2003).

A second model, the poly(C) polymerase model, regards the CCA-adding enzyme as a poly(C) polymerase that undergoes a significant conformational change after the addition of two CMPs, which allows for the addition of a single AMP instead of a third CMP (Seth *et al.*, 2002). The conformational change in the binding site is regulated by ATP. CCC addition in the absence of ATP has been found in class II rabbit liver and *E. coli* enzymes (Seth *et al.*, 2002) as well as in class I *S. shibatae* and *Methanococcus*

jannaschii enzymes (Tomita and Weiner, 2002). Adding CCC onto the 3'end of a tRNA instead of CCA when ATP is absent suggests that those enzymes possess an ATP-binding site and that the occupation of ATP at this site alters the specificity at the active site from C to A. This model also was supported by the isolation of the *E. coli* CCA-adding enzyme with a tightly bound ATP (Tomari *et al.*, 2000). The purified enzyme from *E. coli* can add a CCA sequence to the 3'-end of a tRNA in the absence of added ATP, suggesting that the enzyme to some extent contained some bound ATP (Tomari *et al.*, 2000). One problem with this model is that the crystal structures reveal a single binding site for ATP and CTP. This observation could be explained if the two binding sites overlap. Perhaps the CTP binding site is at the single catalytic site while the ATP binding site is larger and requires additional amino acids. This hypothesis was supported by the mutagenesis of conserved aspartic acid residues (D106 in *S. shibatae* or D93 in *E. coli*) which leads to abolishing the addition of AMP but not of CMP (Seth *et al.*, 2002).

A third model to explain CCA addition is the collaborative template model (Shi *et al.*, 1998; Yue *et al.*, 1998). This model suggests that a single catalytic site alters its specificity during the addition of CCA by cooperating with the growing 3' end of the tRNA to synthesize the CCA sequence (Yue *et al.*, 1998). Fixing a tRNA in position on the surface of the *S. shibatae* CCA-adding enzyme by cross-linking did not affect the enzyme's ability to add the CCA to this molecule (Shi *et al.*, 1998). So the change in specificity of addition from C to A is owing to cooperation between the growing 3'-end of the tRNA and the enzyme and the cooperation progressively creates a binding pocked specific for the addition of the next nucleotide.

Another model which emphasized the cooperation between the enzyme and the growing 3'end of the tRNA in altering the specificity for C addition or A addition is the scrunching-shuttling model (Li *et al.*, 2000). This model was suggested by studies that a tRNA molecule induced the dimerization of dimers of *S. shibatae* CCA-adding enzyme to form a tetramer and that the resulting tetramer could bind two tRNAs. This model argues that there are two pairs of active sites on the tetramer adjacent to the 3' termini of bound tRNA molecules (Li *et al.*, 2000). This model with two quasi-equivalent active sites, one adding CTP and the other adding ATP was proven to be wrong as a single catalytically active subunit can carry out all three steps of CCA addition (Cho and Weiner, 2004).

Recently, another model was proposed based on the complex of the *A. fulgidus* CCA-adding enzyme and tRNA (Xiong and Steitz, 2004). This model argues that the 3'end of the tRNA unstacks from the acceptor stem to position the 3' nucleotide of the tRNA correctly to react with the appropriate NTP bound in the active site. This model also requires bound tRNA substrate for the selection of the correct nucleotide because the enzyme can bind all NTPs in the absence of the tRNA substrate.

In summary, the collaborative template model seems to be the most favored because it combines the merits of other models like the poly(C) polymerase model and the tRNA unstacking model which emphasize that the 3'end of the tRNA participates in the selection of the correct NTPs. The common feature of the three models (collaborative template, poly(C) polymerase and tRNA unstacking) is that there exists some collaboration between the enzyme and the tRNA primer and this collaboration finally decides the selection of the nucleotide and the orderly addition of CCA.

1.5 Kinetic studies on the CCA-adding enzyme

In addition to the extensive analysis of tRNA nucleotidyltransferase based on the various crystal structures described above a considerable amount of effort has been invested in using a classical enzyme kinetics based approach to understand how this interesting enzyme works. CCA addition to the 3'end of a tRNA is reversible and is inhibited by PP_i (Deutscher, 1982) and CCA-adding enzymes have optimal activity *in vitro* in the range of pH 8.5-10 (Deutscher, 1982). The reversible reaction catalyzed by the rabbit liver CCA-adding enzyme has an apparent equilibrium constant for the forward reaction of 1500 at pH 9.4 but only 50 at pH 7.0 (Evans and Deutscher, 1978) which is mainly due to a large difference in the release of a proton at the two pHs during the incorporation reaction. In the presence of a single nucleotide, the enzyme can use tRNA-, tRNA-C or tRNA-C-C as substrate and incorporate CCA, CA or A into those respective substrates (Deutscher, 1982). Previous studies have defined the kinetic parameters for a number of different CCA-adding enzymes under a number of different conditions (Deutscher, 1982). The values of K_m for nucleotides vary depending on organism and purification procedure. The apparent K_m for the various tRNA substrates is 5-15 μM (Deutscher, 1982). Generally, the K_m for ATP (0.1-2 mM) is much higher than the K_m for CTP (15-200 μM) (Seth *et al.*, 2002; Yue *et al.*, 1996). For the yeast enzyme, previous studies (Rether *et al.*, 1974) have shown the apparent K_m for substrates tRNA-C-C, tRNA-C, tRNA-N, ATP and CTP to be 5.5 μM, 11 μM, 7.8 μM, 0.45 mM and 0.26 mM, respectively. A more recent study (Chen *et al.*, 1990) on the native CCA-adding enzyme purified from *S. cerevisiae* as well as from a strain that overproduces this activity reported kinetic constants for substrate ATP (0.56 mM) and CTP (0.18 mM), which are

similar to the previous reports. In each of these experiments the enzymes were shown to maintain classic Michaelis-Menten kinetics (Rether *et al.*, 1974; Williams and Schofield, 1977; Evans and Deutscher, 1978).

Kinetic studies show that CCA-addition is biphasic with the addition of two Cs occurring in the first fast phase with the addition of one A defining the second slow phase (Seth *et al.*, 2002). Studies on the *E. coli* enzyme showed its kinetic mechanism to follow steady state random (Williams and Schofield, 1977). In contrast, the kinetic mechanism for the rabbit liver enzyme was rapid equilibrium random (Evans and Deutscher, 1978). The kinetic mechanism of CCA addition in other organisms is not well understood even though some kinetic constants have been reported (Deutscher, 1982).

1.6 A temperature-sensitive mutant in *Saccharomces cerevisiae* (yeast)

In yeast, the isolation of a temperature-sensitive mutant (Aebi *et al.*, 1990) showed that the CCA-adding enzyme was essential for viability. At the non-permissive temperature, yeast cells with the mutant gene (*ts352 cca1-1*) accumulated tRNA molecules with incomplete 3'end (Aebi *et al.*, 1990) and led to a rapid decrease in protein synthesis (Peltz *et al.*, 1992). Initial characterization of crude extracts from the temperature-sensitive yeast strain showed no tRNA nucleotidyltransferase activity or less than 9% activity as compared to crude extracts from strains carrying the wild-type gene even at the permissive temperature (Aebi *et al.*, 1990). DNA sequencing of the mutant *cca1-1* gene (D. Kushner, personal communication) showed a single nucleotide substitution (G→ A) in the gene, leading to the substitution of an amino acid glutamate by a lysine in the resulting protein (Fig. 1-7). How this single amino acid substitution

confers the temperature-sensitive phenotype and results in a dramatic decrease in the enzyme activity even at the permissive temperature are still not known. To address this question, site-directed mutagenesis of the *CCA1* gene was used to alter the amino acid at this position (Shan *et al.*, in preparation).

Wild-type

GT GAA GTG GAA GAT TT
Gly Glu Val Glu Asp Phe

Mutant

GT GAA GTG **A**AA GAT TT
Gly Glu Val Lys Asp Phe

Fig. 1-7. Sequence of the wild-type and mutant *CCA1* genes from *S. cerevisiae* in the region coding for amino acid 172. The resulting protein sequence is shown below the DNA sequence. The base that changes is shown in bold and the resulting amino acids are underlined.

In addition to generating the original glutamate 172 to lysine variant protein, position 172 also was changed to glutamine, histidine, or phenylalanine. Yeast strains bearing these mutations were tested for growth at the permissive and non-permissive temperatures (D. Kushner, personal communication) (Fig. 1-8). As expected the strain bearing the mutation generating lysine at position 172 of tRNA nucleotidyltransferase was unable to grow at the non-permissive temperature. The strain bearing the glutamine 172 variant protein grew almost as well as the wild-type strain indicating that Glu172 is not required for growth. Strains carrying the histidine and phenylalanine variant proteins grew less well at the non-permissive temperature indicating that the temperature-sensitive phenotype does depend on the amino acid at position 172 (Fig. 1-8).

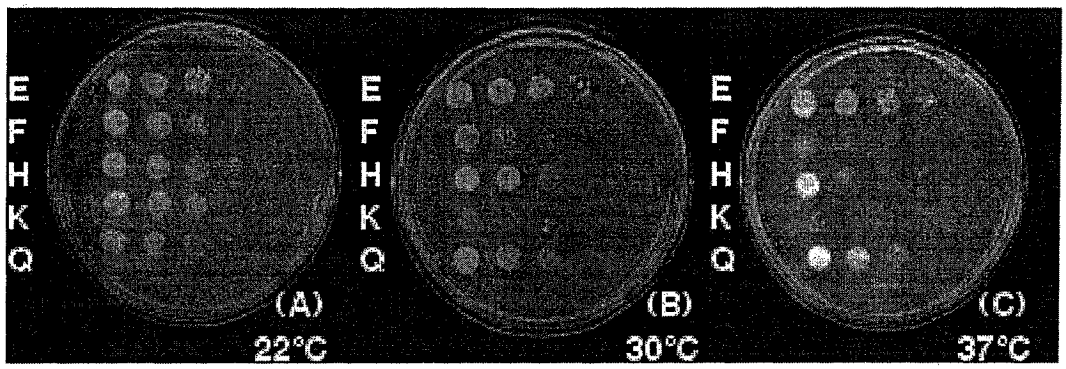

Fig. 1-8. Increasing temperature impairs growth of *S. cerevisiae* with isogenic mutations at Glu172 of *CCA1*. In each panel, growth of serial dilutions of yeast strain YPH500 with the wild-type amino acid, Glu (E), is shown at the top; isogenic mutants of Phe (F), His (H), Lys (K), and Gln (Q), respectively, are shown in the following rows. (A) 22°C, (B) 30°C, (C) 37°C.

1.7 This study

In light of the recent advances in the characterization of tRNA nucleotidyltransferase, particularly the available crystal structures, it seemed worthwhile to revisit the temperature-sensitive mutation either to provide additional insights into how tRNA nucleotidyltransferase functions or into how this mutation generates a temperature-sensitive phenotype. To do this the mutation defining the temperature-sensitive phenotype was identified and the variant protein resulting from this mutation was characterized biochemically and biophysically and compared to the wild-type enzyme. Enzyme activity assays were carried out to compare the relative activities of the wild-type and variant enzymes at permissive and non-permissive temperatures and biophysical techniques (CD and fluorescence) were used to compare the secondary and tertiary structures of these enzymes. Changes in structure as a function of this mutation or with respect to increasing temperature were monitored by recording the changes in the fluorescence and CD spectra.

To further investigate the role of this specific amino acid on enzyme structure and activity, other variant enzymes were characterized. As the obvious result of the conversion of glutamate to lysine is the conversion of a negatively charged residue to a positively charged residue other variants (glutamine, histidine and phenylalanine) reflecting various levels of a change in charge were analyzed. The change of glutamate to glutamine removes the negative charge from this position while keeping a hydrophilic residue here, the substitution of glutamate to histidine could leave a positive charge or no charge at that position depending on the local environment around the amino acid. Finally, phenylalanine, a large non-polar aromatic residue, was introduced into this position. Substituting the large phenylalanine side chain in the place of the smaller glutamate side chain also helps to address the question of the importance of the size of the residue at this position. All the variant enzymes were characterized enzymatically at the permissive and non-permissive temperatures and compared to the wild-type enzyme. In addition, circular dichroism and fluorescence spectroscopy were used to correlate any changes in structure with the changes in enzyme activity.

2. MATERIALS AND METHODS

2.1 Strains, growth media and buffers

E. coli strain XL2-Blue (Stratagene) was kindly provided by Dr. Pam Hanic-Joyce. Growth media and some buffers used in this study are listed in Table 2-1. Unless otherwise indicated all chemicals and reagents were from Bioshop. IPTG (isopropyl-β-D-thiogalactopyranoside) and ampicillin (sodium salt, BioTech grade) were typically prepared as 1 M and 100 mg/ml stock solutions respectively and filtered through a 0.2 μm sterilized syringe filter and stored at - 20°C in small aliquots (1ml). Thrombin was kindly provided by Dr. Joanne Turnbull. Deoxyribonucleotide triphosphates were from Promega. ATP and CTP were from Sigma and ICN Biochemicals respectively and baker's yeast tRNA (Cat. No.109 495) was from Roche.

2.2 Construction of expression system

2.2.1 Plasmid used in fusion protein expression

Commercial plasmid pGEX-2T engineered to contain a *Sal*I restriction site downstream of the *Bam*HI restriction site was used to construct the expression system. Genes of interest were inserted into the vector between the *Bam*HI and *Sal*I restriction sites to generate fusion proteins with glutathione S-transferase.

Table 2-1 Recipes for media and buffers

Growth medium	Recipe	Reference
YT	0.8% Bacto-tryptone 0.5% Bacto-yeast extract 0.5% NaCl (plates: 1.5 % agar)	Sambrook *et al.*,1989
Luria Bertani (LB)	1% Bacto-tryptone 0.5% Bacto-yeast extract 1% NaCl (plates: 1.5 % agar)	Sambrook *et al.*,1989
4X-PAGE loading buffer	0.0625 M Tris-HCl [pH 6.8], 10% glycerol, 2% SDS, 5% β-mecaptoethanol, 0.01% bromophenol blue	
5X SDS-PAGE running buffer (pH 8.3)	Tris 15g/l, glycine 72g/l, SDS 5g/l	
SDS-PAGE Resolving gel (10%)	10% acrylamide (29:1 acrylamide:bis acrylamide, 0.1% SDS, 0.1% APS, 0.375 M Tris-HCl [pH 8.8], 0.1% TEMED	
SDS-PAGE Stacking gel	3.9% acrylamide (29:1 acrylamide:bis acrylamide), 0.1%SDS, 0.1% APS, 0.125 M Tris-HCl [pH6.8], 0.1% TEMED)	
5X TBE	1 M Tris, 1 M Boric acid, 20 mM EDTA [pH8]	
TE	10 mM Tris-HCl [pH8], 1 mM EDTA	
PBS	140 mM NaCl, 10 mM Na_2HPO_4, 1.8 mM KH_2PO_4	

2.2.2 Polymerase chain reaction (PCR) and the purification of PCR products

To generate an expression system to over-express *S. cerevisiae* tRNA nucleotidyltransferase, the *S. cerevisiae CCA1* wild-type and mutant genes in vector pDK200 or derivatives (supplied by D. Kushner, Dickinson College) were amplified by polymerase chain reaction (PCR) using oligonucleotides 5'-ACTAGT**GGATCC**ATGACGAA-3' and 5'-ATCGATGTCGACTACTACAG-3' containing *Bam*HI and *Sal*I restriction sites bolded and underlined, respectively.

Oligonucleotides were obtained from BioCorp Inc. (Montreal). The PCR reactions were performed in a PERKIN ELMER DNA thermal cycler using an initial hot start cycle of 96°C/4 min, 40°C/1min, and 72°C/4min followed by 35 cycles of 96°C/0.5 min, 40°C/1min, 72°C/4min. The last cycle was finished at 72°C for 10 minutes to ensure complete extension of PCR products. The reaction mixture contained 100 pmoles of each primer, 10-100 ng of template DNA, 200 μM dNTPs, 1.5 mM $MgCl_2$, 1 U Pfu DNA polymerase (Stratagene) and 1X Pfu polymerase buffer in a final volume of 100 μl adjusted with distilled water. Mineral oil (100 μl) was layered over the reaction mixture to avoid evaporation at high temperature.

After the reaction, 10 μl PCR product was characterized by agarose gel electrophoresis (section 2.2.5) to check the quality of the products. The remaining 90 μl PCR product was concentrated by adding 1/10 volume of 3 M sodium acetate and two volumes of 99% ethanol. After complete mixing, the samples were frozen at -80°C for 30 minutes and centrifuged at 4°C for 30 minutes at 14 000 rpm in an Eppendorf microcentrifuge. The pellets were washed with 100 μl 80% ethanol, desiccated and resuspended in 10 μl distilled water.

2.2.3 **Plasmid DNA preparation** (modified from Sambrook *et al.*,1989)

E. coli XL2-Blue cells carrying the plasmid of interest were grown overnight at 37°C with shaking in 5 ml YT medium containing 100 μg/ml ampicillin. Aliquots of 1.5 ml were collected in Eppendorf tubes by centrifugation for 3 minutes and the supernatant was discarded. The pellet was resuspended in 100 μl of ice-cold resuspension buffer (50 mM glucose, 25 mM Tris [pH8], 10 mM EDTA) and left for 5 minutes at room

temperature. Next, 200 µl of fresh lysis buffer (0.2 M NaOH, 1% sodium dodecylsulfate) was added and the samples were inverted several times gently and placed on ice for 5 minutes. Next, 150 µl of neutralization buffer (3 M potassium acetate [pH 5.2] adjusted with acetic acid) was added and mixed thoroughly by inverting the tubes. After centrifugation at 4°C for 10 minutes, the clear liquid was collected and 1 µl of 10 mg/ml RNase A was added. After incubation at 50°C for one hour, 400 µl of phenol was added and the samples were vortexed and centrifuged for 3 minutes to separate the phenol and aqueous phases. The aqueous layer was collected and the plasmid DNA was precipitated as described previously (section 2.2.2). DNA concentrations were determined by UV absorbance assuming an A_{260} of 1 equals 50 µg/ml of DNA. DNA samples were sequenced by Bio S&T (Lachine, Quebec) to confirm the sequences.

2.2.4 Restriction digestions

*Bam*HI (10 U/µl) and *Sal*I (10 U/µl) were used with the digestion buffers from the supplier (MBI Fermentas). An appropriate amount of PCR product or plasmid DNA was digested with 2-5 units of *Sal*I in 10 µl $1XO^+$ buffer at 37°C for 2 hours and the DNA was precipitated as described previously (section 2.2.2). Next the DNA sample was digested with 2-5 units of *Bam*HI in 10 µl $1XG^+$ buffer at 37°C for 2 hours. For the plasmid DNA, after 90 minutes of digestion, 1 unit of CIAP (calf intestinal alkaline phosphatase, MBI) was added into the digestion mixture. The digested samples were separated by agarose gel electrophoresis (2.2.5) and the desired fragments were excised (2.2.6).

2.2.5 Agarose gel electrophoresis

Agarose (genetic technology grade) was from ICN. Agarose gels were prepared by dissolving agarose in 1X TBE buffer. Ethidium bromide was added to a final concentration of 1 μg/ml before the gel solidified. Samples, mixed with loading dye (Promega), were separated on 1% agarose gels at 102 volts for 30-40 minutes. DNA markers (λ DNA digested with *Eco*RI and *Hin*dIII, 500 μg/μl from Promega) were used as standard.

2.2.6 Fragment purification

Excised DNA fragments were purified using the SpinPrep™ Gel DNA Kit by the procedure recommended by the supplier (Novagen). SpinPrep™ Gel Melt Solution (300 μl) was added per 100 mg of gel slice. The solution was incubated in a water bath at 50°C for 10 minutes and vortexed for 30 seconds at 2 minute intervals to melt the gel. The SpinPrep™ Filter was placed into a 2 ml receiver tube. A maximum of 700 μl of the dissolved gel solution was added and centrifuged at top speed in a microcentrifuge for 30 seconds. Then 400 μl of fresh SpinPrep™ GelMelt solution was added to wash away the residual agarose on the DNA sample. The sample was centrifuged again as before and 600 μl of SpinPrep™ Wash buffer (with ethanol) was added to wash the DNA sample on the filter. Samples were centrifuged for another 2 minutes to remove the residual wash buffer and the SpinPrep™ Filter was transferred into a 1.5 ml Eluate Receiver Tube and 45-50 μl pre-warmed distilled water was added with incubation for 3 minutes at 50°C. The sample then was centrifuged for 1 minute to collect the eluted DNA.

2.2.7 Ligation

The *Bam*HI and *Sal*I digested PCR products (wild-type and mutant *CCA1* genes) were inserted into *Bam*HI and *Sal*I digested pGEX-2T vector. Insert (100-200 ng) and vector DNA (100 ng) were ligated in 1X ligase buffer (MBI) containing 1 unit of T4 DNA ligase (MBI) and 0.25 mM ATP in a final volume of 20 μl at 4°C overnight. Linearized vector alone and dephosphorylated vector without insert were used as controls.

2.2.8 Preparation of competent XL2 Blue cells (modified from Sambrook *et al.*, 1989).

XL2 Blue cells were streaked on a YT agar plate and incubated overnight at 37°C. One colony was picked and inoculated into 5 ml of YT medium and grown at 37°C with shaking at 225 rpm overnight. Next morning, the overnight culture was diluted 100 fold with fresh YT medium and incubated with shaking at 225 rpm until an optical density of 0.5-0.6 at 600 nm had been reached. The culture was transferred to a sterile 500 ml centrifuge bottle and left on ice for 40 minutes. Then, the cells were collected by centrifugation in a JA-10 rotor at 5000 rpm for ten minutes at 4°C. The supernatant was discarded and the cell pellet was resuspended in sterile ice-cold 50 mM $CaCl_2$ solution (to 25% of original volume) and left on ice for 15 minutes. The cells were recovered by centrifugation as before and the cell pellets were resuspended in sterile ice-cold 50 mM $CaCl_2$ with 15% glycerol (to 4% of original volume). The competent XL2 Blue cells were transferred to pre-chilled sterile Eppendorf tubes in 0.5 ml aliquots and frozen at -80°C.

2.2.9 *E. coli* transformations

E. coli transformations were based on a protocol described by Capage and Hill (1979) and Lederberg and Cohen (1974). Briefly, 5 µl of ligation mixture was added to 50 µl of competent XL2 Blue cells in a sterile Eppendorf tube and incubated for 30 minutes on ice. After heat shocking for 45 seconds at 42°C, the cells were cooled on ice for 2 minutes and 100 µl sterile YT medium was added with subsequent incubation at 37°C for an hour with vigorously shaking. Finally, the mixture was plated onto YT agar plates with 50 µg /µl ampicillin and incubated at 37°C overnight.

2.2.10 Screening for transformed cells

The screening process was adapted from the rapid screening procedure of Promega with minor modifications. The transformed colonies were selected and patched onto YT agar plates containing 50 µg/µl ampicillin and incubated at 37°C overnight. Patched cells were smeared in Eppendorf tubes and resuspended in 50 µl of 10 mM EDTA (pH 8) by vortexing. Then 50 µl of freshly made cracking buffer (0.2 M NaOH, 20% sucrose and 1% SDS) was added and the samples were vortexed and incubated at room temperature for 5 minutes. After moving the tubes to 70°C for 5 minutes, 1.5 µl 4 M KCl and 1 µl 0.4% bromophenol blue were added, the samples were vortexed and incubated on ice for 10 minutes. After centrifugation at top speed at 4°C for 4 minutes in the microcentrifuge, 20 µl samples was loaded onto a 0.8% agarose 1X TBE gel and electrophoresed at 90 volts for about 2 hours. Plasmid DNA without insert was used as a control.

2.3 Protein expression and purification

2.3.1 Over-expression of fusion proteins

XL2-Blue cells carrying pGEX-2T vectors containing the genes of interest were inoculated into 10 ml YT medium containing 50 μg/μl ampicillin and incubated at 37°C with shaking at 225 rpm overnight. The overnight culture was diluted 100 fold into 1 l YT ampicillin medium and incubated at 37°C until an optical density of 0.7 at 600 nm had been reached. Expression of the fusion protein was induced by addition of 1M IPTG (isopropyl-β-D-thiogalactopyranoside) to a final concentration of 1 mM with growth at 18°C overnight (14-16 hours). The cells were collected by certrifugation at 5 000 rpm in a JA-10 rotor at 4°C for fifteen minutes and the cell pellets were stored at -80°C or resuspended in resuspension buffer to purify fusion protein.

2.3.2 Cell lysis

Fusion proteins expressed from pGEX-2T derivatives were purified according to the procedure outlined in Current Protocols in Protein Science (Harper and Speicher, 1997). Cells were resuspended in resuspension buffer (50 mM Tris [pH 8.0], 1 mM EDTA, 0.3 mM PMSF and 0.01% lysozyme) and incubated on ice for 15 minutes before sonication. Resuspended cells were sonicated on ice using the large tip of the Branson Sonifier 250 with ten 10 second pulses with a 20 second pause between each pulse. The sonicated solutions were centrifuged at 18 000 rpm in a JA-20 rotor at 4°C for 40 minutes. The supernatant was removed from the cell debris pellets and aliquots of supernatant or resuspended cell debris pellet (containing the same amount of protein) were analyzed by SDS-PAGE (denaturing polyacrylamide gel electrophoresis) (see

section 2.3.4) to check the fusion protein expression level. The supernatant containing the desired protein was used for column purification.

2.3.3 Measurement of protein concentration

Protein concentrations were determined according to the procedure accompanying the Bio-Rad protein assay kit. A 200 µl aliquot of dye reagent was added to 800 µl of protein sample and water to give a final volume of 1 ml. Absorbance at 595 nm was measured on a UV spectrophotometer. A standard curve was produced by measuring absorbance at 595 nm of different amounts of bovine serum albumin (0, 5, 10, 15, 20, 25 µg). The colour development of the mixture of protein and dye reagent was time dependent, so the incubation time of the BSA standard and unknown samples was kept the same (5-10 minutes). The concentration of proteins was determined by linear regression analysis from the standard curve.

2.3.4 Sodium dodecyl sulfate-polyacrylamide gel electrophoresis (SDS-PAGE)

SDS polyacrylamide separating and stacking gels (5 ml and 2 ml, respectively) were made according to the instructions accompanying the Bio-Rad apparatus and cast between 4 cm by 10 cm gels plates separated by 4 mm spacers. SDS and ammonium persulfate were prepared as 10% stock solutions at room temperature; the acrylamide/*bis*-acrylamide mixture was prepared as a 30% (29:1 acrylamide to *bis*-acrylamide) solution and stored at 4°C. To prepare 10 ml stacking gel 1.3 ml 30% acrylamide/bis-acrylamide, 100 µl SDS, 100 µl APS, 2.5 ml 0.5 M Tris [pH6.8], 6.1 ml dH_2O and 10 µl TEMED were mixed, an appropriate aliquot taken and allowed to polymerize at room temperature.

To prepare 10 ml separating gel 3.3 ml 30% acrylamide/*bis*-acrylamide, 100 μl SDS, 100 μl APS, 2.5 ml 1.5 M Tris [pH6.8], 4 ml dH_2O and 10 μl TEMED were mixed, an appropriate aliquot taken and allowed to polymerize at room temperature. Boiled protein samples mixed with loading dye (see Table 2-1) were loaded into the wells of the stacking gel and electrophoresed in pre-chilled running buffer at constant voltage (200 volts) for about one hour. The proteins on the polyacrylamide gel were visualized by staining in Coomassie blue staining solution (0.1% Coomassie blue R-250, 40% methanol, 10% acetic acid) for 30-50 minutes and destaining in destaining solution (40% methanol, 10% acetic acid) three hours, changing the destaining solution every hour.

2.3.5 Glutathione Sepharose 4B column chromatography

GST-fusion proteins were purified by affinity chromatography using Glutathione Sepharose 4B following the manufacturer's instructions (Amersham Pharmacia Biotech). The fresh affinity matrix was packed by gravity in a 1 cm X 20 cm column to a height of 3-5 cm. The gel matrix was equilibrated by rinsing with 10 bed volumes of distilled water followed by 10 bed volumes of loading buffer (50 mM Tris [pH8], 140 mM NaCl). The gel could be used many times and regeneration of used gel was achieved by washing with 2 bed volumes of 6 M guanidine-HCl followed by 5 bed volumes of distilled water and equilibration with 5 bed volumes of 1XPBS (140 mM NaCl; 10 mM Na_2HPO_4; 1.8 mM KH_2PO_4, pH 7.4). Alternatively, the resin was regenerated by washing with 3 bed volumes of alternating high (0.1 M Tris [pH 8.5], 0.5 M NaCl) and low pH (0.1 M sodium acetate [pH 4.5], 0.5 M NaCl) buffer. The cycle was repeated 3 times and finally the gel was re-equilibrated with 5 bed volumes of 1XPBS.

2.3.6 Fusion protein purification and thrombin cleavage

Cell lysate containing GST fusion protein was applied to the resin equilibrated with loading buffer (PBS) with incubation for 30 minutes at 4°C to promote the binding of GST-fusion protein to the affinity matrix. The column then was packed and drained, and washed with 100 bed volumes of PBS or 50 mM Tris buffer with 140 mM NaCl (pH 8.0) to remove impurities. Thrombin cleavage to remove the GST-tag was carried out by adding 8-10 μg thrombin to the column resin loaded with the protein of interest in 6-8 mls of 50 mM Tris buffer with 140 mM NaCl, 2.5 mM $CaCl_2$ (pH 8.0) with incubation at 4°C overnight on a rotary mixer. After cleavage the column buffer and a further two bed volumes of wash buffer were collected. Alternatively, the fusion protein could be eluted from the column by 3 bed volumes of elution buffer (15 mM glutathione, 50 mM Tris-HCl [pH8.0], 140 mM NaCl) and thrombin added to the eluted protein at a ratio of 1 μg thrombin for 1 000 μg fusion protein. Thrombin digestion was carried out overnight at 4°C in a dialysis bag (Spectrum laboratories, Inc., Molecular cutoff 6 000-8 000) in a large volume (4 l) of buffer (50 mM Tris-HCl [pH8.0]; 140 mM NaCl) which also removed the glutathione. The next morning, the overnight dialyzed and thrombin cleaved sample was loaded onto the affinity column to remove the GST-tag and any uncut fusion protein. The flow-through and the following two bed volume wash fractions were kept and analyzed by SDS-PAGE. Purified proteins were stored at -80°C in small aliquots with 10% glycerol.

2.4 Enzyme activity assay

2.4.1 Treatment of substrate tRNA

The treatment to remove any intact 3'-cytidine-cytidine-adenosine sequences from the commercial yeast tRNA was achieved by snake venom phosphodiesterase (0.029 units/mg, Sigma) treatment according to the procedure described by Yue *et al.* (1998) with some modifications. Generally, 28 mg tRNA was treated with 5.6 mg (0.1623 units) snake venom phosphdiesterase for one hour at 22°C in 100 mM Tris-HCl (pH 9.0), followed by two extractions with equal volumes of fresh phenol, two extractions with equal volumes of chloroform and one ether extraction. The ether layer was discarded and the tRNA was precipitated as described previously as for DNA except that the final pellet was resuspended in RNase free water (Integrated DNA Technologies, INC). The quality of the treated tRNAs was analyzed by 7 M urea polyacrylamide gel electrophoresis.

2.4.2 Polyacrylamide urea gel electrophoresis

The gel used to separate tRNAs was made by mixing 9.5 g acrylamide, 0.5 g *bis*-acrylamide, 21 g urea and 10 ml 5XTBE and adjusting with water to 50 ml. Cross-linking was catalyzed by adding 30 μl 10% APS and 1 μl TEMED. After loading 4-6 μg tRNA mixed with loading buffer (95% formamide, 20 mM sodium EDTA, 0.2% xylene cyanol and 0.2% bromophenol blue) electrophoresis was carried out in pre-chilled 1XTBE buffer on ice for 4 hours at constant voltage (200V). The gel was stained in 0.1% ethidium bromide solution for one half hour and visualized using the UV transilluminator.

2.4.3 Standard activity assay of tRNA nucleotidyltransferase

CCA-adding enzyme activity was assayed by measuring incorporation of [α^{32}P] ATP (3000 Ci/mmol, 10 mCi/ml, MPI Biochemical) into substrate tRNAs which were pretreated with snake venom phosphodiesterase to remove any intact CCA sequences (section 2.4.1). The activity assay was a modification of the procedure of Cudny *et al.* (1978). The concentration of tRNAs was determined by UV absorbance assuming an A_{260} of 1 at 40 μg/ml. Enzyme activity assays were carried out in duplicate in glass tubes in 100 μl final volumes containing 100 mM glycine buffer (pH 9.0), 10 mM $MgCl_2$, 0.4 mM CTP, 1.0 mM ATP, 0.2-0.5 μl [α^{32}P] ATP and 20 μM tRNA. Purified wild-type enzyme (100 ng) was added to the reaction mixture to initiate the reaction and the assay was carried out for 2 minutes and stopped by addition of the same volume of 2 M HCl with incubation on ice for 20 minutes. Under standard conditions, the incorporation of CMP and AMP into substrate tRNA was in the linear reaction range (section 2.4.4). The reaction mixtures were filtered through GF/C (Whatmann) glass fiber filters. Each filter was washed with 100 ml 1M HCl, and then with 10 ml 99% ethanol to remove any unincorporated free [α^{32}P] ATP. The filters were air-dried and 5 ml of scintillation fluid was added and activity was measured in a LKB WALLAC-1218RACKBETA scintillation counter. Each experiment was carried out at least twice and boiled enzyme controls were used to account for non-specific interactions with the protein. The boiled enzyme values were subtracted from the values obtained.

2.4.4 Measuring the initial velocity over a range of tRNA concentrations

For the wild-type enzyme, kinetic studies were carried out under steady-state conditions at room temperature. In the stop-time radioactive assay, the process of the reaction cannot be monitored continuously, therefore, to measure the initial velocity of the reaction, the appropriate amount of enzyme and assay time were optimized experimentally to keep the reaction in the linear range until the reaction was stopped by adding 100 µl 2 M HCl. The average velocity (calculated by dividing the total amount of product by assay time) was taken as the initial velocity.

2.4.4.1 Amount of enzyme to be used

Different amounts of purified wild-type enzyme (18.75 ng, 37.5 ng, 75 ng, 150 ng, 300 ng) in 10 µl 1XPBS buffer were added to give a final 100 µl reaction mixture containing 100 mM glycine buffer (pH 9.0), 10 mM $MgCl_2$, 0.4 mM CTP, 1.0 mM ATP, 0.2 µl [α^{32}P] ATP (3000 Ci/mmol, 10 mCi/ml) and 40 µM tRNA, assayed for 10 minutes at room temperature and processed as described above (section 2.4.3).

2.4.4.2 Time course of the assay

Under standard conditions of glycine, ATP and CTP with 10 µM tRNA and 0.25 µl [α^{32}P] ATP, 30 ng wild-type enzyme in 10 µl 1XPBS was added into a 90 µl reaction mixture. To determine the time course profile, the assays were carried out for 1 min, 3 min, 5 min, 7 min, 9 min and 12 min and processed as described above (section 2.4.3).

2.4.4.3 Measuring the kinetic constant for tRNAs

Wild-type enzyme (140 ng) in 10 μl of 1XPBS was added into a 90 μl standard reaction mixture with varying amounts of tRNA while the concentrations of the other two substrates ATP (1 mM) and CTP (0.4 mM) were kept relatively high (two fold the K_m reported by Chen *et al.* (1990)). The concentration of tRNA in two assays were 10, 15, 20, 25, 30 and 60 μM or 0.5, 5, 25, 50, 100 and 250 μM. The radioactivity of the final product was converted to moles of AMP incorporated by comparison to the radioactivity of an aliquot of labeled ATP with known specific activity (a sample calculation is shown in Appendix A). The initial velocity versus concentration of substrate tRNA was plotted by SigmaPlot or GraFit.

2.4.5 Activity assays at different pHs

S. cerevisiae CCA-adding enzyme was assayed under a variety of conditions to assess the requirements for optimal activity. To assay the effect of pH on wild-type enzyme activity, standard assay conditions described above were used except a three-component buffer of 50 mM MES, 50 mM MOPS and 100 mM diethanolamine (kindly provided by Dr. J. Turnbull) was used for pH values between 6.0 and 10. The pH of the buffer system was adjusted with KOH.

2.4.6 Comparison of wild-type and variant enzyme activities at 22°C

To compare the relative activities of wild-type and variant enzymes at room temperature, activity assays were carried out at 22°C under the standard assay conditions as described above. It was important that each reaction was sampled in the linear range

to compare relative activities. The comparison of relative activities was based on the linear range determined for variant E172K, which was established by optimizing the amount of enzyme and the assay time. Using a 5 min assay and keeping the glycine, $MgCl_2$, ATP, CTP and tRNA concentrations at standard levels with 0.285 μl [α -^{32}P] ATP while increasing the E172K protein concentration (150 ng, 300 ng, 600 ng, 1200 ng, or 1920 ng), the amount of enzyme required to keep the assays in the linear range could be determined. From this result, a time course could be produced using the appropriate amount of enzyme. Based on the conditions determined to define the linear range for E172K, amounts of variant enzymes E172H (1400 ng, 700 ng and 350 ng), E172F (1700 ng and 850 ng) and E172K (2400 ng and 1200 ng) were added to reaction mixtures with incubation at 22°C for 2 minutes to compare their relative activities.

2.4.7 Effect of elevated temperature (37°C) on enzyme activity

To determine the effect of 37°C temperature on enzyme activity, the enzyme was pre-incubated at 37°C for different times and the enzyme activity assay was carried out under the standard conditions described above (section 2.4.3) but at 37°C. The reactions were repeated for some of the variants using modified reaction conditions which showed activity at 22°C (section 2.4.6) but after pretreatment of the protein at 37°C.

2.5 Biophysical studies on the CCA-adding enzyme of *S. cerevisiae*

2.5.1 Far-UV circular dichroism spectroscopy

CD spectra in the far-UV region (200-250 nm) were recorded on a Jasco 710 spectropolarimeter under a constant nitrogen flow. The spectra were recorded in a 0.5 cm

cell using a protein concentration of 0.1-0.2 mg/ml in PBS buffer (pH 7.3), 0.2 nm step resolution, 20 nm/minute scan rate, 0.25 second response time, 1.0 nm bandwidth and accumulated over 5 scans. Buffer was scanned under the same conditions to define a baseline and CD signals of proteins were baseline subtracted using the Jasco standard analysis software.

2.5.2 Thermal denaturation of the enzyme monitored by CD spectroscopy

To investigate the thermal stability of the proteins, thermal denaturation was recorded by monitoring the changes in α-helices as a function of temperature. A 1 ml protein sample was placed in a 0.5 mm path length quartz cell. The change of CD signal at 222 nm as temperature increased from 20°C to 70°C was recorded. The rate of temperature increase was 30°C/h. Response time was 1 second and bandwidth was 1.0 nm. The thermal denaturation curves were constructed by conversion of the CD signal to the fraction of unfolded proteins and the transitional points of wild-type and variant proteins were calculated.

2.5.3 Fluorescence study

2.5.3.1 Intrinsic fluorescence of wild-type and variant enzymes

Intrinsic fluorescence of the proteins was measured on an SLM-2 Aminco Bowman Luminescence spectrophotometer. All samples were dissolved in 1X PBS and UV absorbance at 280 nm was used to determine the concentration of samples. All emission spectra were recorded with an excitation wavelength of 280 nm and an emission wavelength of 340 nm in the range between 300 and 400 nm with a scan rate of 1 nm/sec

and a 4 nm bandwidth. The excitation energy was 800-900V. PBS buffer was scanned under the same conditions to define a baseline and all of the spectra were baseline subtracted.

2.5.3.2 Effect of temperature on intrinsic fluorescence of wild-type and variant enzymes

To follow the possible tertiary structural changes at 37°C, intrinsic fluorescence emission spectra of samples at different time points at 37°C were recorded under the same conditions. The intensity and maximal emission wavelength at different time points were compared. Fluorescence spectra of wild-type and variant proteins also were recorded at 22°C and 37°C under the conditions described above. Because the intensity of fluorescence is temperature dependent, only the maximal emission wavelengths of the spectra at these two temperatures were compared. Emission spectra of buffer recorded at 22°C and 37°C under the same conditions were used for baseline correction.

2.5.3.3 Interaction of tRNA nucleotidyltransferase with substrate tRNA

The interaction of substrate tRNAs with tRNA nucleotidyltransferase can be monitored by intrinsic fluorescence quenching. The fluorescence of the protein samples was measured at 340 nm after excitation at 280 nm as described previously (section 2.5.3) except that the excitation bandwidth was 2 nm. Wild-type enzyme was titrated by the serial addition of 2 μl of 100 μM tRNAs into 1 ml protein sample (OD_{280}=0.05, 0.25 μM) in PBS buffer. Fluorescence titration spectra were recorded at 20°C after the serial addition of tRNAs for 2 minutes. As tRNAs absorb at the excitation wavelength (280 nm), the absorption of samples at 280 nm and 340 nm will be recorded and corrected for

the inner filter effect. PBS buffer (1 ml) was titrated with the same amount of tRNAs and the spectra of buffer titration were corrected for the inner filter effect and used as the baseline for corresponding protein-tRNA titration samples.

Fluorescence quenching was performed by adding 10 μl and 20 μl aliquots of tRNAs (2.5 μg/μl, 100 μM) into 1 ml of protein solution (OD_{280}=0.05, 0.25 μM) in PBS buffer. For the fluorescence spectra of protein alone, the spectrum of PBS recorded under the same conditions was used as background. However, for tRNAs quenched protein samples, the fluorescence spectrum of equal amounts of tRNAs alone in PBS buffer was used as background. Those spectra were corrected for the inner filter effect first, and then background subtracted to get the protein spectra quenched by tRNAs. Fluorescence emission spectra of proteins and proteins quenched by tRNAs were compared to see if the addition of tRNAs decreased the intensity of fluorescence spectra. The inner filter effect was corrected using this equation.

$$F_c=F_o \times (V_f/V_0)\times\text{antilog}((OD_{ex}+OD_{em})/2)$$

F_c and F_o refer to the corrected and observed fluorescence respectively; OD_{ex} and OD_{em} refer to the absorbance at excitation wavelength and at emission wavelength and V_f and V_0 refer to the volume of the solution after the addition of tRNAs and the initial volume.

2.6 H/D exchange and MALDI-ToF analysis

2.6.1 H/D exchange of tRNA nucleotidyltransferase and fragmentation by pepsin. (Mandell *et al.*, 1998)

To initiate the H/D exchange, 18 μl of 5 mM KH_2PO_4 buffer, in D_2O (pD7) was added to 2 μl protein (4 μg/μl), then the sample was incubated at room temperature for 30 min to permit H/D exchange. Next 40 μl 0.1% trifluoracetic acid (TFA) was added to

quench the exchange (decreasing pH to 2.5). As a control, 18 μl of 5 mM KH_2PO_4 buffer, in H_2O (pH7) were added to 2 μl protein and incubated and quenched in the same way. Deuterated buffer was prepared by drying 5 mM KH_2PO_4 buffer [pH6.6], in H_2O and resuspending the dried KH_2PO_4 sample in the same volume of D_2O. To investigate the thermally induced conformational changes, 2 μl of protein was incubated at 37°C for 30 min and labeled and quenched in the same way. Immobilized pepsin 10 μl (about 10 μg of pepsin, Pierce) was washed twice in a 1.5 ml Eppendorf tube with chilled 0.05% TFA by vortexing and subsequently centrifuged for 3 min at 10 000 g, then stored on ice. The quenched protein sample was added to the pepsin and digested for 5 min on ice with mixing by pipette continuously. The digested protein then was separated from the pepsin by centrifugation for 1 min at 14 000 g and the supernatant was transferred to a 0.5 ml Eppendorf tube. Samples were immediately frozen in liquid N_2 and stored at –80°C. All operations were conducted in the cold room after deuterium incorporation into the protein had been quenched.

2.6.2 Preparation of samples for MALDI-TOF MS (Mandell *et al.*, 1998)

The matrix solution was freshly prepared by dissolving α-cyano-4-hydroxycinnamic acid in a solution containing ratio (V/V/V) of 1:1:1 acetonitrile, ethanol, 0.1%TFA (pH2.5). The matrix (kindly provided by Dr. A. English) was centrifuged and kept on ice before use. Frozen samples were quickly thawed to 0°C. A 2 μl sample was mixed with 2 μl matrix solution, and 1 μl was spotted onto the chilled MALDI target (supplied by Dr. A. English). The target was placed under nitrogen flow to dry the spot in 2 minutes.

2.6.3 MALDI-TOF Mass Spectrometry

Micromass MALDI-ToF-LR with a flight tube length of 1.0 m (linear mode) or 2.3 m (reflectron mode) was equipped with a N_2 UV laser (337 nm wave length) and was set to deliver a pulse at a rate of 5 Hz, with 10 shots per spectrum for reflectron mode. Peptides were analyzed in positive ion mode with a pulse reflectron voltage of 2600 V. In reflectron mode, the reflectron voltage is 2000 V and the detector voltage is 1800 V, and accuracy is less than 100 ppm. Theoretical maximum resolution in reflectron mode is 10 000. Each spectrum represents the average of a minimum of 10 scans. External calibration for peptide detection was achieved using a mixture of angiotensin (MW 1296.5), renin (MW 1759.0) and ACTH (MW 2465.7). All standards were dissolved in 0.1% TFA to yield 10 pmol/μl. Three microliters of each peptide or protein standard solution was mixed with 9 μl of α–cyano-4-hydroxycinnamic acid and then 1 μl of this was spotted on the target plate. Data analysis software utilized was MassLynx 4.0 (MicroMass).

2.6.4 MW determination by Electrospray ionization mass spectrometry.

Wild-type protein was desalted using a NAP-10 column (Amersham Biosciences). Methanol and TFA were added to the protein solution to a final concentration of 0.1% to improve the efficiency of ionization. ESI was performed on a Q-ToF mass spectrometry (Micromass, Manchester, England) equipped with a Micromass electrospray ionization source. The instrument parameters were as follows: capillary voltage: 3500 V; cone voltage: 50 V; multiplier: 550V; MCP: 2200V; TOF: -9.1kV; source block temperature: 80°C; desolvation temperature: 30°C. Q-ToF instrument calibration was achieved using

Human [Glu1]-Fibrinopeptide B Human from Sigma (MW=1570). The average mass resolution is 8 000 and the accuracy for proteins at these conditions is less than 100 ppm.

3. RESULTS

3.1 Plasmid construction

The region of the *S. cerevisiae CCA1* gene (wild-type and various mutants) coding for the open reading frame from ATG3 of tRNA nucleotidyltransferase was PCR amplified from vector pDK200 (or derivatives) using primers to generate *Bam*HI and *Sal*I restriction sites. An aliquot of each PCR reaction was analyzed by 1% agarose gel electrophoresis and products corresponding to the expected size of the open reading frame (1557 bp) were observed (Fig.3-1).

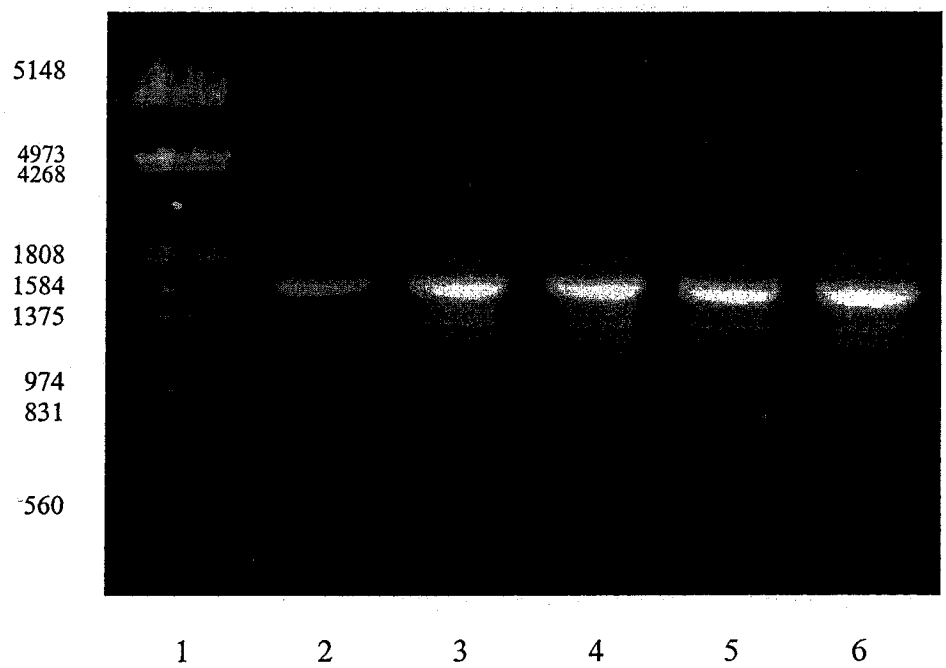

Fig. 3-1. Agarose gel electrophoresis of PCR products of amplification of *CCA1* wild-type and mutant genes. Lane 1 *Eco*RI-*Hin*dIII digested lambda marker DNA, lanes 2-6 PCR products generated from wild-type or mutant *CCA1* genes.

The PCR products were restriction digested with *Bam*HI and *Sal*I and ligated into the modified pGEX-2T expression vector (section 2.2) digested with the same enzymes.

After transformation into *E. coli*, the resulting colonies were screened by restriction digestion and the correct colonies were further characterized by DNA sequencing of the insert. All sequences were as expected with no unanticipated mutations arising.

3.2 Recombinant protein over-expression and purification

The five recombinant fusion proteins (E172, E172K, E172Q, E172H and E172F) were over-expressed and purified. The predicted size of the GST-fusion protein of *S. cerevisiae* tRNA nucleotidyltransferase is 84 KDa, which is in good agreement with what was seen on the gel (Fig. 3-2). The expression levels of the wild-type and variant proteins showed no major differences.

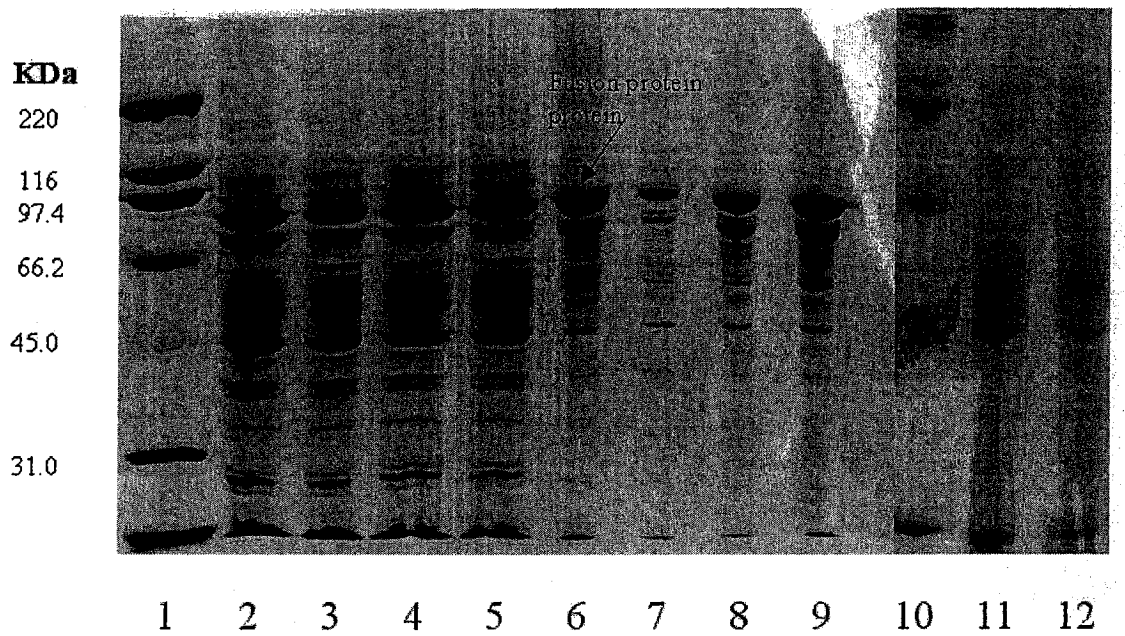

Fig. 3-2. Coomassie blue stained SDS-polyacrylamide gel of over-expression of glutathione S-transferase (GST) fusion proteins. Lanes 1 and 10 are Bio-Rad SDS-PAGE molecular weight standards (broad range). Soluble fusion proteins from overexpressing cells are shown in lanes 2, 3 (wild-type) and 4, 5 (E172H variant). Fusion proteins contained in the pellets from the same cells are shown in lanes 6, 7 (wild-type) and 8, 9 (E172H variant). Soluble proteins from cells carrying the wild-type gene but without induction are shown in lanes 11 and 12.

When proteins in the supernatant fraction were purified by affinity column chromatography using glutathione Sepharose 4B resin, fusion proteins eluted by 15 mM glutathione from the column showed approximately 80% purity as judged by SDS-PAGE (Fig. 3-3, lanes 3-8) although some other proteins also eluted under these conditions. When the GST-tag was cleaved from the fusion protein by thrombin protease on the column, a purified protein with a theoretical molecular mass of 60 782 Da (wild-type) should elute in the wash while the GST-tag, any remaining undigested fusion protein and any other proteins binding to the column should remain on the column. Although on-column cleavage could produce protein with higher purity (Fig. 3-4, panel A), the efficiency of thrombin cleavage was lower and the overall yield of protein was lower. It proved to be easier to control the digestion conditions and more efficient to cleave the GST tag in solution (Fig. 3-3, lane 2) such that the removal of GST-tag, any uncleaved protein, and any proteins that bind non-specifically to the column can be achieved by reloading the samples onto the glutathione column and collecting the flow-through (Fig. 3-5). The molecular mass of the wild-type enzyme was determined to be 60 784 D by ESI-Q-ToF mass spectrometry (Fig. 3-4, panel B), which is consistent with the theoretical molecular mass of 60 781.9 D.

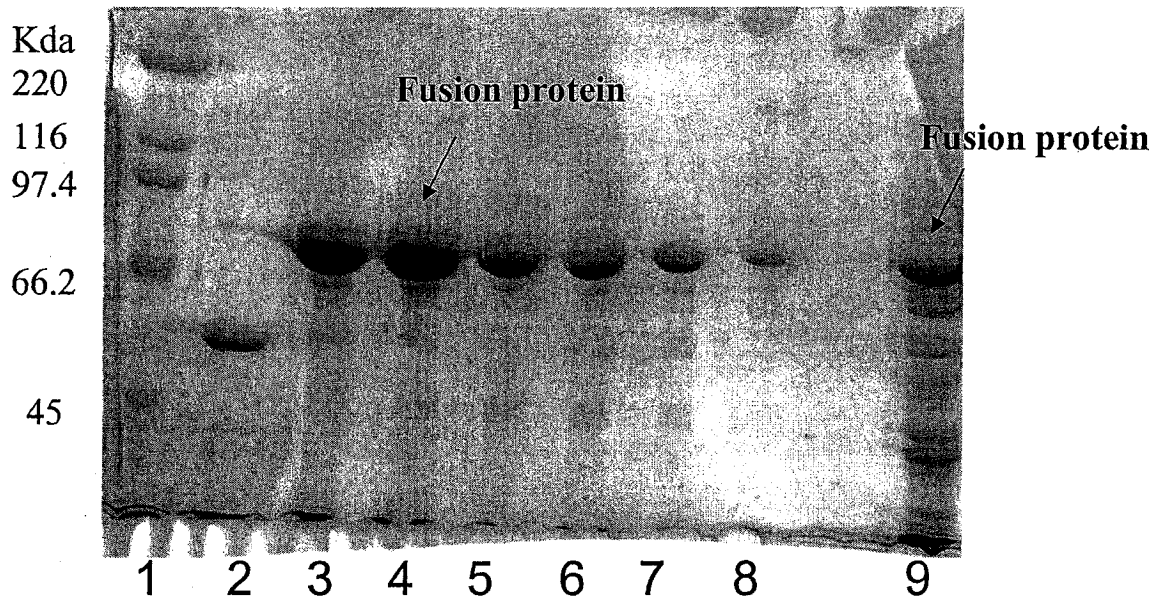

Fig. 3-3. Coomassie blue stained SDS-polyacrylamide gel of GST fusion protein purified by glutathione Sepharose 4B column. Lane 1 is the Bio-Rad molecular weight standard (broad range). Lane 2 is an aliquot of fusion protein digested with thrombin in solution. Lanes 3-8 are different fractions of the fusion protein eluted from the glutathione Sepharose 4B column using 15 mM glutathione buffer. Lane 9 is the flow through fraction of the crude supernatant after loading onto the glutathione Sepharose 4B column.

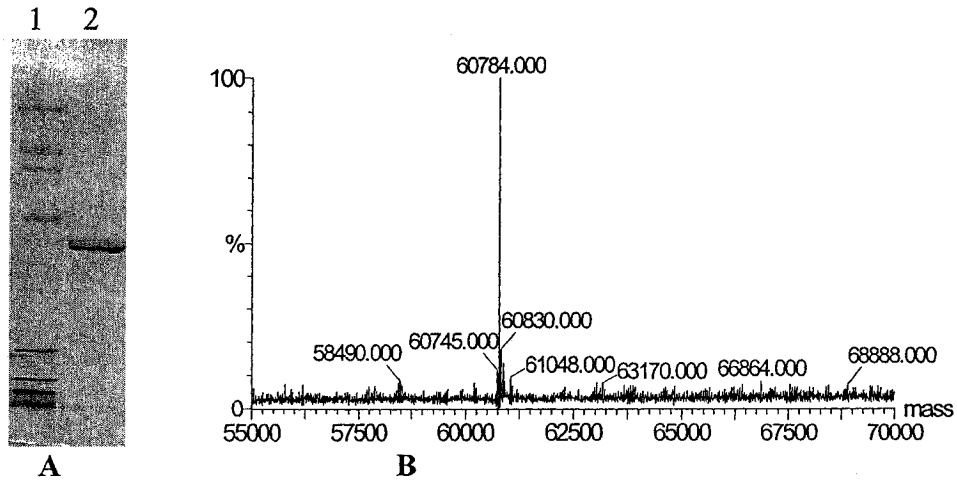

Fig. 3-4. Characterization of purified wild-type protein. (A) SDS-PAGE analysis. Lane 1: Bio-Rad broad range protein standard, Lane 2: wild-type protein with the GST-tag cleaved on column. **(B) ESI-Q-ToF mass spectrum of the purified protein**.

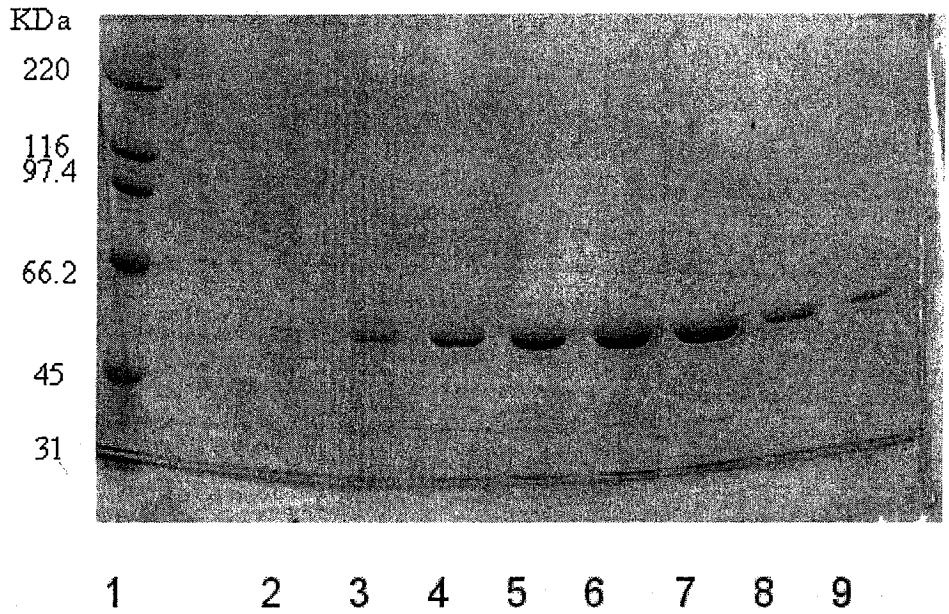

Fig. 3-5. SDS-polyacrylamide gel electrophoresis of purified protein. Lane 1 is the BioRad molecular weight standards (broad range). Lanes 2-7 are different fractions of tRNA nucleotidyltransferase with the GST-tag cleaved by thrombin in solution and removed by chromatography on glutathione column.

3.3 tRNA nucleotidyltransferase activity assay

3.3.1 pH profile

Wild-type enzyme was assayed over a wide pH range to optimize the assay conditions. Under standard conditions, the wild-type enzyme shows maximal activity at pH 10 and much lower activity at pH 7 (9 % of activity as compare to pH 10) (Table 3-1). These data were consistent with previous experiments showing maximal activity for CCA-adding enzymes at pH 9-10 (Deutscher, 1982).

pH	6	7	8	9	10
Relative activity (%)	3.16	8.76	11.01	26.35	100

Table 3-1. The relative activity of the wild-type CCA-adding enzyme at different pHs. Standard assay conditions were used except that a three-component buffer was used to change the pH.

3.3.2 Activity at room temperature

When activity assays of the wild-type and variant enzymes were carried out at 22°C under the standard assay conditions, the variants E172Q and E172H showed measurable but lower activity than the wild-type enzyme, while variants E172K and E172F showed almost no activity (Fig. 3-6).

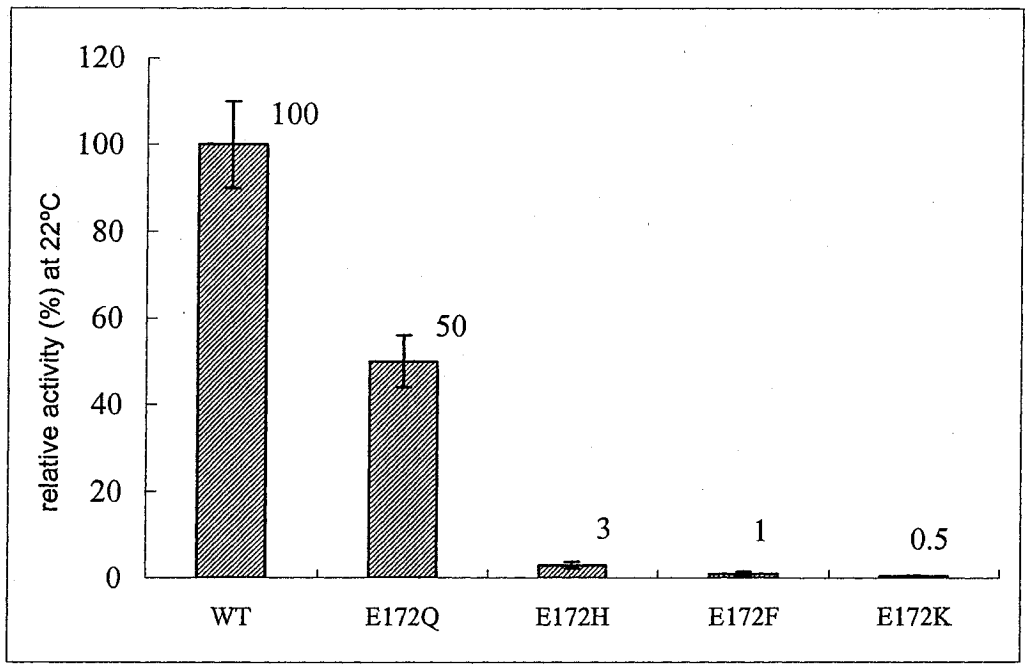

Fig. 3-6. The relative enzyme activity of wild-type and variant enzymes at 22°C. The assays were carried out under standard conditions and were terminated after 2 minutes. The number over each bar indicates relative activity as compared to wild-type taken as 100%.

Because the activities of the variant enzymes were lower under the standard assay conditions, increased amounts of enzymes were used in the activity assays to increase the activity to measurable levels. The amount of variant enzymes used to compare the relative activities was based on how much enzyme E172K can be used in the linear reaction range. First, the linear reaction range for E172K was determined by optimizing enzyme amounts and assay time. When the assay time was fixed at 5 minutes, this

reaction is in the linear range with up to 1920 ng enzyme under the conditions 1.0 mM ATP, 0.4 mM CTP, 20 μM tRNA (Fig. 3-7).

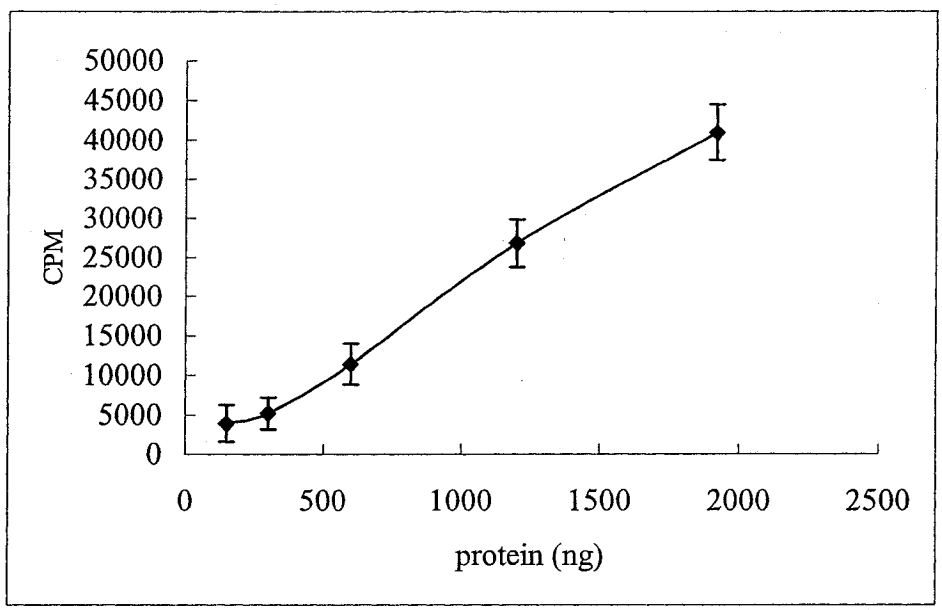

Fig. 3-7. Progress curve of product as a function of enzyme (E172K) amount. The assays were initiated by adding different amounts of enzyme E172K (150 ng, 300 ng, 600 ng, 1200 ng, 1920 ng) in 10 μl 1X PBS into a 90 μl reaction mixture giving final concentrations of 1.0 mM ATP, 0.4 mM CTP, 20 μM tRNA and 0.285 μl [α ^{32}P] ATP. The reactions were terminated after 5 minutes.

Based on this result, with the same substrate concentrations, 600 ng of enzyme were used to produce the time course (Fig, 3-8) and the assay was in the linear range for up to 20 minutes.

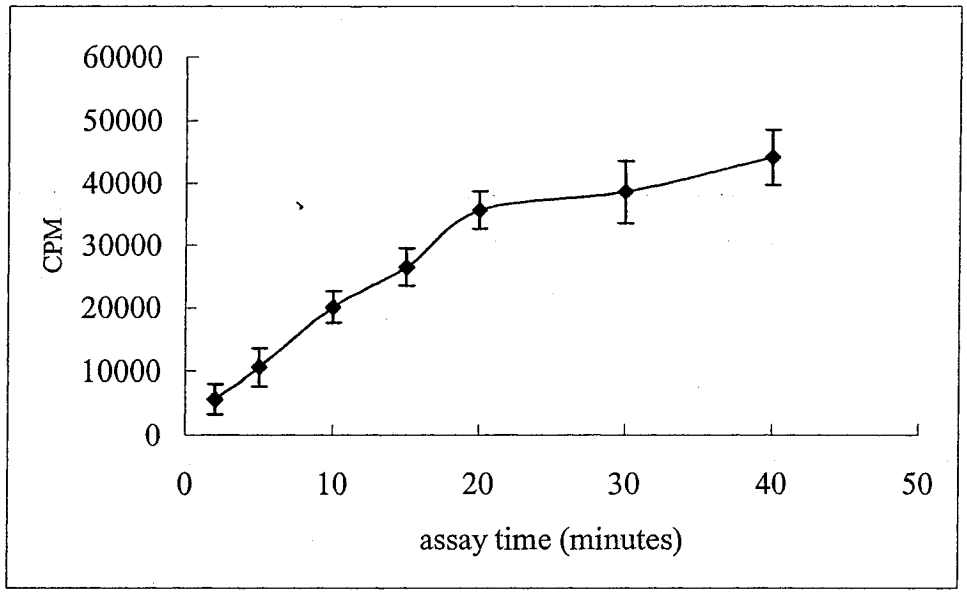

Fig. 3-8. Time course profile of enzyme (E172K) activity at 22°C. The assays were initiated by adding 600 ng of enzyme E172K in 10 μ 1X PBS into a 90 μl reaction mixture giving final concentrations of 1.0 mM ATP, 0.4 mM CTP, 20 μM tRNA and 0.285 μl [α ^{32}P] ATP.

The reaction for E172K was shown to be linear for up to 1920 ng protein with 5 minutes incubation or 600 ng protein with 20 minutes incubation with substrate concentrations of 1.0 mM ATP, 0.4 mM CTP and 20 μM tRNA. To compare the relative activity of the other variant enzymes to wild-type, the assay time was kept at 2 minutes and the enzyme amounts were 100 ng for wild-type and E172Q enzymes (based on the results of 3.3.4) while the amount of E172H was increased to 350 ng, 700 ng and 1400 ng, E172F was increased to 850 ng and 1700 ng, and E172K was increased to 1200 ng and 2400 ng. For variants E172H, E172F and E172K, the incorporation of AMP into substrate tRNA increased with the increasing enzyme amount used suggesting that the reactions are in their linear range (Fig. 3-9).

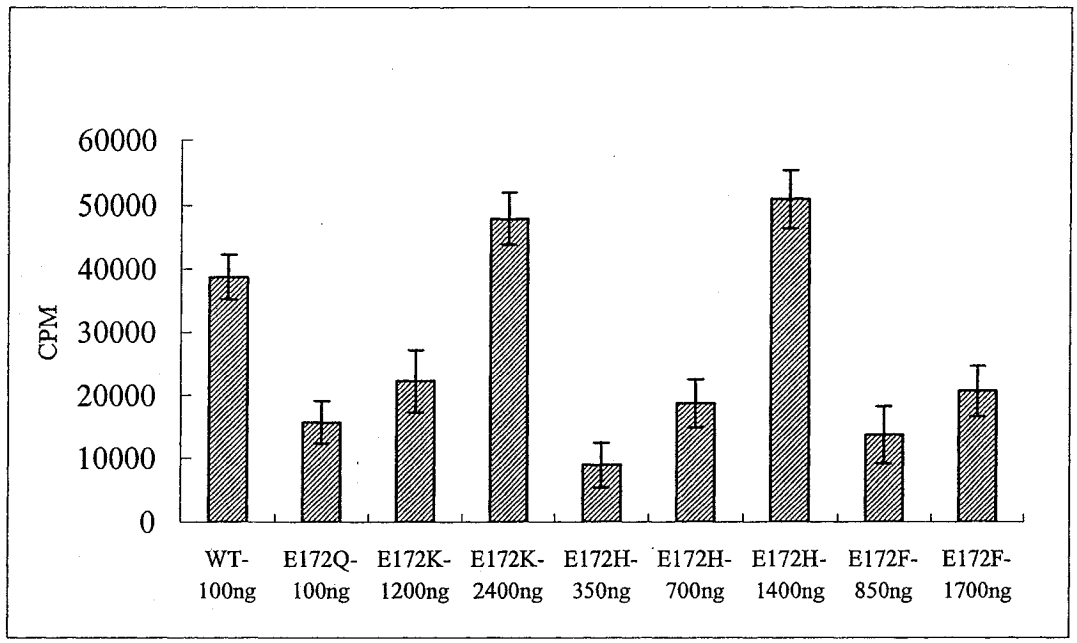

Fig. 3-9. Enzyme activity of wild-type and variant proteins at 22°C. Increasing amounts of enzymes were used in the activity assay. The assays were carried out for 2 minutes under the conditions 1.0 mM ATP, 0.4 mM CTP, 20 μM tRNA and 0.36 μl [α -P^{32}] ATP.

The activities of the enzymes were converted to specific activity (×μmol/min.mg) (sample calculation of specific activity determination is shown in Appendix A) and show the wild-type enzyme as the most active, followed by variants E172Q and E172H with E172F and E172K having the lowest specific activity (Fig. 3-10). The specific activities of the E172Q and E172H variants are 40% and 7% of the wild-type enzyme, respectively while the specific activities of the E172F and E172K variants are only 4-5% of the wild-type enzyme.

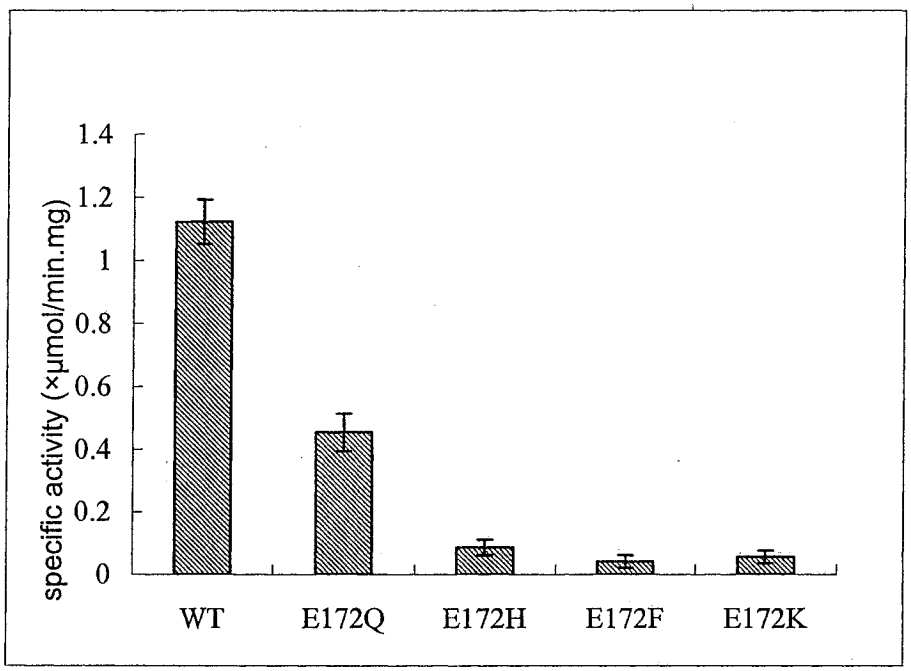

Fig. 3-10. Specific activities of wild-type and variant enzymes at 22°C.

3.3.3 Effect of elevated temperature (37°C) on enzyme activity

To investigate the effect of elevated temperature (37°C) on enzyme activity, wild-type enzyme and variants E172H and E172K were incubated at 37°C for different time points and assayed under standard conditions but at 37°C. Under standard conditions the wild-type enzyme showed increased activity at 37°C as compared to 22°C when the protein was assayed without pretreatment at 37°C. However, the activity at 37°C decreased with the increase of pre-incubation time at 37°C (Fig. 3-11). Even pre-incubation for 1 minute at 37°C caused the activity of the wild-type enzyme to drop to 75% of its initial activity at 37°C. Incubation for longer times at 37°C led to an increased loss of activity.

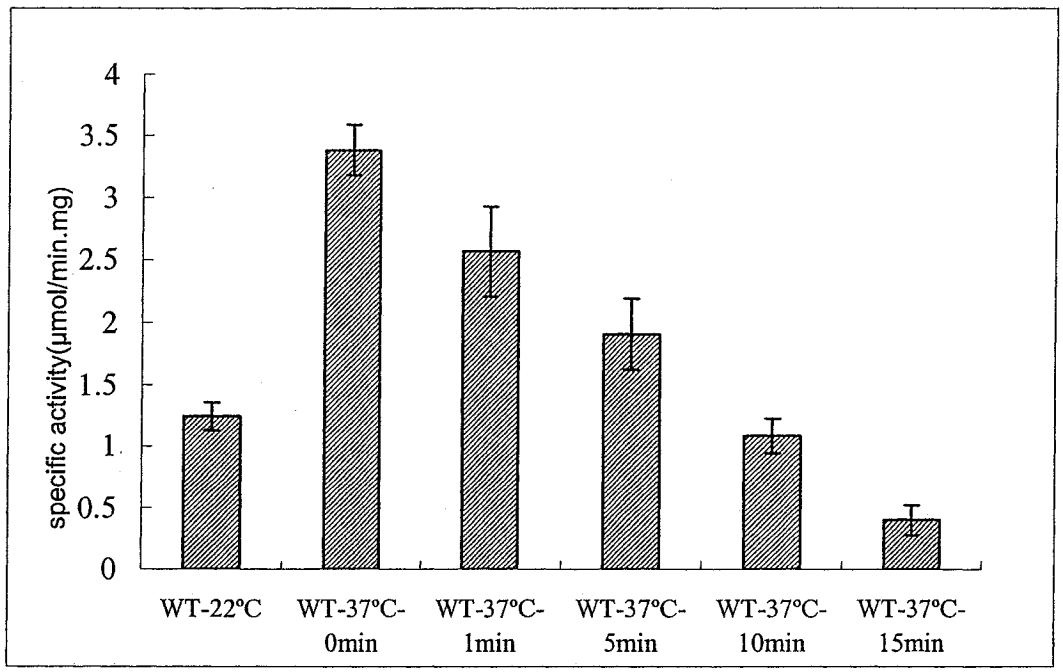

Fig. 3-11. Effect of elevated temperature (37°C) on enzyme activity. Wild-type enzyme pre-incubated at 37°C for 0, 1, 5, 10 and 15 minutes and assayed under the standard conditions but at 37°C for 2 minutes.

When assayed at 37°C under the standard conditions variants E172H and E172K showed no activity even without any pre-incubation at 37°C (data not shown). By increasing the amount of variant enzyme in the assay by 20 fold (2000 ng) for E172K and 17 fold (1700 ng) for E172H, the variants could be shown to have activity at 37°C although even with no pre-incubation they showed less activity at 37°C than they did under the same conditions when assayed at 22°C (Fig. 3-12). Pre-incubation at 37°C for only 1 minute almost completely eliminated the activity of the variant enzymes and increasing the incubation time does not lead to any additional obvious decrease in activity (Fig. 3-12). The specific activities of the variant enzymes at the non-permissive temperature are very low as compared to wild-type. (Compare Fig. 3-11 and Fig. 3-12, note scale on Y axes).

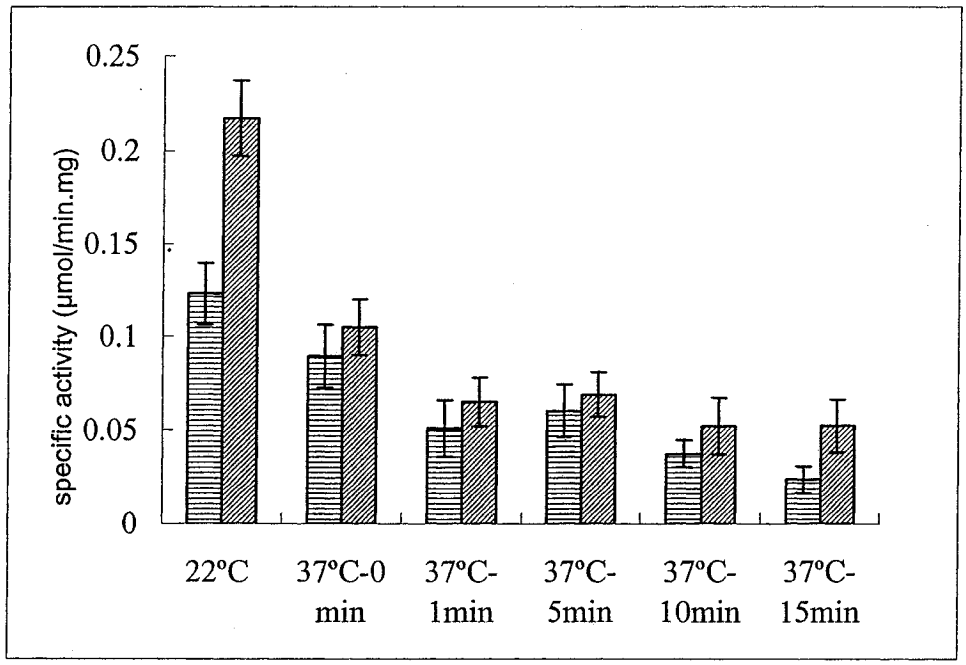

Fig. 3-12. Effect of elevated temperature (37°C) on the activity of variants E172K and E172H. Enzyme was pre-incubated at 37°C for 1, 5, 10, 15 minutes and assayed under the standard conditions but at 37°C with 20 fold excess of enzyme E172K (▤) or 17 fold excess of enzyme E172H (▨).

Assay Temperature	Pre-incubation at 37°C	Specific activity (µmol/min.mg)		
		WT	E172K	E172H
22°C	–	1.25	0.106	0.217
37°C	0 min	3.38	0.072	0.105
	1 min	2.57	0.059	0.065
	5 min	1.91	0.041	0.068
	10 min	1.09	0.036	0.052
	15 min	0.40	0.017	0.052

Table 3-2. Specific activities at 22°C and 37°C for wild-type and E172K and E172H variant enzymes.

For the wild-type enzyme there is an increase in specific activity at the higher temperature. The increase is maintained for up to almost 10 minutes at 37°C, but is reduced over time such that even after one minute pre-incubation, the specific activity

drops to 75% of its specific activity at 37°C but without pre-incubation. In contrast, with the variant enzymes there is no increase in specific activity at the elevated temperature and, in fact, even without pre-incubation there is a decrease in the specific activity of these two enzymes.

3.3.4 Linear reaction range of wild-type tRNA nucleotidyltransferase

Under the standard conditions except with 40 μM tRNA, different amounts of wild-type enzyme (see material and methods) in 10 μl 1X PBS were added into a 90 μl reaction mixture and the activity assay was carried out for 10 minutes at room temperature. The number of counts per minute generated by the radiolabelled tRNA products was plotted as a function of the amount of enzyme used in the assay (Fig. 3-13). Under the same conditions but using 10 μM tRNA and keeping the enzyme amount constant at 30 ng, the activity assay was carried out for 1, 3, 5, 7, 9, 12 minutes to define a time course (Fig. 3-14).

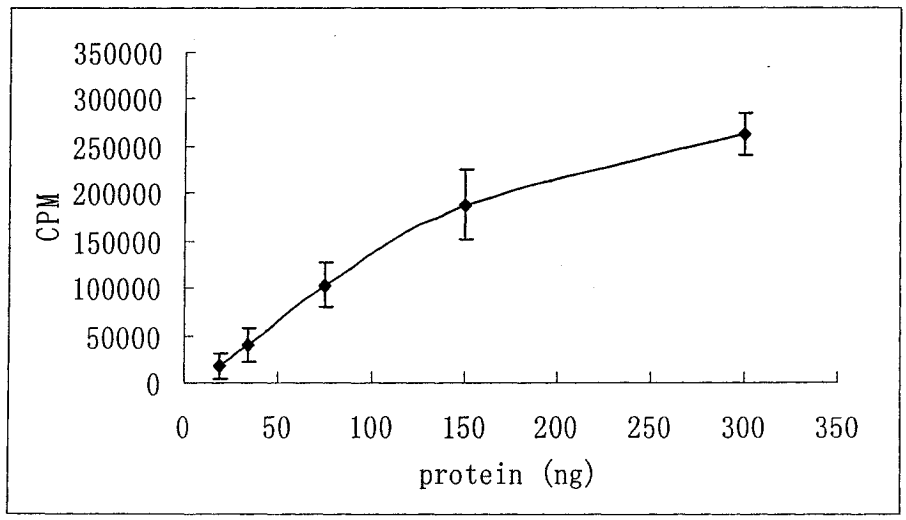

Fig. 3-13. Optimizing enzyme amounts used in the study of the kinetic mechanism. The assay conditions are 1.0 mM ATP, 0.4 mM CTP, 0.25 μl [α ^{32}P] ATP and 40 μM tRNA, various amounts of enzyme were added and assayed for 10 minutes at 22°C.

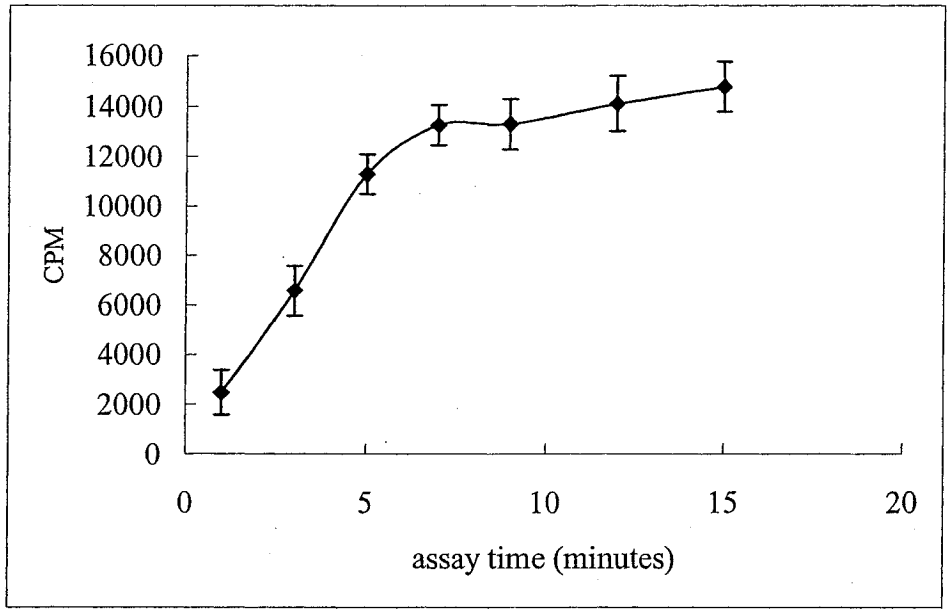

Fig. 3-14. Optimizing the assay time used in kinetic mechanism studies. The assay conditions are 1.0 mM ATP, 0.4 mM CTP, 0.25 μl [α ^{32}P] ATP and 10 μM tRNA, 30 ng enzyme were used and samples were taken at the indicated time points.

3.3.5 Measuring the initial velocity

Under standard conditions (section 2.4.3), the reaction catalyzed by wild-type enzyme was linear for up to 5 minutes and 150 ng of protein (Fig. 3-13, 3-14). Based on these experiments, 140 ng of enzyme were used in the kinetic analyses with a reaction time of 2 minutes. When the kinetic assay was carried out in the range of 0.5 to 250 μM tRNA, the velocity versus substrate graph (Fig. 3-15) suggests Michaelis-Menten kinetics. From this a K_m for tRNA (10.9 μM) and V_{max} (2.36 μmol/min.mg) for the reaction were calculated. When the assay was carried out using tRNA concentrations at smaller increments (10, 15, 25, 30, 60 μM), the velocity versus substrate concentration graph (Fig. 3-16) did not appear to follow standard Michaelis-Menten kinetics, but seems to fit better

to the Hill equation, so an apparent $K_{0.5}$ value for tRNA was determined by fitting initial velocities versus tRNA concentrations (10 μM to 60 μM) to the Hill equation (Fig. 3-17). From the data analysis of those experiments, kinetic constants of the wild-type enzyme are $K_{0.5}$ app (μM) $= 16.5 \pm 1.0$, V_{max} app ($\times 0.1$ μmol/min.mg)$= 9.2 \pm 0.5$ and $n=2.8 \pm 0.4$.

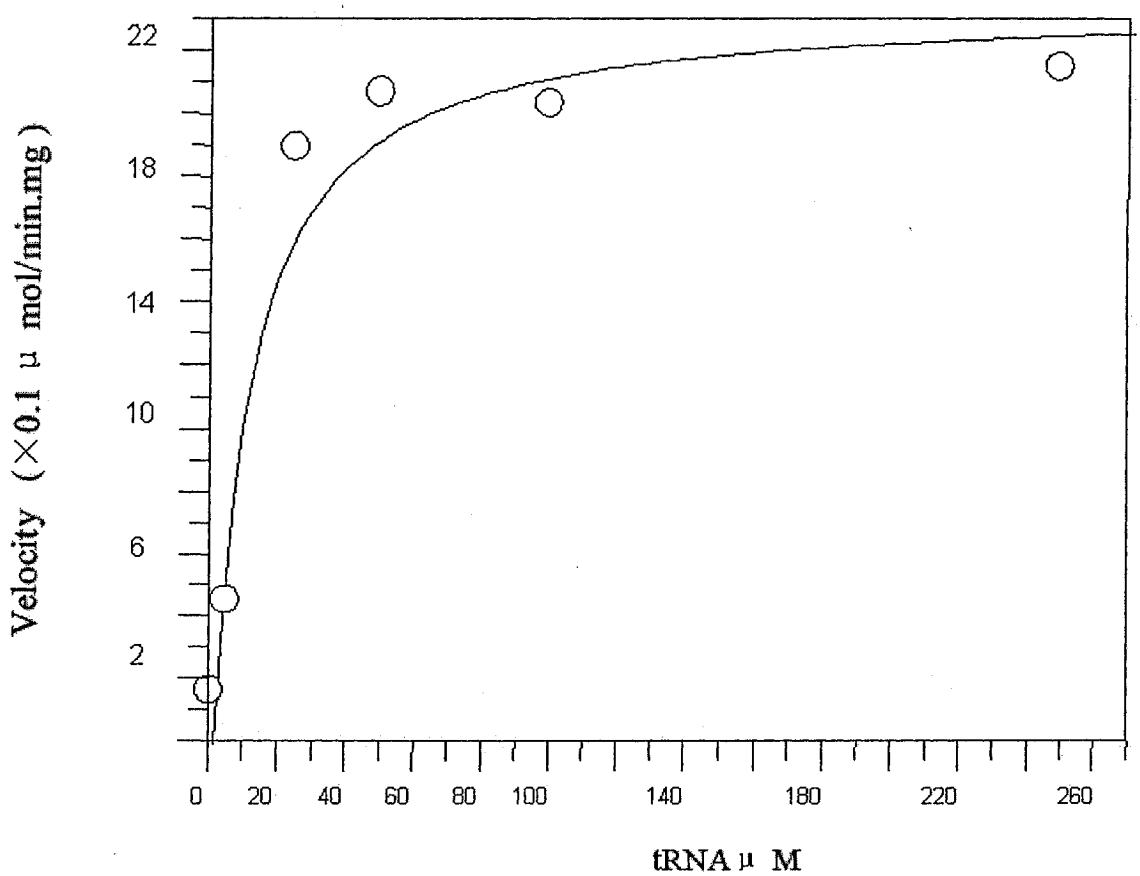

Fig. 3-15. Substrate saturation curve for tRNA. The dots represent velocity at specific tRNA concentrations in the range 0.5, 5, 25, 50, 100, 250 μM while the line represents a fit to the Michaelis-Menten equation.

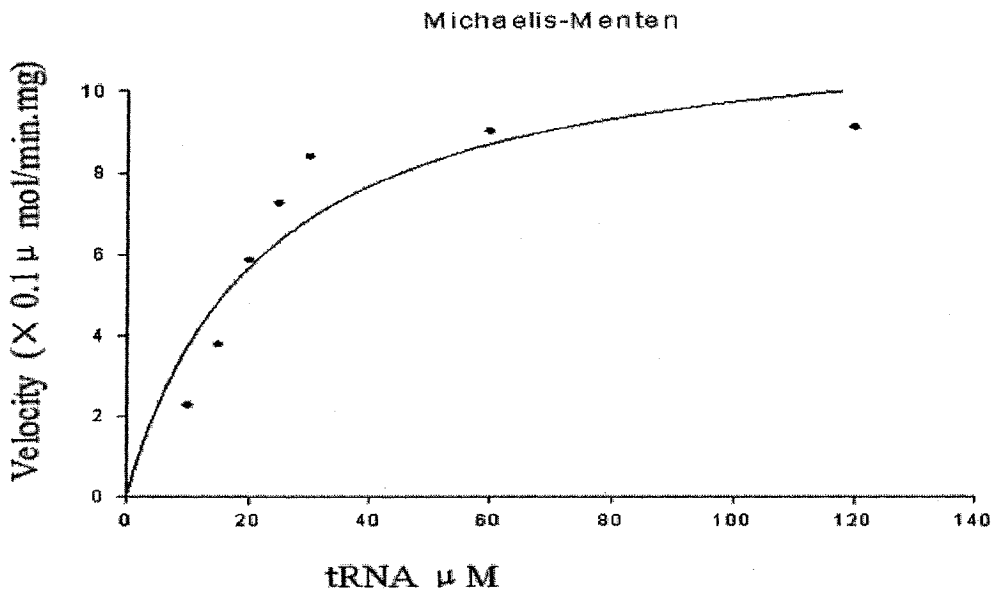

Fig. 3-16 The substrate saturation curve for tRNA was fit to the Michaelis-Menten equation. The dots represent velocity at specific tRNA concentrations in the range 10, 15, 25, 30, 60 μM while the line represents a fit to the Michaelis-Menten equation.

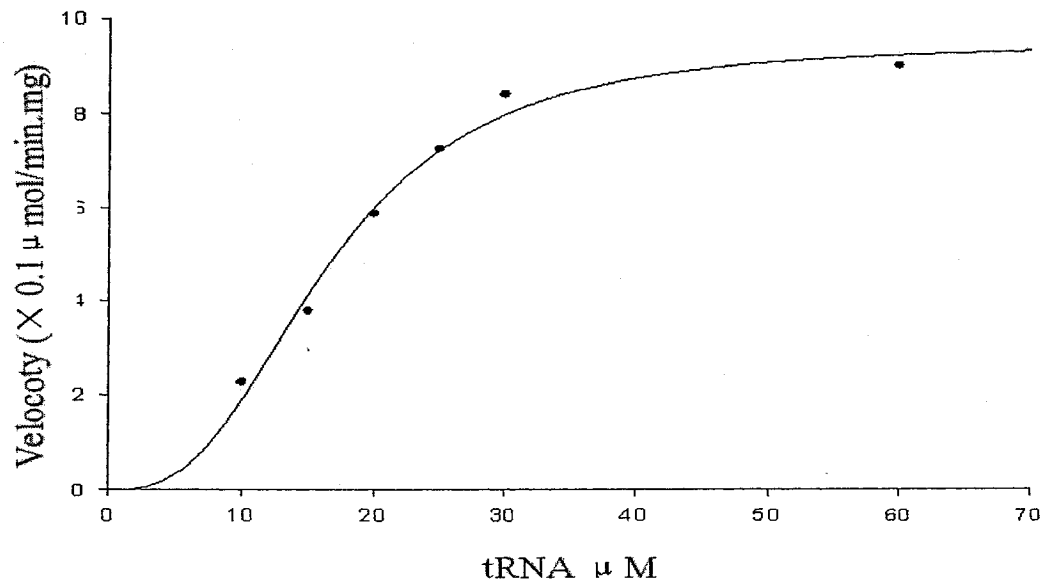

Fig. 3-17. Substrate saturation curve for tRNA was fit to Hill equation. The dots represent velocity at specific tRNA concentrations in the range 10, 15, 25, 30, 60 μM while the line represents a fit to the Hill equation.

3.4 Biophysical study of tRNA nucleotidyltransferase

3.4.1 Secondary structural features

The secondary structure of variant and wild-type proteins was detected using peptide bond (far-UV) circular dichroism (CD) at 22°C. The far-UV CD spectra of all of the proteins are virtually indistinguishable and dominated by typical α-helix structures with two reasonably intense negative bands at 208 nm and 222 nm (Fig. 3-18).

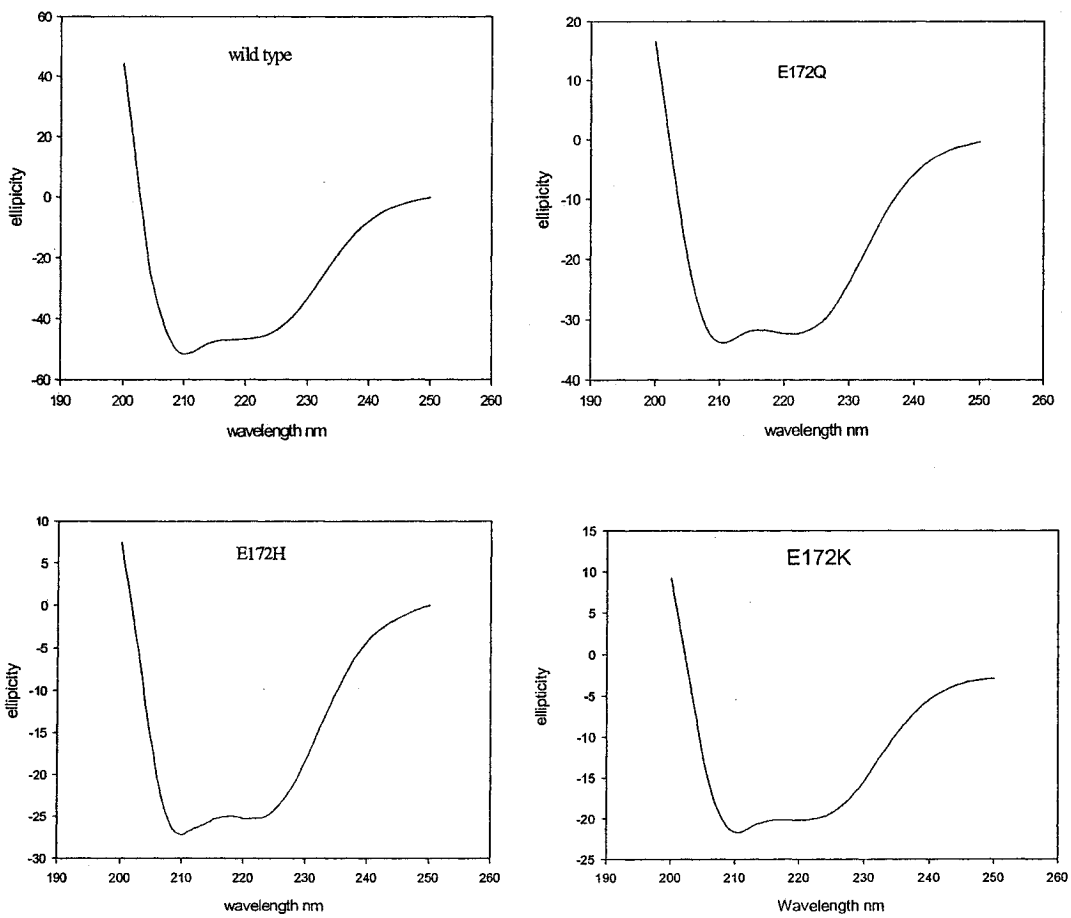

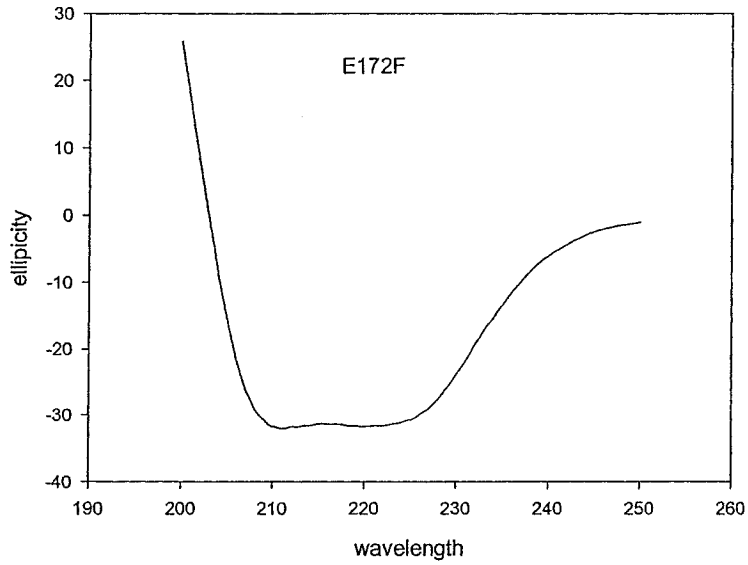

Fig. 3-18. The far-UV CD spectra of wild-type and variant proteins. Protein samples were scanned in 1X PBS with 5 accumulations.

All of the proteins exhibit similar far-UV spectra at 22°C, indicating that these mutations at position 172 have no detectable effect on the secondary structure of the protein.

3.4.2 Temperature-induced denaturation of wild-type and variant proteins

To investigate the thermal stability of the secondary structure, thermal denaturation was recorded by monitoring the changes in α-helices as a function of temperature using circular dichroism spectroscopy (Fig. 3-19). As denaturation takes place, a progressive loss of secondary structure occurs. The melting temperature (T_m) indicates the temperature at which 50% of the secondary structure is lost. Based on the thermal denaturation curves, the transitional points of wild-type and variant proteins were calculated (Table 3-3). The wild-type protein and variant proteins E172H and E172Q have similar transitional temperatures while E172F and E172K are less thermally stable

with lower transitional temperatures (Fig. 3-19). As an indication of the remaining secondary structure at 37°C, the ellipicity θ_{222} at 37°C as compared to ellipicity θ_{222} at 22°C was calculated (Table 3-4). While the wild-type, E172H and E172Q variant proteins maintain a high level of secondary structure; the E172K and E172F variant proteins have lost approximately half of their secondary structure at 37°C as defined by this parameter.

Using the parameters described in materials and methods, the process of thermal denaturation took a total of 90 minutes so that the proteins were exposed to high temperature for a long time. The spectra of the denaturated proteins after cooling to room temperature were similar to those of denaturated proteins at high temperature (data not shown) suggesting that thermal denaturation is not reversible.

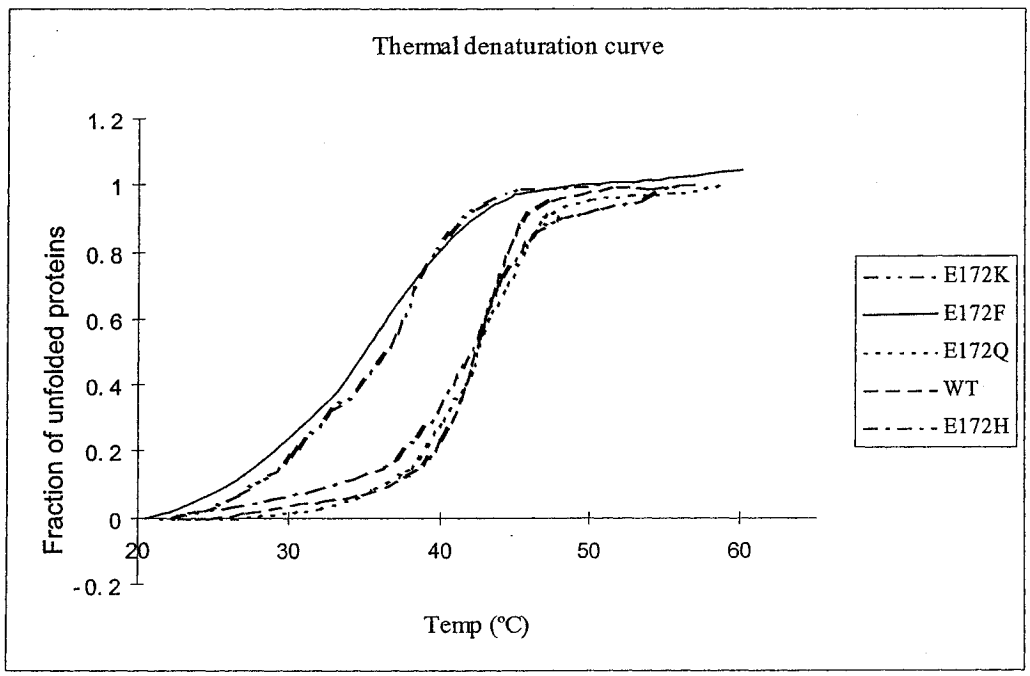

Fig. 3-19. Thermal denaturation curves of wild-type and variant proteins. Ellipicity θ_{222} was monitored as a function of temperature between 20°C and 60°C. The fraction of unfolded protein was used to construct the thermal denaturation curve.

Protein	WT	E172Q	E172H	E172K	E172F
Tm (°C)	42.5±0.4	42.8±0.5	41.7±0.4	36.5±0.4	36±0.4

Table 3-3. Transitional points of wild-type and variant proteins obtained from the thermal denaturing curves.

Protein	WT	E172Q	E172H	E172K	E172F
% of θ_{222} at 37°C	90	89	88	51.4	52.9

Table 3-4. Ellipicity (θ_{222}) at 37°C as compared to 22°C, representing the remaining secondary structure at 37°C during the thermal denaturation.

3.4.3 Fluorescence spectra of wild-type and variant proteins at 22°C

The fluorescence spectra of wild-type and variant proteins were recorded and normalized spectra were compared (Fig. 3-20). Even at room temperature, the maximal emission wavelength of the variant proteins shows a red-shift as compared to the wild-type protein.

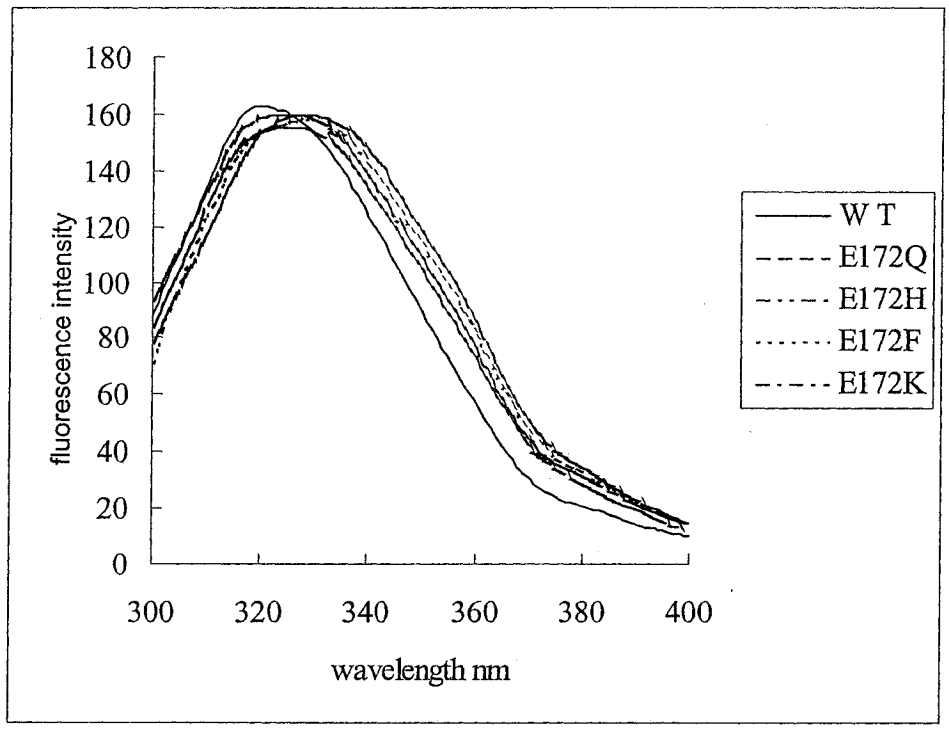

Fig. 3-20. Comparison of emission spectra of the wild-type and variant proteins at 22°C.

3.4.4 Monitoring thermal denaturation by fluorescence spectroscopy

To investigate the possible change in conformation caused by thermal denaturation, protein fluorescence spectra were recoded at 37°C at different incubation times for the wild-type enzyme and the E172Q, E172H and E172K variants (Fig. 3-21). For all proteins, the fluorescence intensity decreased and the maximal wavelength shifted to the red with the increase of the incubation time. For the wild-type protein, the maximal wavelength did not shift in the first 2 minutes even though the fluorescence intensity decreased. For the other variants, the red-shift occurred immediately once the proteins were added into the 37°C buffer (Fig. 3-21). When these data are presented as wavelength of maximum fluorescence intensity as a function of time (Fig. 3-22), it is

clear that the rate of red shift for the wild-type protein is much slower than for the other proteins. By approximately 20 minutes the wavelength of maximum fluorescence has plateaued for the wild-type enzyme suggesting that any changes in tertiary structure have stabilized at this point. In contrast, the E172Q, E172H and E172K variant proteins show a very rapid shift in wavelength of maximum fluorescence within the first few minutes. By 5 minutes the E172Q and E172H variants have reached a plateau with respect to wavelength of maximum fluorescence while the wavelength of maximum fluorescence for the E172K variant enzyme continues to rise for as long as data were collected (25 minutes). These data suggest that the E172Q and E172H variant proteins denature rapidly at 37°C, but only to a certain extent while the E172K variant denatures rapidly and continues to denature to an even greater degree.

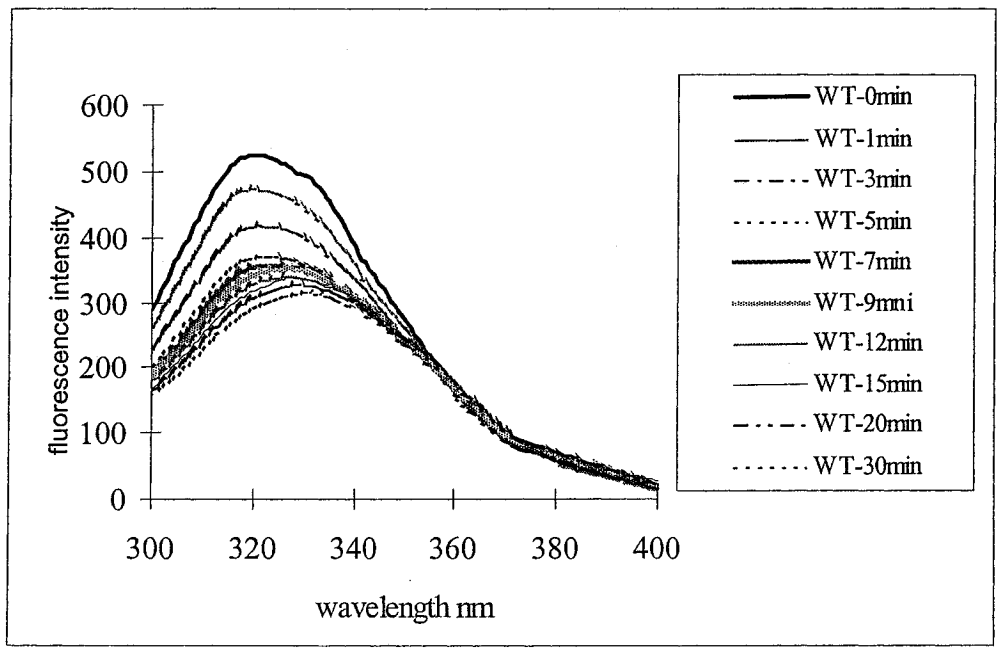

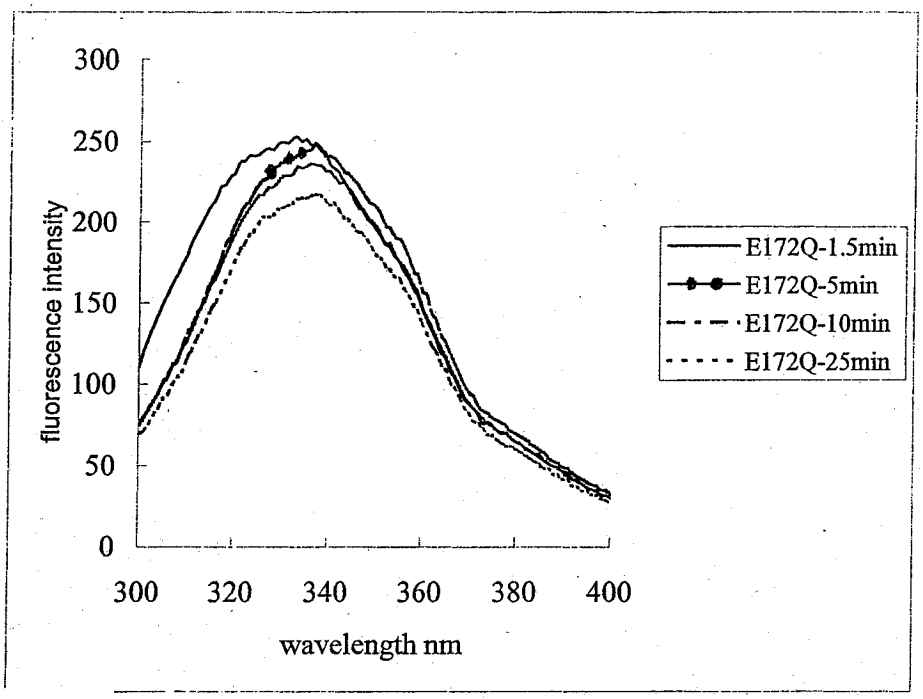
300
250
200
150
100
50
0
fluorescence intensity
300
320
340
360
380
400
wavelength nm
E172Q-1.5min
E172Q-5min
E172Q-10min
E172Q-25min

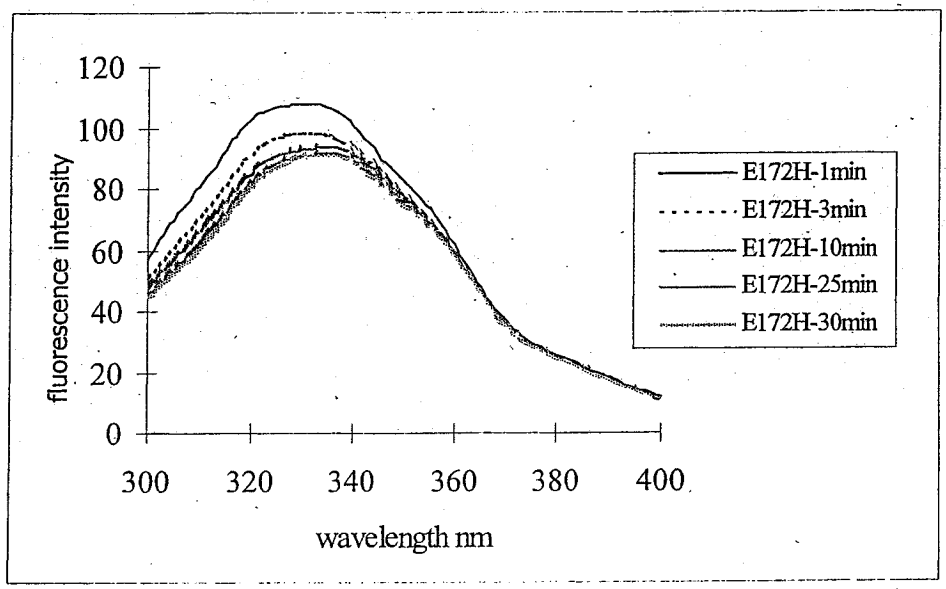
120
100
80
60
40
20
0
fluorescence intensity
300
320
340
360
380
400
wavelength nm
E172H-1min
E172H-3min
E172H-10min
E172H-25min
E172H-30min

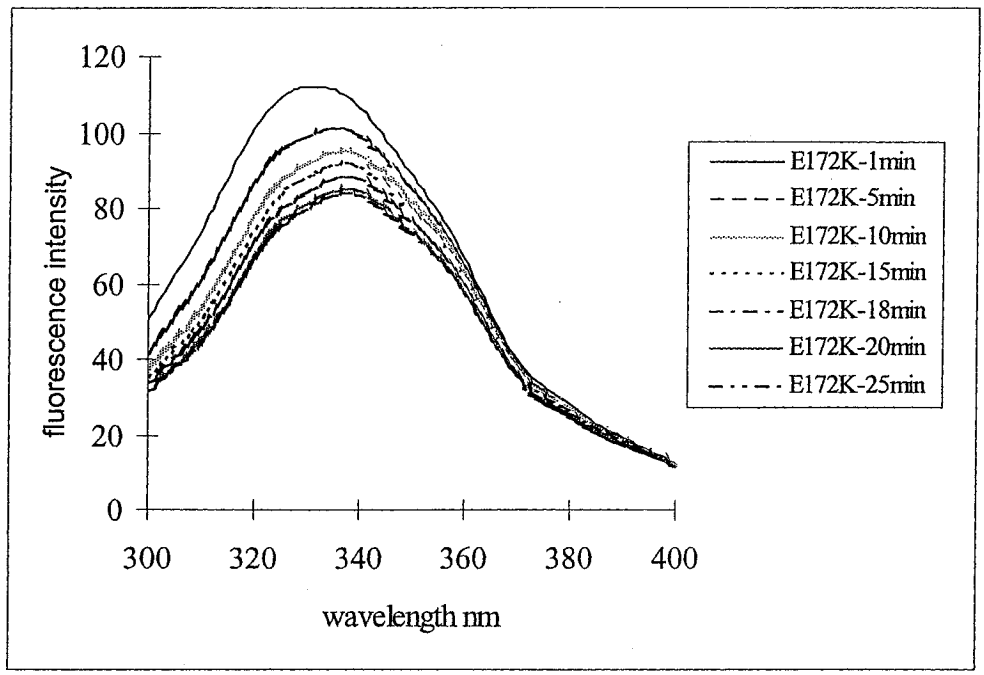

Fig. 3-21. Monitoring thermal denaturation by fluorescence spectroscopy. All the fluorescence emission spectra were recorded at 37°C after different incubation times at 37°C.

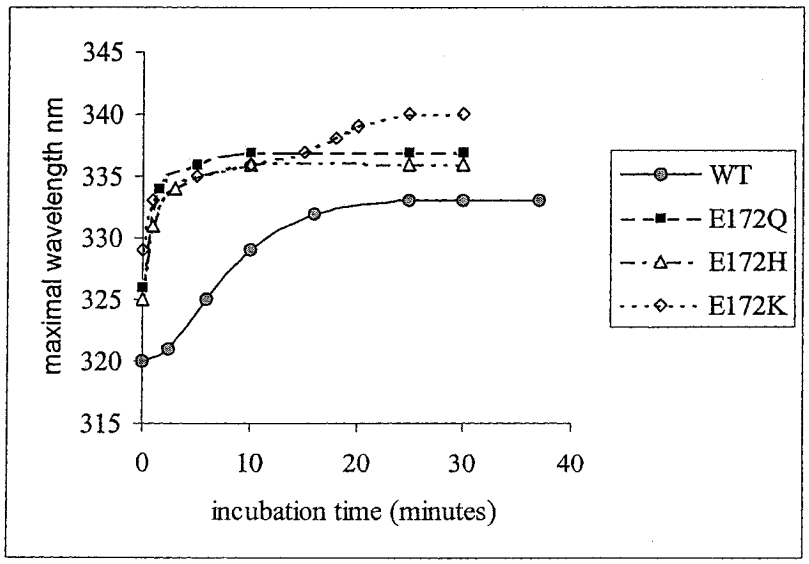

Fig. 3-22. The maximal emission wavelength varied with the pre-incubation time at non-permissive temperature.

After 30 minutes at 37°C, continued incubation did not result in an additional red shift of the spectra. So, under the conditions described in materials and methods, fluorescence spectra were measured at 22°C for proteins pre-incubated for 30 min at 22°C or at 37°C. The maximal peak emissions from the wild-type and variant proteins at the two temperatures were compared (Fig. 3-23). The E172F and E172K variants show the greatest emission shift to higher wavelengths (Fig. 3-23, Table 3-5) upon incubation at the higher temperature.

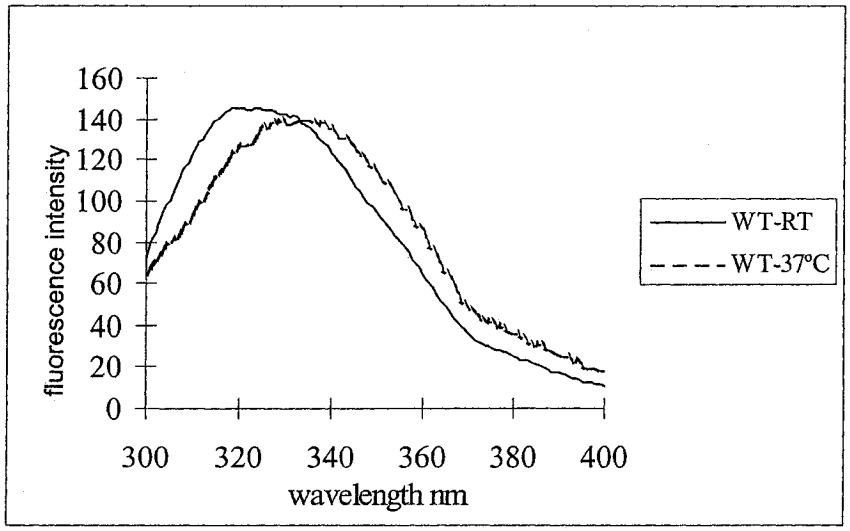

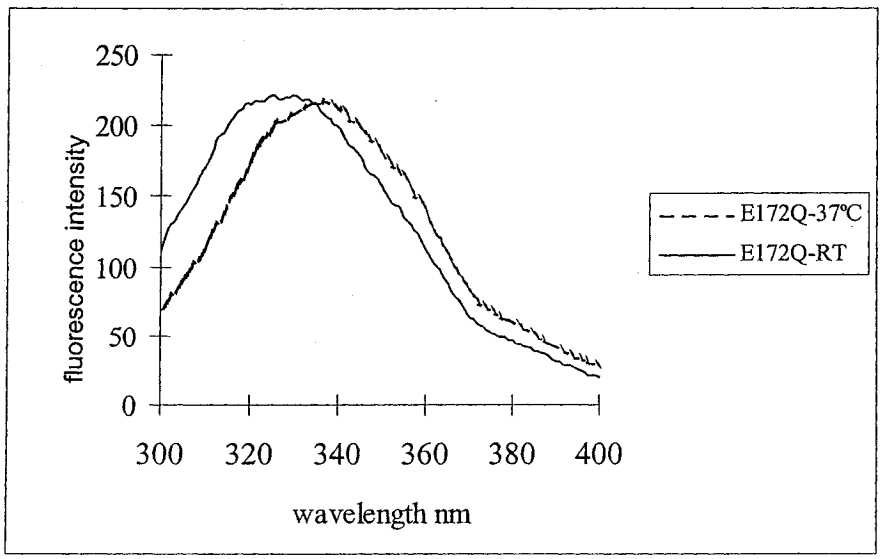

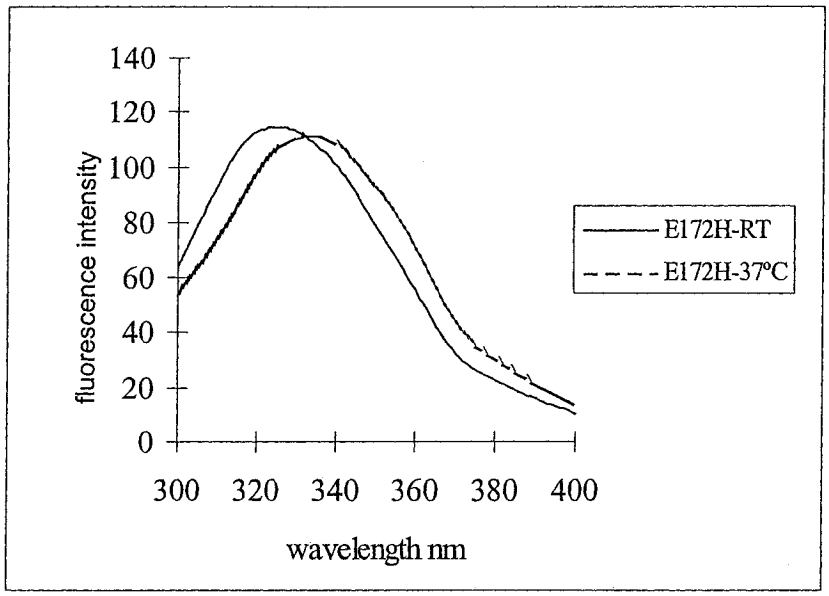
140
120
100
80
60
40
20
0
fluorescence intensity
300
320
340
360
380
400
wavelength nm
E172H-RT
E172H-37°C

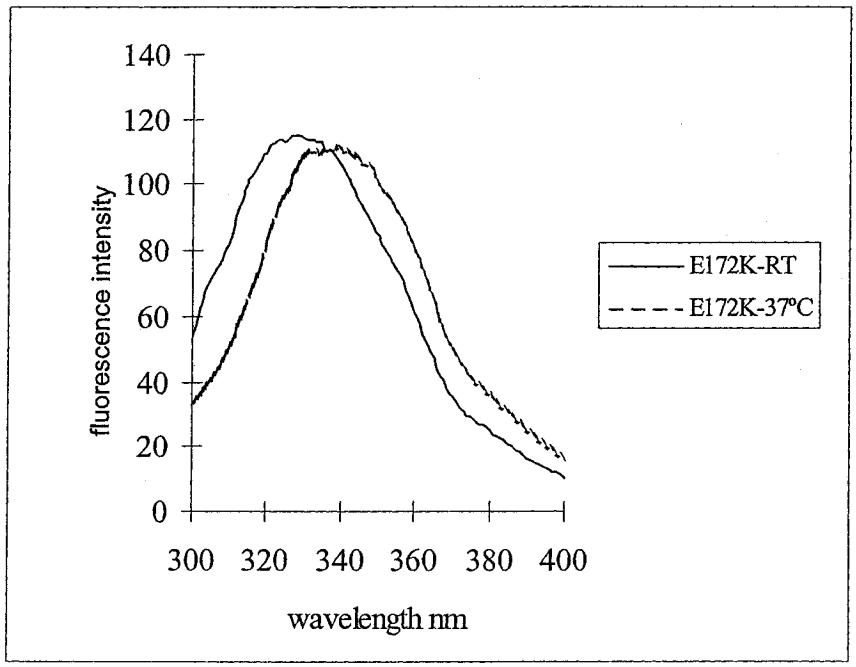
140
120
100
80
60
40
20
0
fluorescence intensity
300
320
340
360
380
400
wavelength nm
E172K-RT
E172K-37°C

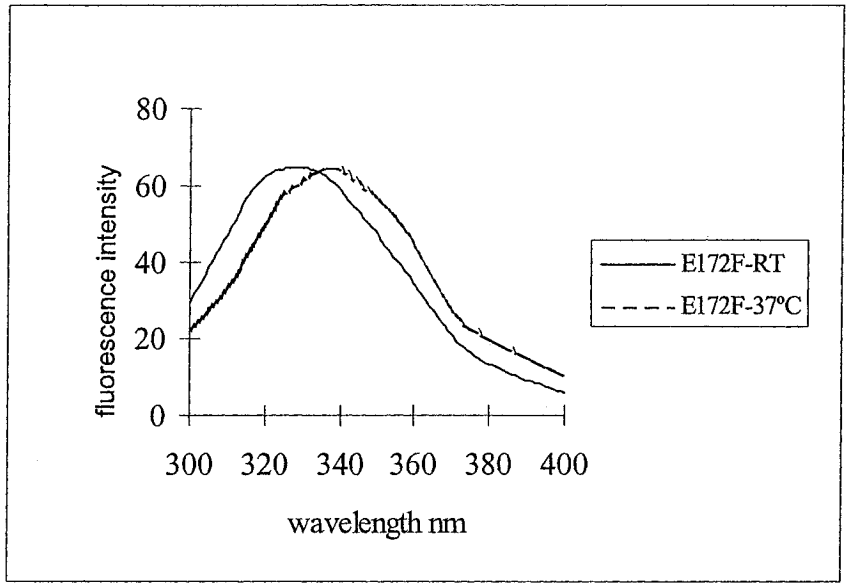

Fig. 3-23. Comparison of fluorescence spectra of enzymes at 22°C and 37°C. The spectra were normalized to compare the maximal emission wavelength.

Protein	Wild-type	E172Q	E172H	E172F	E172K
λmax (nm) at 22°C	320	326	325	328	329
λmax (nm) at 37°C	334	336	336	338	340
Δλmax (nm)	14	10	9	10	11

Table 3-5. The maximal wavelength of fluorescence emission of wild-type and variant proteins at 22°C and 37°C as well as the changes in λ max between the two temperatures.

3.5 Mass spectrometry analysis of tRNA nucleotidyltransferase

3.5.1 Peptide Mass Fingerprinting (PMF)

Peptic peptides from wild-type tRNA nucleotidyltransferase were analyzed by MALDI-ToF. Twenty-one out of thirty-seven peptic peptides covering 35% of the sequence of the protein were identified (Table 3-6) by ExPASy-PeptideMass or ExPASy-FindPept (http://ca.expasy.org/).

MH^+ (observed)	Position	Sequence	Method to identify
741.41	213-218	KSKHLE	PeptideMass
749.41	505-509	IRWQF	PeptideMass
768.51	272-277	ENVIFF	PeptideMass
790.37	49-55	TGGWVRD	FindPept
817.55	22-28	QNICNLL	PeptideMass
820.46	60-67	LGQGSHDL	PeptideMass
849.43	405-411	KFADRSQ	PeptideMass
896.52	210-216	IRFASRF	PeptideMass
949.52	140-147	SRIPKVCF	PeptideMass
989.52	331-339	KIGRSPGFQ	PeptideMass
994.47	509-517	FDNPTGTDQ	PeptideMass
1157.66	36-44	NQKYHNKPE	PeptideMass
1365.69	277-287	FWHNDSSVVKF	PeptideMass
1373.79	238-249	NSKISRERVGVE	PeptideMass
1462.79	140-152	SRIPKVCFGTPEE	PeptideMass
1516.83	431-444	AHFASLSDAFLKIP	FindPept
1744.96	341-356	NFILSAILSPMANLQI	FindPept
1761.95	238-252	NSKISRERVGVEMEK	FindPept
1796.05	351-366	MANLQIIGNPKKKINN	FindPept
1819.93	173-188	VEDFTKRGLQDLKDGV	FindPept
1891.02	316-330	ELYPMFLEKLPILRE	FindPept
2223.47	241-260	ISRERVGVEMEKILVGPTPL	FindPept

Table 3-6. Peptide Mass Fingerprinting. Identification of peptic peptides observed in the MALDI Spectrum.

3.5.2 Hydrogen/Deuterium (H/D) exchange coupled with MALDI-ToF to detect the conformation of the protein at two temperatures

H/D exchange experiments monitored by MALDI-ToF on protein incubated at 22°C or at 37°C for 30 min showed that three peptic peptides (amino acids 431-444, 36-44 and 341-356) of the protein from 37°C incorporated more deuterium than did the same peptides in the protein at 22°C (Table 3-7). A fourth fragment showed more deuterium incorporated at the higher temperature, but its identity could not be defined as

there are two peptides with the same mass (Table 3-7). The four peptides (36-44, 431-444, 341-356, 489-503 or 45-59) were found to incorporate 2, 4, 5, or 5 deuterium per peptide when incubated at 22°C representing 22%, 28%, 33%, or 33% of the available amide hydrogens of those peptides. In contrast, the same peptides incorporated an additional 5, 3, 5, or 4 deuterium (representing 77%, 50%, 60%, or 60% of the available amide hydrogens of the peptides) after the enzyme was heat treated at 37°C.

Mass (MH^+) of peptides	Mass (MH^+) D-peptides	Mass (MH^+) Thermal D-peptides	Position	Sequence
1157.66	1160	1165	36-44	NQKYHNKPE
1516.93	1520.84	1523.89	431-444	AHFASLSDAFLKIP
1744.96	1749.93	1754.08	341-356	NFILSAILSPMANLQI
1724.97	1729.96	1733.04	489-503	LQMKPGPWLGKINNE
			45-59	PLTLRITGGWVRDKL

Table 3-7. Deuterium incorporated into protein pre-incubated at 22°C or 37°C.

3.6 Quenching of protein fluorescence by the binding of tRNA

In this study, the interaction of tRNA nucleotidyltransferase with tRNA was monitored by the change in the intrinsic fluorescence intensity of the enzyme. Fluorescence spectra were recorded under the conditions described in materials and methods and the inner filter effect was corrected when the OD_{280} of samples was above 0.05. Titration of wild-type protein clearly showed that the fluorescence intensity decreases with increasing amounts of tRNA added (Fig. 3-24). When the concentration of tRNA in the protein solution reached 1.6 μM, the quenching of the fluorescence

spectrum by tRNA was close to saturation and the addition of more tRNA did not decrease the fluorescence intensity significantly.

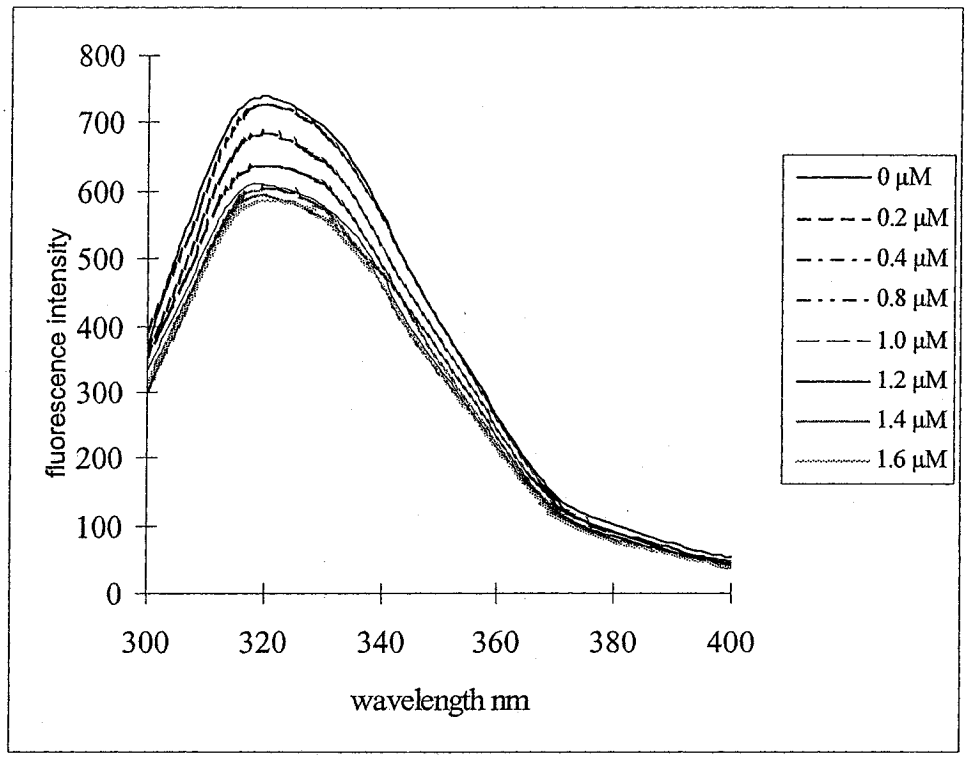

Fig. 3-24. Fluorescence titration of wild-type tRNA nucleotidyltransferase with tRNAs treated with snake venom phosphdiesterase. Intrinsic fluorescence of wild-type protein was titrated with yeast tRNAs in PBS at 20°C and a buffer titrated with the same tRNA were used as baseline. All of the titration spectra were obtained by inner filter effect correction and baseline subtraction.

Based on the result of titration of the wild-type protein, 10 μl of 100 μM of tRNA (final concentration of tRNA in the protein samples is 1 μM) was used to quench the E172Q, E172H and E172K variant proteins. For wild-type protein, the addition of tRNA to a final concentration of 1 μM quenches the fluorescence spectrum (Fig. 3-24) while the inner filter effect caused by absorbance of tRNA at the excitation wavelength was kept relatively low. The fluorescence emission spectra of the variant proteins with and without tRNA were compared to see if the addition of tRNA decreased the intensity of

the fluorescence spectra. The amount of tRNA (1 μM) which efficiently quenches the wild-type enzyme (Fig. 3-25) cannot quench the fluorescence spectra of the E172H and E172K variant proteins (Fig. 3-25). Even for the E172Q variant which showed higher activity than the other variants, the fluorescence spectrum cannot be quenched obviously by the addition of this amount of tRNA. When the amount of added tRNA was increased two-fold, the E172Q, E172H and E172K variants do show some quenching of the fluorescence intensity (Fig. 3-25). As a control experiment, the quenching of heat-treated wild-type protein was tested. For this protein 1 μM tRNA cannot quench the fluorescence intensity (Fig. 3-26)

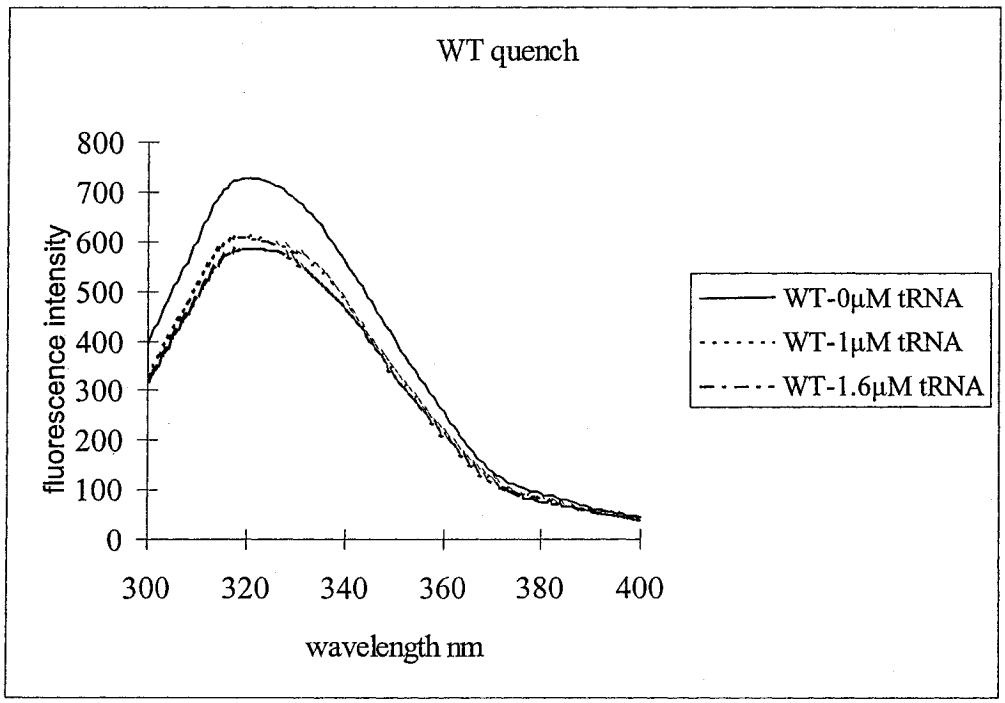

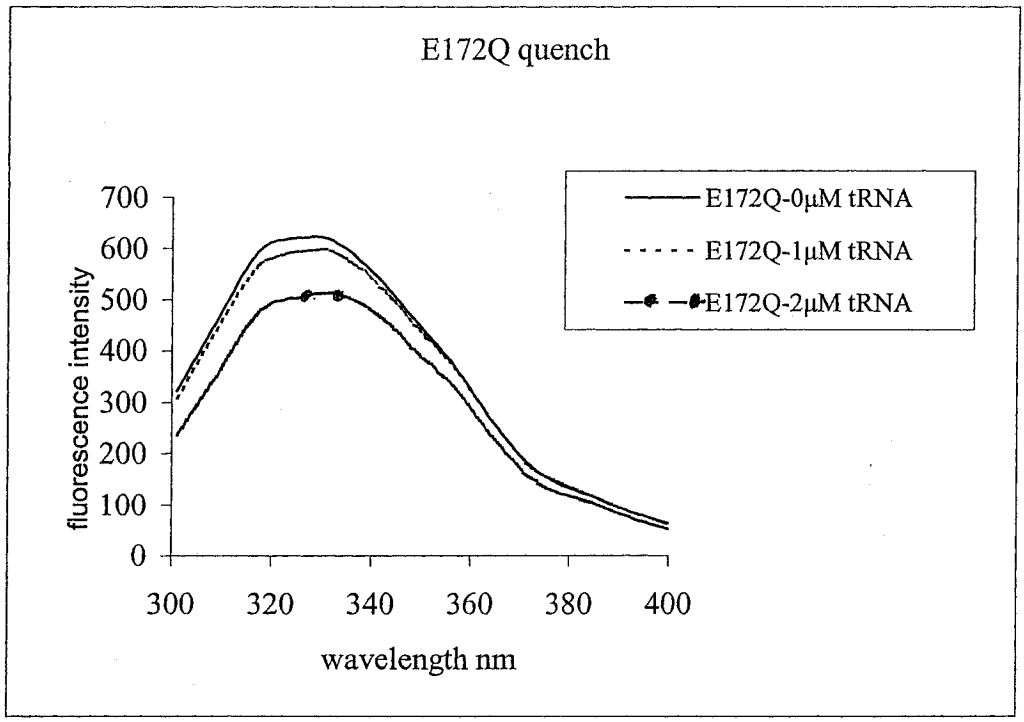
E172Q quench
700
600
500
400
300
200
100
0
fluorescence intensity
300
320
340
360
380
400
wavelength nm
E172Q-0μM tRNA
E172Q-1μM tRNA
E172Q-2μM tRNA

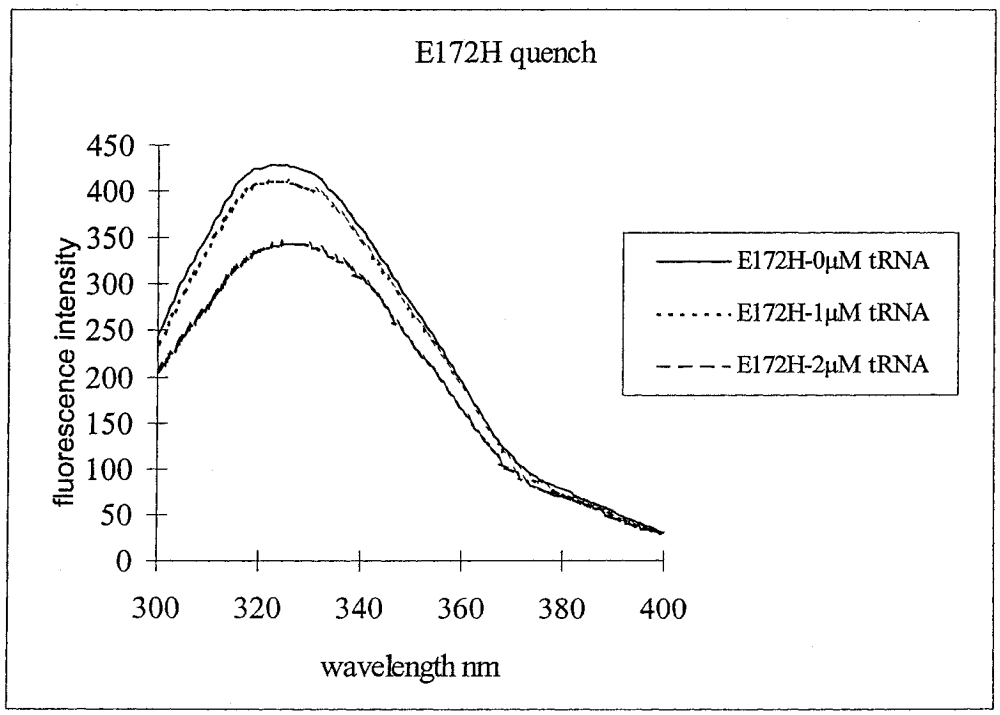
E172H quench
450
400
350
300
250
200
150
100
50
0
fluorescence intensity
300
320
340
360
380
400
wavelength nm
E172H-0μM tRNA
E172H-1μM tRNA
E172H-2μM tRNA

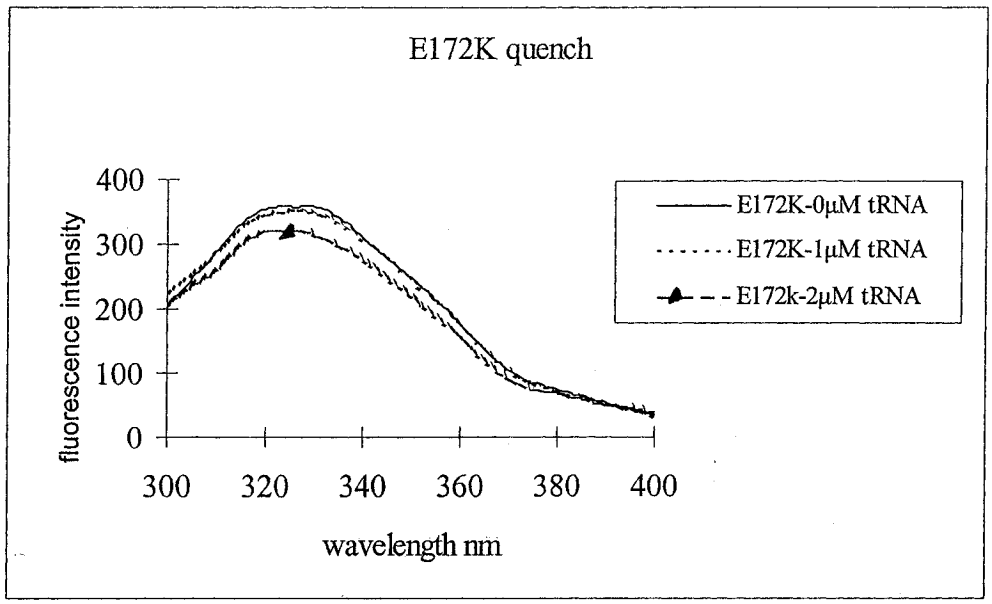

Fig. 3-25. The intrinsic fluorescence spectra quenched by tRNA. Intrinsic fluorescence spectra of proteins were quenched by adding 1 μM (10 μl), 1.6 μM (16 μl) and 2 μM (20 μl) of tRNAs as shown.

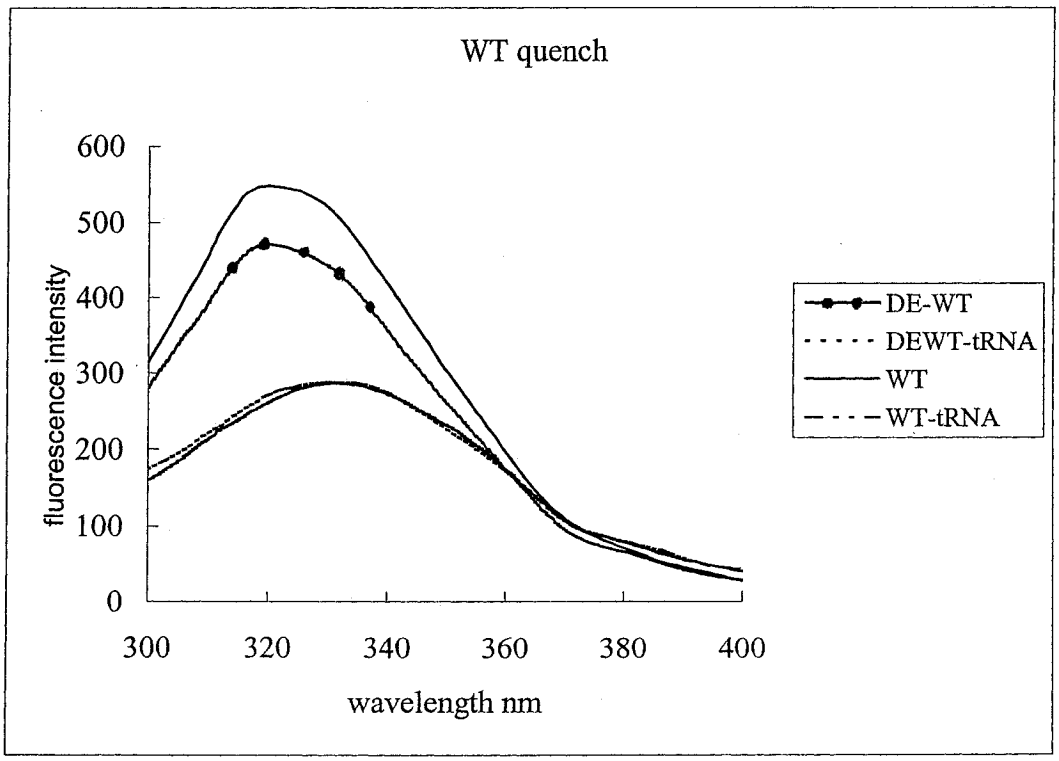

Fig. 3-26. Comparison of the quenching of the intrinsic fluorescence of native and heat-treated wild-type enzyme. WT Native wild-type enzyme, WT-tRNA native enzyme with 1 μM tRNA, DE-WT heat-treated wild-type enzyme (incubated at 37°C for 30 minutes), DEWT-tRNA the heat-treated enzyme with 1 μM tRNA.

4. DISCUSSION

4.1 Expression and purification of tRNA nucleotidyltransferase

Wild-type and mutant *S. cerevisiae CCA1* genes were cloned into pGEX-2T and the resulting tRNA nucleotidyltransferases were expressed as GST fusion proteins in *E. coli*. The soluble GST fusion proteins were purified to approximately 80% purity using a signal-step glutathione-Sepharose 4B affinity column (Fig. 3-4). There always was some fusion protein found in the flow-through fraction from the column (Fig. 3-3, lane 9) perhaps because the conformation of the GST moiety is changed by fusion to the large tRNA nucleotidyltransferase polypeptide such that the affinity of GST to glutathione is reduced.

The subsequent cleavage of the fusion protein to release the GST-tag could be carried out on column or in solution. Cleaving off the GST-tag in solution is more effective and allows easier control of digestion conditions (Fig. 3-4, lane 2), however, it takes longer and makes it more difficult to remove the cleaved GST-tag completely from the solution. After cleavage in solution the cleaved protein must be loaded again onto the glutathione Sepharose affinity column to remove the GST-tag from the solution. Prior to this it is important to completely remove any glutathione present from the first purification step by extensive dialysis otherwise the GST moiety and any uncleaved fusion protein will not bind well to the GST-affinity column. Taken together all of these steps add to the amount of preparation required to generate a pure protein and as a result, the proteins are more likely to degrade and lose activity. In fact, there are smaller protein bands evident on the SDS-PAGE gel after cleavage of the GST-tag from the fusion protein in solution which may indicate degradation of the fusion protein (Fig. 3-5). These

bands are less evident in the on column cleaved samples (Fig. 3-4 A). So while on column cleavage resulted in a lower efficiency of cleavage and a lower yield of product as well as decreased control of digestion conditions and difficulty in monitoring the extent of cleavage (Harper and Speicher, 1977), this method was much faster and yielded a higher purity and less degraded product than cleavage of the protein to remove the GST-tag in solution (compare Fig. 3-4 A and Fig. 3-5). Therefore, in this study, the desired proteins were obtained by cleavage on column.

The final purity of the desired protein was 90~95% with some smaller polypeptides evident which could be products of degradation of tRNA nucleotidyltransferase or some host cell proteins. Because the yields were sufficiently good, a further purification step was not carried out. The purified enzyme was stored in small aliquots at -80°C in 10% glycerol and maintained activity for at least two years.

4.2 Enzyme activity assay

4.2.1 Linear reaction range for wild-type enzyme

The well-established assay for CCA-adding enzymes is a stop-time radioactive assay where the enzyme activity is assayed by measuring the incorporation of radiolabeled AMP into substrate tRNA as acid-precipitable counts. It was important to find the linear reaction range so that the relative activities of different enzymes could be compared and the initial velocities could be determined by stop-time assay. Over the linear range of a reaction, the average rate in a period of time at the beginning of the reaction can be assumed to be the initial rate velocity for the calculation of K_m and V_{max} according to steady-state kinetics (Gao and Leary, 2003). The linear reaction range for

the wild-type enzyme was determined by generating two reaction progress curves by monitoring the formation of product as a function of time or of enzyme concentration (enzyme amount in a constant reaction volume). The optimum reaction time and enzyme concentration should be within the linear region of each progress curve with the conversion percentage of the substrate kept as low as possible (Gao and Leary, 2003). Based on the two reaction progress curves, a standard assay condition was established. For the wild-type enzyme, the reaction was shown to be linear up to 150 ng of enzymes and 5 minutes reaction time under the conditions of 1.0 mM ATP, 0.4 mM CTP and 20 μM tRNA at 22°C (Fig. 3-13, Fig. 3-14). The assay time was kept short even though under these conditions the reaction shows linearity up to 5 minutes because by keeping the assay time relatively short; the amount of enzyme could be increased while the reaction was still kept in the linear range.

4.2.2 Optimum pH of CCA addition

Under standard conditions, the optimal pH for the yeast tRNA nucleotidyltransferase was shown to be pH 10 (Table 3-1). This is consistent with the high pH optima shown for a number of tRNA nucleotidyltransferases from many organisms (Williams and Schofield, 1977; Evans and Deutscher, 1978; Shanmugam *et al.*, 1996; Yue *et al.*, 1998). The overall trend in activity with respect to pH seen here (Table 3-1) is similar to that seen with the *Lupinus albus* tRNA nucleotidyltransferase (Shanmugam *et al.*, 1996) where lower activity was seen at pH 7. The rapid drop in activity as pH drops below pH 8.5 may be due to the inability of products to dissociate from the enzyme at the lower pH (Deutscher, 1982). These *in vitro* relative levels of

activity with respect to pH are interesting in the context of how this enzyme functions *in vivo* at physiological pH. As this is an essential enzyme it must work *in vivo* where the pH is neutral. Perhaps the reaction pathway is different *in vitro* and *in vivo,* or other factors can promote a more rapid dissociation of the product from the enzyme *in vivo* (Deutscher, 1982)

4.3 Kinetic analysis of the wild-type enzyme

4.3.1 Biochemical analysis

To calculate K_m and V_{max} values in the presence of increasing amounts of substrate tRNA, the concentrations of the other two substrates (ATP and CTP) were kept constant at apparently saturating values, two-fold the reported K_m (Chen *et al.*, 1990). The kinetic assay of the wild-type enzyme was carried out in the range of 0.5 to 250 μM tRNA (Fig. 3-15) and again with 10 to 60 μM tRNA (Fig. 3-16). Interestingly, in the first case the data suggest Michaelis-Menton kinetics (Fig. 3-15) while in the second case the data can be fit to the Hill equation (Fig. 3-16). In either case though the apparent K_m or apparent $K_{0.5}$ representing the affinity of substrate tRNA for the enzyme is consistent with a value of 10-16 μM. This is in good agreement with the literature value of 5.6-7.5 μM for the rabbit liver (Evans and Deutscher, 1978) and *E. coli* tRNA nucleotidyltransferases (Deutscher, 1972a; Evans and Deutscher, 1978; Williams and Schofield, 1977) when yeast tRNA treated with snake venom phosphodiesterase was used as substrate. Similar values, 3 μM (Li *et al.*, 1996) or 5.3 μM (Wang *et al.*, 1984) were obtained with the yeast enzyme when more well-defined substrates: a precursor Glu tRNA or yeast $tRNA^{Phe}CpC$-, respectively, were used. In contrast, the V_{max} values in the two sets of experiments are

quite different (compare Fig. 3-15 and Fig. 3-17). The main reason for the large difference in V_{max} values likely is caused by the large differences in the value determined for counts per minute (CPM) contained in an aliquot of [α-^{32}P]-ATP with known specific activity as measured in the scintillation counter. The number of CPMs in a known volume of [α-^{32}P]-ATP was used as a reference to convert the CPMs of products generated in each reaction to moles of AMP incorporated (see Appendix A for sample calculation). For different batches of radiolabeled ATP on a given reference date, the number of CPM/10^{-14} mol [α-^{32}P]-ATP varied by approximately 6-fold (from 45 143 to 272 193). This variability was due either to errors between experiments, *e.g.*, pipetting or to variability between different batches of [α-^{32}P]-ATP. On the reference date, the radiolabeled ATP was said to have a specific activity of 3000 Ci/mmol at a concentration of 10 μCi/μl (ICN, Biochemicals; Inc). In a typical experiment around 5 μl (50 μCi) [α-^{32}P]-ATP was used to prepare the reaction mixture in 500 μl. Of this, 2 μl were diluted into 100 μl and 10 μl (0.02 μCi) of this reaction mixture were counted directly to get the CPM and to calculate the value of CPM/mol [α-^{32}P]-ATP. Any errors arising in these steps would lead to errors in calculating V_{max} in different experiments. To minimize the error in the calculation of the value of CPM/mol, several aliquots of radiolabeled ATP from a single batch were counted and the average value was used for all of the experiments when using the same batch of radiolabeled ATP to convert the final products to moles of AMP incorporated. Any differences in the value of CPM/mol [α-^{32}P]-ATP between experiments will affect the calculated velocity at every tRNA concentration. If the same value for CPM/mol [α-^{32}P]-ATP is used in the calculation of V_{max} for different

experiments then these values will be matched well (see sample calculation). The difference in the value of CPM/mol only affects the V_{max} value but not the K_m value.

When the kinetic assay was carried out in the range 0.5 to 250 μM tRNA (Fig. 3-15), the steps between the tRNA concentrations (0.5, 5, 25, 50, 100 and 250 μM) may have been too large to provide precise information on the reaction at the lower tRNA concentrations. While it seems, based on these data (Fig. 3-15), that the reaction is approaching V_{max} at 25 μM, the large increase from 5 μM to 25 μM may omit some useful information. When the assay was carried out at 10-60 μM (Fig. 3-17) more finely mapping this region with tRNA concentrations of 10, 15, 20, 25, 30, and 60 μM more detail may have been revealed. The data derived from these experiments seem to more closely fit a Hill plot than Michaelis-Menten kinetics. While more points may be needed at concentrations lower than 10 μM, the sensitivity of the assay makes it difficult to detect an initial velocity when the concentration of tRNA is kept this low. Furthermore, the linear reaction range of the reaction would be made narrow with the decrease in substrate tRNA concentration.

If the data fitting the Hill plot are to be believed they suggest possible cooperative binding of tRNA to this enzyme. A Hill coefficient of 2.8 was calculated from the data presented in Fig. 3-16 and suggests that the binding of tRNA to the enzyme assists further tRNA binding. Early kinetic studies on the *S. cerevisiae* tRNA nucleotidyltransferase did not show any regulation of enzyme activity by substrate tRNA (Rether *et al.*, 1974; Sternbach *et al.*, 1976). The reaction conditions in those earlier studies were 100 μl reaction volumes containing 1 mM ATP and CTP, 12.5 mM $MgCl_2$, 50 mM glycine (pH 9.3) and 3-20 μM tRNA (Rether *et al.*, 1974). These assay conditions are similar to what

was used in this study even though more enzyme (500-1000 ng) was used in their reactions. Maybe the enzyme that they purified was not as active as ours due to the different procedure of purification. More recently, Li *et al.* (1996) used 0.5 mM ATP and 0.05 mM CTP concentrations and a 60 min time point in their assays. Based on the literature values (Chen *et al.*, 1990) of the K_ms for these substrates (0.56 mM for ATP and 0.18 mM for CTP), the concentrations of ATP and CTP used by Li *et al.* (1996) were apparently too low to produce a tRNA saturation curve in steady state kinetics. Moreover, a 60 minutes assay time was likely too long to represent steady state kinetics.

Even though cooperative binding can produce a sigmodial substrate saturation curve (Fushinobu *et al.*, 1998), a sigmodial substrate saturation curve does not guarantee cooperative binding. Other factors also could result in the production of a sigmodial velocity versus substrate concentration curve; for example, a mixture of enzyme isoforms with different K_m values for the substrate could produce a sigmodial curve because of the superposition of the individual curves for the varied isoforms (Copeland, 1996). Or a two–substrate reaction following a random order mechanism can display sigmoidal kinetics without true cooperativity if one of the two ordered reactions is faster than the competing ordered reaction (Copeland, 1996). Even a monomeric enzyme also could show cooperative behavior, for example, ribonuclease. In this case the cooperativity is caused by the combination of a fast catalytic turnover with a slow conformational transition between an inactive and active enzyme form (Copeland, 1996). For the CCA adding enzyme, kinetic studies show that CCA-addition is biphasic with the addition of two Cs occurring in the first fast phase with the addition of one A defining the second slow phase (Seth *et al.*, 2002). Perhaps this is similar to the findings of Evans and

Deutscher (1978) and suggests a random ordered mechanism for this enzyme. In our case, the treatment of baker's yeast tRNA substrate with phosphodiesterase could lead to non-uniform substrate with no CCA, one C, two Cs or a complete CCA attached. So the velocity measured could be a combination of the velocities of three reactions, *i.e.*, the addition of -CCA, -CA or just -A. Furthermore, Rether *et al.* (1974) found that for the yeast tRNA nucleotidyltransferase, tRNA without a CCA end was a competitive inhibitor of AMP attachment to tRNA-CC and that tRNA-CCA was a non-competitive inhibitor for both CMP attachment to tRNA and AMP attachment to tRNA-CC. The different batches of treated substrate tRNAs could possess different amounts of tRNA, tRNA-C, tRNA-CC and tRNA-CCA. As a result, the velocity could be affected differently. Moreover, Li *et al.* (1996) showed that precursor tRNA substrate concentrations above 40 μM led to substantial inhibition of the yeast enzyme. In addition, as ATP and CTP are competitive inhibitors of each other (Rether *et al.*, 1974), perhaps the different ATP and CTP concentrations used in the previous study changed the catalytic conditions of the reaction from those discussed here, resulting in initial velocities reflecting different reactions. In addition, the possible chemical hydrolysis of ATP and CTP to their dinucleotide and mononucleotide analogues makes the reaction system even more variable and complex. So while based on this information the standard assay conditions can be used to compare relative enzyme activities; it is difficult to make the reaction system constant to probe the kinetic mechanism. So another approach was needed to investigate the interaction of enzyme with tRNA.

4.3.2 Biophysical analysis

To more clearly define what is happening in the reaction with increasing amounts of tRNA a biophysical approach was used to study tRNA binding. A number of factors such as ligand binding, protein-protein association/dissociation and denaturation can affect fluorescence signals (Lakowics, 1999). The intrinsic fluorescence of tryptophan and tyrosine can be used as a signal to characterize the interaction of proteins with other molecules. For example, if a protein interacts with another molecule, *e.g.*, a substrate, this molecule may absorb the incident light activating Trp or Tyr residues, it also could quench the fluorescence given off by a Trp or a Tyr residue that had been activated, or it could cause a conformational change in the protein such that the Trp or Tyr is in a different environment and has changed emission spectra (Lakowics, 1999). For example, the interaction between *E. coli* Arginyl-tRNA synthetase and $tRNA^{Arg}$ was monitored by the decrease in the intrinsic fluorescence intensity as substrate $tRNA^{Arg}$ was added to the enzyme (Lin *et al.*, 1988). Fluorescence titration also was used to characterize the interaction between human immunodeficiency virus type 1 (HIV-1) reverse transcriptase and $tRNA^{Lys}$ (Thrall *et al.*, 1996). Titration of this enzyme with $tRNA^{Lys}$ resulted in up to a 30% maximal quenching of fluorescence (Thrall *et al.*, 1996) upon addition of $tRNA^{Lys}$. The interaction of tRNA with tRNA nucleotidyltransferase was detected by monitoring the change of intrinsic fluorescence of the enzyme with and without tRNA. The intrinsic fluorescence of the wild-type enzyme was quenched upon incubation with tRNA by as much as 25% (Fig. 3-23). This decrease in fluorescence could be due to a change in conformation induced by binding with tRNA such that the microenvironment of tryptophan or tyrosine residues was changed leading to the quenching of fluorescence

(Lakowics, 1999) or aromatic groups were in the binding site. A small excitation slit (2 nm at 280 nm) was used to minimize photodecomposition of the protein and a large emission slit (4 nm at 340 nm) was used to provide an adequate signal. The fluorescence intensity decreased with increasing amounts of tRNA added to the protein solution and was almost saturated at 2 μM tRNA final concentration (Fig.3-24).

Initial titration of the enzyme (0.25 μM) with tRNA may suggest an S-shaped curve indicating that the binding of tRNA to the enzyme is cooperative (Hammamieh and Yang, 2001; Wu *et al.*, 1994) in agreement with what was seen enzymatically (Fig. 3-17).

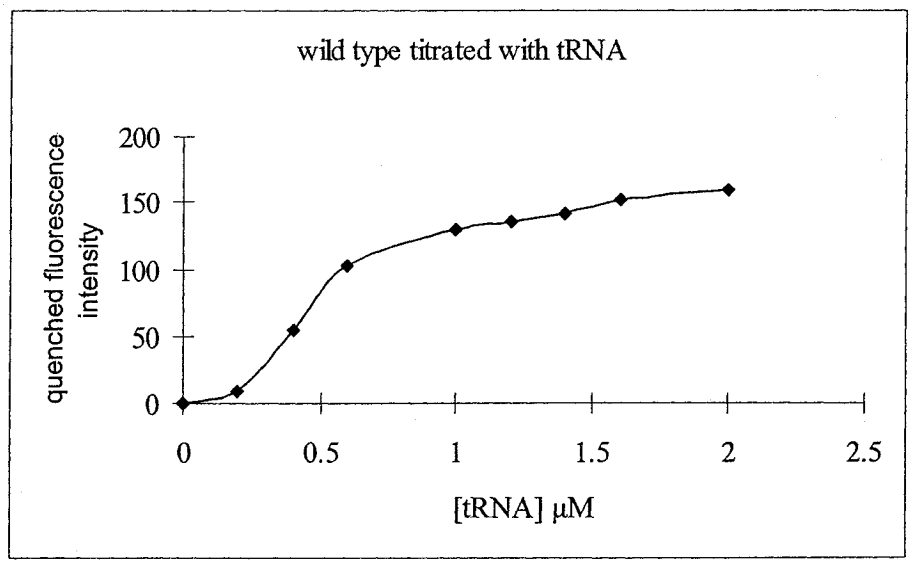

Fig. 4-1 The titration of intrinsic fluorescence of wild-type enzyme with tRNA at 20°C.

Considering the size of tRNA nucleotidyltransferase (~60 000 D) and substrate tRNA (>20 000 D), it seems impossible for a single enzyme molecule to bind multiple tRNA molecules. All of the resolved crystal structures of tRNA nucleotidyltransferases show the enzymes as dimers even though the interface of the subunits is different (Li *et al.*, 2002; Augustin *et al.*, 2003; Okabe *et al.*, 2003; Tomita *et al.*, 2004; Xiong and Steitz,

2004). How the tRNA interacts with the enzyme has been revealed by the resolved crystal structures of the *A. fulgidus* and *A. aeolicus* enzymes complexed with tRNA (Xiong and Steitz, 2004; Tomita *et al.*, 2004). In the *A. fulgidus* structure, one tRNA molecule contacts only one AfCCA subunit of the dimer and the second tRNA binds to the other monomer. This is consistent with native gel shift experimental results that showed a molar ratio of 1:1 for the AfCCA enzyme and tRNA (Xiong *et al.*, 2003). Similarly to the *A. fulgidus* enzyme, the crystal structure of the *A. aeolicus* A-adding enzyme (Aa.LC) complex with a primer tRNA lacking the terminal adenosine and an incoming ATP analogue (AMPcPP) shows that one Aa.LC molecule bound one tRNA molecule (Tomita *et al.*, 2004). In contrast, the CCA adding enzyme of *S. shibatae* has been shown to bind one tRNA molecule per dimer and two protein/tRNA complexes assemble further to form an active homo-tetramer and the resulting tetramer could bind two tRNAs (Li *et al.*, 2000). The molar ratio of protein to tRNA is 2:1. The bound tRNA molecule seems to have a function in inducing the dimerization of dimers of *S. shibatae* CCA-adding enzyme to form a tetramer. Interestingly, a resolved crystal structure of a AfCCA enzyme, with a tRNA minihelix and ATP shows a tetramer binding with three tRNA analogues (Xiong and Steitz, 2004). The middle tRNA seems to function as a cross-linking reagent to induce the formation of the tetramer. Based on the available information from enzyme-tRNA complexes, CCA-adding enzymes are likely to exist as dimers and the interaction with tRNA could be in a 1:1 ratio or a 2:1 ratio. So while both the biochemical and biophysical data suggest that tRNA may bind to tRNA nucleotidyltransferase in a cooperative manner, further experiments need to be done to address this.

4.4 Variant enzymes: linear reaction range and relative activities

Enzyme activity assays for the variant enzymes were carried out under the standard conditions of 1.0 mM ATP, 0.4 mM CTP, 20 μM tRNA and 100 ng enzyme with an assay time of 2 minutes. All of the variant enzymes showed much lower activity than the wild-type enzyme except for the most conserved variant (E172Q) which maintained 40%~50% of the wild-type activity under these conditions (Fig. 3-6). Initially, these observations may seem surprising as *in vivo* any of these amino acid changes allow the cells to remain viable at the permissive temperature (Aebi *et al.*, 1990, D. Kushner, personal communication). On examination of the originally characterized temperature-sensitive strain, segregants carrying the temperature-sensitive mutation showed either 0 or 9% of wild-type enzyme activity when assayed in crude lysates at the permissive temperature (Aebi *et al.*, 1990). These findings are similar to the low levels of activity observed here for the purified E172K variant enzyme. There are a number of explanations that allow the *in vitro* and *in vivo* observations to conform. For example, perhaps only low levels of enzyme activity are required to maintain viability such that a variant enzyme that functions poorly still functions well enough to keep the cells alive. Moreover, while in the *in vitro* assay the amount of enzyme is limited to how much is added, *in vivo* protein synthesis may be increased to produce enough of the variant enzyme to meet the cell's needs. Perhaps *in vivo* there are some factors that help to stabilize the enzyme which are lost during cell lysis and purification. The role of pH in the relative activity of the enzyme *in vivo* and *in vitro* also cannot be excluded. As discussed above, the fact that physiological pH (<8.5) results in low levels of activity *in vitro* even for the wild-type enzyme suggests that there may be a difference in the

reaction pathway *in vivo* and *in vitro*. Perhaps it is this difference that allows the E172K variant enzyme to manifest its defect more dramatically at the permissive temperature *in vitro* than *in vivo*.

Given that the low level of enzyme activity seen with the E172K variant enzyme *in vitro* is still sufficient to maintain viability, the relative activities of the other variant enzymes are not unexpected. For example, the E172Q substitution is the most conservative of the substitutions made in terms of the characteristics of the amino acid and this substitution has the least effect on enzyme activity. The most interesting observations of enzyme activity are with respect to the activities of the E172F and E172H variant enzymes. The E172F variant enzyme has approximately the same level of reduced activity as the E172K variant enzyme while the E172H variant enzyme has only slightly more activity. Under the standard conditions, the sensitivity of the assay was too low to reliably measure the incorporation of label with the variant enzymes, so a wider range of enzyme concentrations and reaction times were assayed.

The linear reaction range was determined for variant E172K (the least active variant) to improve the sensitivity of the assay (Fig. 3-7, Fig. 3-8). For E172K, the reaction remains linear up to 1920 ng of enzyme and 5 minute reaction time or for 20 minutes when 600 ng of enzyme is used under the conditions of 1.0 mM ATP, 0.4 mM CTP and 20 μM tRNA. Based on the linear reaction range of the modified activity assay for the E172K variant, increased amounts of variant E172K, E172H and E172F were used to compare the relative activities of all enzymes at 22°C. Although for E172H and E172F, the linear reaction range was not known, the assay time was kept at 2 minutes as for the E172K variant enzyme. The conditions for the E172Q variant enzyme were kept the

same as for the wild-type enzyme. Under these conditions it was hoped that initial velocities for all of the reactions could be assumed from a comparison of the final product in the time-stopped assay.

The incorporation of AMP into substrate tRNA increased with increasing amounts of variant enzymes (E172K, E172H and E172F) indicating that for each variant enzyme the reaction was in the linear range (Fig. 3-9). Therefore, by increasing the enzyme amount in the assay and staying in the linear range more reliable indications of enzyme activity could be calculated even for the variant enzymes showing low levels of activity. The specific activity of all of the enzymes was calculated and the relative specific activities (Fig. 3-10) are in good agreement with the relative activities obtained under the standard conditions (Fig. 3-6). Using these values, the specific activities of the E172Q, E172H, E172F and E172K variant enzymes are 40%, 7%, 5% and 4% of wild-type (Fig. 3-10). The approximately 60% loss of activity on conversion of the glutamate at position 172 to a glutamine suggests that a carboxylate at this position is important but not essential for enzyme activity. In this context it is interesting that natural variation at this position results in an aspartic acid in a number of tRNA nucleotidyltransferases (Fig. 1-4). The position of this amino acid on the exterior of the protein away from the active site, based on positioning this amino acid on the resolved crystal structures (Fig. 4-2), suggests that this amino acid is not directly involved in catalysis or contact with any of the substrates. This suggests that alteration of this amino acid could more likely affect overall protein structure or stability.

4.5 Thermal inactivation of wild-type and E172K and E172H variant proteins

To investigate how a single glutamate to lysine amino acid substitution at position 172 of tRNA nucleotidyltransferase could generate a temperature-sensitive phenotype, thermal inactivation studies of wild-type and variant (E172K and E172H) enzymes were carried out *in vitro*. For the wild-type enzyme, its specific activity when assayed directly at 37°C was almost three fold its specific activity when assayed at 22°C (Fig. 3-11, Table 3-2). This is not unexpected as enzyme activity tends to increase with increasing temperature. In fact, a rough rule of thumb (Piszkiewicz, 1977) suggests that enzyme activity should double for approximately every 10°C increase in temperature. The data for the wild-type enzyme fit nicely with this suggestion. However, an activity increase correlation with temperature increase only applies if the increase in temperature does not lead to thermal denaturation of the protein (Piszkiewicz, 1977). In the case of the wild-type enzyme extended incubation leads to a decrease in enzyme activity (Fig. 3-11, Table 3-2). This decrease in activity may result from thermal denaturation of the protein or from proteolysis as any proteases present in solution also will have increased activity at the elevated temperature. By 15 minutes, activity of the wild-type enzyme has dropped by 70% of activity at 22°C (Fig. 3-11) at which point no additional decrease in activity was seen (data not shown). This suggests that the decrease in activity was brought about by thermal destabilization of the protein and was not simply due to degradation of the enzyme by contaminating proteases. In fact, SDS-PAGE of a sample maintained at elevated temperature for 90 minutes did not show any increase in degradation (data not shown).

In contrast, when the variant enzymes E172H and E172K were assayed directly at 37°C they showed no increase in specific activity and only 50%-70% of their specific activity at 22°C (Fig. 3-12, Table 3-2). This suggests that the variant enzymes are less thermally stable than the wild-type enzyme. In fact, while the wild-type enzyme retained 75% of its activity after pre-incubation for one minute at 37°C (higher than its activity at 22°C), both E172K and E172H were almost completely inactivated after one minute pre-incubation at 37°C (Fig. 3-12, Table 3-2).

If one compares the specific activities of the three enzymes (Table 3-2) it is apparent that at any temperature the wild-type enzyme has the highest specific activity. At 22°C the specific activity of the wild-type enzyme is approximately 12 fold or 5.7 fold higher than the lysine and histidine variant enzymes, respectively. When assayed at 37°C with no pre-incubation these values rise to 47 fold and 32 fold respectively, indicating that the initial exposure to the elevated temperature is able to reduce the activity of the variant enzymes more dramatically than the wild-type enzyme. After 15 minutes pre-incubation when the loss of activity has stabilized the wild-type enzyme retains on the order of 23 times the specific activity of the lysine variant and 8 times the specific activity of the histidine variant. So while at the permissive temperature the E172K and E172H substitutions reduce enzyme activity they also serve to make the resulting protein less active at the non-permissive temperature. This increased loss of specific activity at the non-permissive temperature may be responsible for the temperature-sensitive phenotype observed *in vivo*.

It might be particularly important that the greatest change in the loss of activity occurs on the initial transfer to the "non-permissive" temperature such that at this time

the enzyme functions extremely poorly. *In vivo*, if this happened to this extent, it would alter the cell's ability to carry out protein synthesis and affect viability. One could argue that only reducing enzyme activity to a small degree would allow the cell to adapt to these new conditions and survive, for example, by producing more of the variant protein as described in the introduction. However, inactivating tRNA nucleotidyltransferase to the degree seen with the lysine variant enzyme would dramatically inhibit protein synthesis because as the cell's growth rate is increased by the increase in temperature more tRNAs would be synthesized but would not have complete 3'-termini. These tRNAs could then compete for binding at tRNA synthetases or even at the ribosome and compound the problem further disrupting protein synthesis and leading to cell death. So while it seems possible to connect this loss of activity with the temperature-sensitive phenotype it is still not clear why the mutations in the gene leads to a less active protein or to a protein that loses activity at the higher temperature. To address this question, biophysical character of the wild-type and mutant gene products were carried out.

4.6 Biophysical study of wild-type and variant enzymes

The results of the enzymatic analysis have shown that at the permissive temperature any of the tested amino acid substitutions resulted in a decrease in enzyme activity *in vitro*. This decrease in activity ranged from roughly 50% for the most conservative substitution (E172Q) tested to up to approximately 96% for the E172K mutation that defined the original temperature-sensitive mutant. Moreover, the E172H and E172K substitutions resulted in an almost complete loss of enzyme activity on shifting to 37°C (the non-permissive temperature). There is also good *in vivo* data to correlate the loss of

enzyme activity at 37°C to loss of viability (Fig. 1-8). Based on these findings it was important to determine whether a structural change in the protein could be linked to these enzymatic and biological observations. To do this fluorescence and CD spectroscopy were used.

4.6.1 The secondary structure of the wild-type and variant enzymes

The various elements of secondary structure, such as helices, sheets and turns, within a protein each possess a distinctive pattern in how they absorb circularly polarized light (Greenfield, 1996). Far-UV CD scans of the wild-type and variant tRNA nucleotidyltransferases show typical α-helical structure (Fig. 3-18) with characteristic troughs at 208 nm and 222 nm (Greenfield, 1996). This is not unexpected as the resolved crystal structures of the human (Augustin *et al.*, 2003), *Bacillus stearothermophilus* (Li *et al.*, 2002) class II tRNA nucleotidyltransferases and *Aquifex aeolicus* A-adding enzyme (Tomita et al., 2004) show that these proteins contain abundant α-helices representing 50% (*B. stearothermophilus*), 44% (human) and 45% (*A. aeolicus)* of the secondary structure in these proteins. It is likely that the structure of the yeast tRNA nucleotidyltransferase has an α-helical content similar to these values but from an evolutionary perspective it is likely more similar to its eukaryotic homologue than to its eubacterial homologues.

In an attempt to place the yeast mutation on the higher order structure of tRNA nucleotidyltransferase the analogous amino acids in the human, *B. stearothermophilus* and *A. aeolicus* sequences were marked. These amino acids all are located in a region of

the protein linking the head and neck domains but do not appear to be involved in the formation of any α-helical structures (Fig. 4-2).

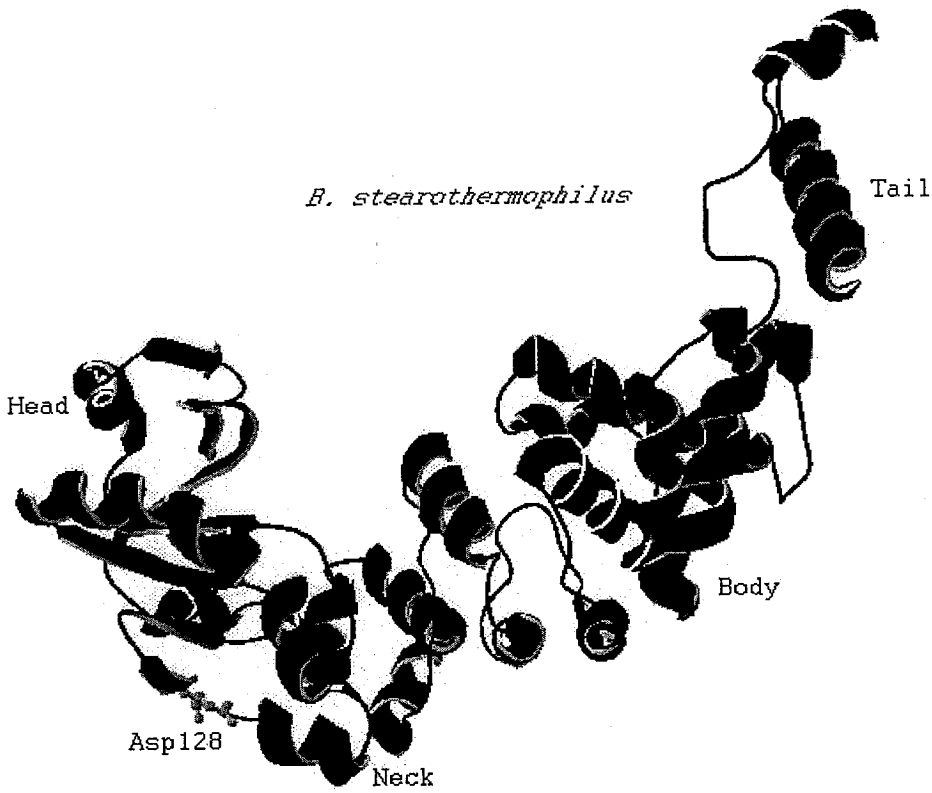

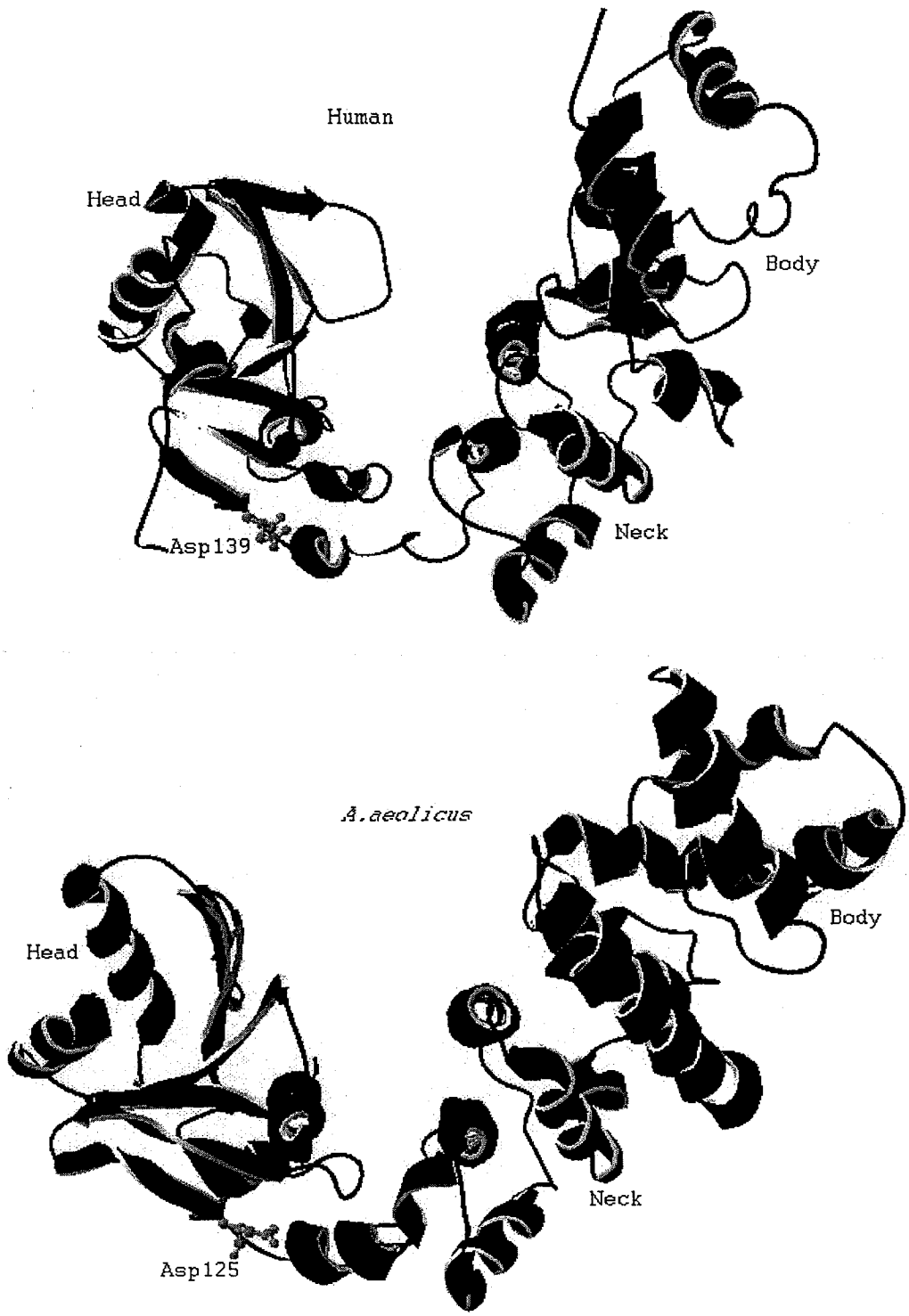

Fig. 4-2. The corresponding position of the altered amino acid of yeast CCA-adding enzyme on the crystal structures of *B. stearothermophilus*, human CCA-adding enzyme and *A. aeolicus* A-adding enzyme. The altered amino acid was assigned to Asp128, Asp139 and Asp125, respectively.

In fact, this amino acid finishes β-strand 7 in the *B. stearothermophilus* enzyme and β-strand 6 in the human enzyme, adjacent to a small number of amino acids (a small loop or turn) connecting this β-strand to an α-helix (helix E in *B. stearothermophilus* and helix 6 in the human enzyme). By comparing the far UV CD spectra of the wild-type enzyme to the variant enzymes (Fig. 3-18) this suggests that changing the glutamate at this position to lysine, glutamine, histidine or phenylalanine does not dramatically alter the secondary structure of the protein at 22°C (Fig. 3-18). Although this amino acid likely does not participate in the construction of an α-helix as shown in Fig. 4-2, it may be an important amino acid in maintaining the higher order structure of tRNA nucleotidyltransferase. The important role of this amino acid can be identified by its conservation in other tRNA nucleotidyltransferase (Fig. 1-4). The alignment of the primary structure of the yeast enzyme with other tRNA nucleotidyltransferases suggests that an amino acid containing a carboxylate (either glutamate or aspartate) is highly conserved at this position and always follows a large hydrophobic amino acid, isoleucine, valine or phenylalanine in these examples (Fig. 1-4), leucine or tyrosine in other tRNA nucleotidyltransferases (not shown).

It could be imagined that altering an amino acid at the end of this β-strand near a small loop or turn could affect the orientation of this β-strand with respect to the nearby α-helix. Loops possess greater structural flexibility than strands and helices and have relatively few contacts with the remainder of the structure (Fiser *et al.*, 2000). The flexibility of a loop makes it more easily disturbed by the introduction of another amino acid with different charge, polarity or size and the disturbance of the loop could affect the framework of the protein and expand to the whole structure of protein. Perhaps in the

case of tRNA nucleotidyltransferase the organization of the β-strand with respect to the nearby α-helix is altered affecting the overall tertiary structure of the protein but having no direct affect on the elements of secondary structure. As the crystal structure of the yeast enzyme is not known, it will be compared to the class II tRNA nucleotidyltransferase enzymes for which crystal structures are known. This region of the yeast enzyme corresponding to the region from the last amino acid in β-strand 7 to the first amino acid of α-helix E in the *B. stearothermophilus* enzyme is composed of 7 amino acids (EDFTKRG). This region is even smaller in the *B. stearothermophilus* (DPFGG), human (DYFNG) enzymes and *A. aeolicus* A-adding enzyme (YFGGL). The common property of this region of the protein is steric compactness with a hydrophobic amino acid preceding the acidic residue and a hydrophobic or proline residue immediately following the acidic residue (except in the case of the yeast enzyme where a hydrophobic residue follows a second acidic residue). Analysis of the crystal structures reveals that the aspartic acid residues corresponding to E172 in the yeast enzyme also participate in forming hydrogen bonds with other amino acids in the adjacent helix to stabilize the higher order structure of the protein. For example, the terminal carboxylate of Asp125 of the *A. aeolicus* A-adding enzyme (corresponding to Glu172 of the yeast enzyme) forms H-bonds with the backbone amides of Tyr126 and Leu130 and with the terminal $-NH_2$ of Arg131 (Fig. 4-3).

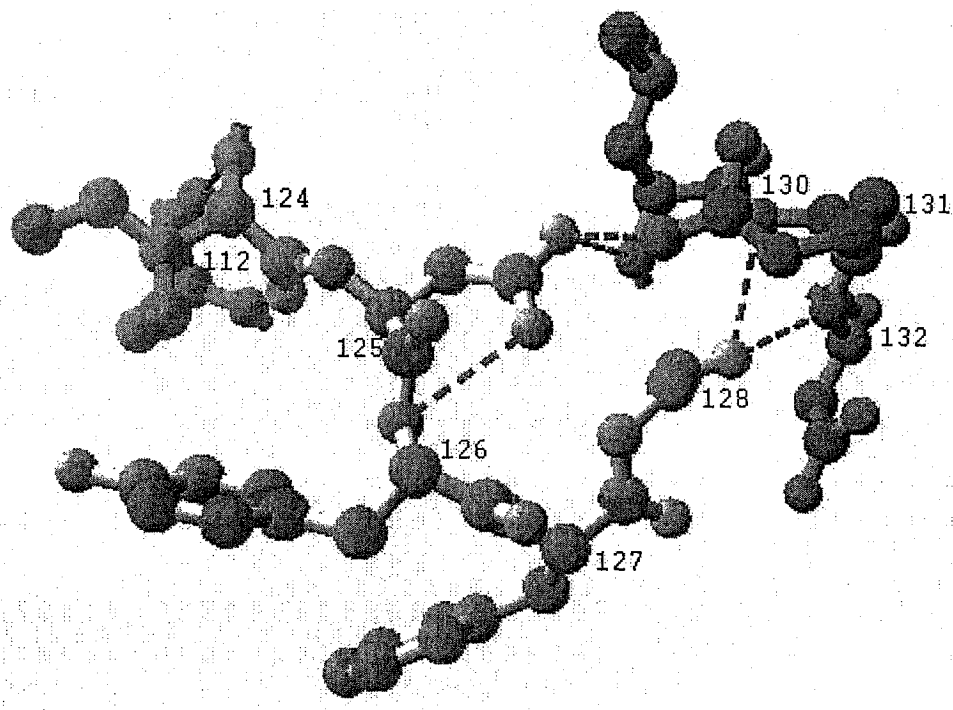

Fig. 4-3 The hydrogen bonding around Asp125 in the crystal structure of *A. aeolicus* A-adding enzyme.

As Tyr126 is in the small loop or turn connecting the β-strand ending at Asp125 (or Glu172 in the yeast enzyme) with the next α-helix which contains both Leu130 and Arg131, it is easy to see how these hydrogen bonds could define the structure of the protein in this area and how altering this amino acid could alter the associated hydrogen bonding and affect the organization of the β-strand with respect to the adjacent α-helix. Moreover, by changing the relative orientation of these two structures the overall structure of the protein may be changed. The introduction of a Gln, His or Lys residue at this position would alter the hydrogen bonding potential while a Phe would eliminate any hydrogen bonding from the side chain. As a result of altering hydrogen bonding or due to steric problems caused by placing a large amino acid (*e.g.*, Phe or Lys) in this position, the relative orientation of the adjacent α-helix could change leading to a change in the

overall structure of the protein. Any change in the overall structure of the protein may be reflected by intrinsic fluorescence changes of tyrosine and tryptophan residues in the protein that may undergo a change in their environment.

4.6.2 The tertiary structure of wild-type and variant enzymes

The intrinsic fluorescence from tryptophan and tyrosine residues is an excellent probe for the structure of proteins (Tsaprailis *et al.*, 1998). The microenvironmant surrounding a tryptophan can be reflected because the maximum fluorescence of tryptophan changes from ~320 nm to 350 nm as its environment changes from nonpolar to polar, for example, when a tryptophan that was buried in the interior of a protein becomes more exposed to solvent as a result of denaturation of the protein (Tsaprailis *et al.*, 1998). For many proteins and especially for large proteins with numerous tryptophan and tyrosine residues, tyrosine fluorescence emission (λmax~305 nm) is not observed because the distribution of tyrosine and tryptophan residues in the higher order structure of the protein leads to a distinct energy transfer from the tyrosine to the tryptophan (Fitter and Haber-Pohlmeier, 2004). Fluorescence emission spectra were collected on protein samples with OD_{280}<0.05 and an excitation wavelength at 280 nm. This excitation wavelength allows for both tyrosyl and tryptophanyl signals to be monitored (Lakowics, 1999). There are five tryptophan and fifteen tyrosine residues in the yeast tRNA nucleotidyltransferase and their distribution in a model of yeast enzyme built based on the crystal structure of the human tRNA nucleotidyltransferase by software Spdbv (http://www.expasy.org/spdbv) is shown (Fig. 4-4). Because the human enzyme (433 amino acids) is smaller than the yeast enzyme (529 amino acids), three tryptophan and

five tyrosine residues at the C-terminus as well as three tyrosine residues in the N-terminus cannot be shown on the model. The distribution of these aromatic residues throughout the entire enzyme makes them a good probe for any structural changes in the protein.

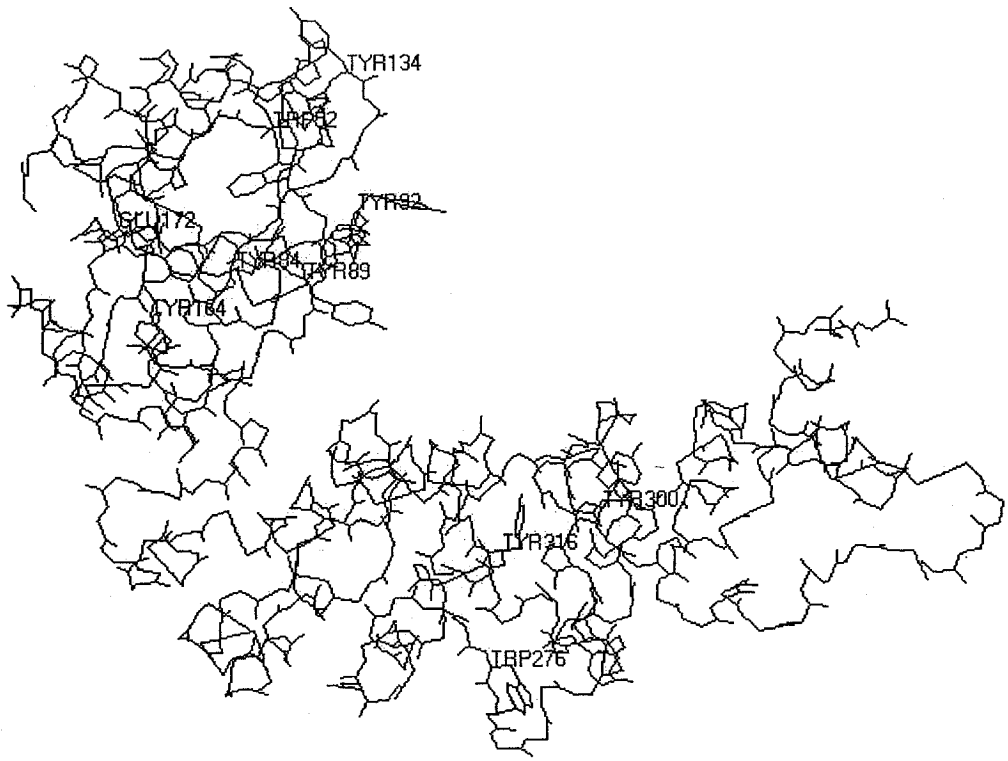

Fig. 4-4 The distribution of tyrosine and tryptophan residues on the model of yeast tRNA nucleotidyltransferase built on the crystal structure of the human enzyme. All Trps, Tyrs and Glu172 are labeled.

Comparing the fluorescence spectra of the wild-type and variant enzymes shows a red-shift of maximal emission at room temperature for all of the variants as compared to the wild-type enzyme (Fig. 3-20). This shift varies from 6 nm (E172Q and E172H) to 8 and 9 nm (E172F and E172K). This observation suggests that one or more aromatic residues in the protein is in a more polar environment perhaps indicating a structural

change such that it is more solvent exposed. It is interesting that the red shift for E172Q and E172H are similar while the red shift with E172K and E172F are also similar. Since the Q and H substitutions gave a similar red shift and the K and F substitutions gave a different red shift it would be interesting to determine if these amino acids had any similar characteristics. Glutamine and histidine are both hydrophilic amino acids capable of hydrogen bonding. Glutamine lacks any charge and histidine may have a positive charge or no charge depending on the local environment. Since the pka of the R group in histidine is 6.04 (Voet and Voet, 1995), it likely has no charge at physiological pH, so both of these amino acids likely reflect uncharged amino acids with hydrogen bonding potential. In contrast, phenylalanine is a hydrophobic residue with no hydrogen bonding potential in its side chain. Lysine can form hydrogen bonds, but at physiological pH likely has a positive charge. So while with respect to their hydrogen bonding potential glutamine and histidine are similar to each other, lysine and phenylalanine are completely different. Therefore the change in red shift does not reflect simply an effect of the hydrogen bonding potential of the newly introduced side chains. If instead of looking at charge as the defining parameter in these amino acids, we look at size, we find that in terms of Van der Waals volume, glutamate has a size of 109 $Å^3$, glutamine has a size of 114 $Å^3$, histidine is 118 $Å^3$ and lysine and phenylalanine are both 135 $Å^3$ (Richard, 1974). Interestingly, as the size of the residue increases, the amount of red shift increases. As discussed previously, this suggests that as the size of the residue increases the relative positions of the β-strand and the α-helix adjacent to this residue (Fig. 4-2) are altered such that the compact structure of the protein is changed causing some tryptophan or tyrosine residues to be more solvent exposed.

Clearly, even at the permissive temperature the alteration of E172 to glutamine, histidine, phenylalanine or lysine has an affect on enzyme structure and function. Even the small alteration from Glu to Gln results in a 50-60% loss of enzyme activity and a change of 6 nm in the fluorescence emission spectrum suggestive of a structural change in the protein. This 6 nm red shift in itself is not sufficient to inactivate the protein, however, when the substitution at position 172 is to a His then enzyme activity is reduced to only 7% of wild-type activity. Although, both the Gln and His residues cause a red shift of the same apparent magnitude, the His is slightly larger than the Gln. Perhaps this additional size or the presence of the imidazole ring plays a role in defining enzyme activity. Clearly, when Phe or Lys is introduced at this position there is an 8-9 nm red shift and the enzyme activity of the E172K and E172F variant enzymes is low. Based on the discussion above, the introduction of amino acids with different size and charge into this compact turn or loop could lead to steric hindrance, or a change in electrostatic or hydrophobic interactions with neighboring amino acids. The final result is the change in the organization of the adjacent sheet and helix. Considering that those sheets and helices are conserved in the catalytic domain of the nucleotidyltransferase superfamily, it seems logical that a disturbance in this region would affect enzyme activity. It is not clear though whether this decrease in enzyme activity is due to a decrease in substrate binding or in catalytic activity or to both.

4.6.3 Quaternary structure

From the resolved crystal structures of tRNA nucleotidyltransferase, it is obvious that tRNA nucleotidyltransferase dimerizes in different orientations: human enzyme -

body domain to body domain contact (Augustin *et al.*, 2003), *B. stearothermophilus* enzyme (Li *et al.*, 2002) - head to head interaction (Fig.1-5) and the *A. aeolicus* - head and neck domains (Tomita *et al.*, 2004). Since no crystal structure is available for the yeast tRNA nucleotidyltransferase whether this enzyme also forms a dimer is unknown. However, it is interesting that the enzyme kinetic and fluorescence quenching data suggest possible multimer formation. Further research will be required to address this question and the role, if any, of amino acid 172 in dimer formation.

4.7 The comparison of thermal stability of wild-type and variants

4.7.1 Fluorescence

When wild-type tRNA nucleotidyltransferase is incubated at 37°C, a decrease in fluorescence intensity and a red-shift in the wavelength of maximum intensity are observed (Fig. 3-21). The red-shift in maximum wavelength reflects a change in the environment of the tryptophan residues indicative of protein unfolding (Lakowicz, 1999) such that tryptophan residues are more exposed to the aqueous environment. The exposure and an increase in temperature lead to a decrease in fluorescence intensity. Even though the wild-type protein shows the greatest red-shift (14 nm) when comparing 22°C with 37°C, it appears to be more folded at 37°C than either the E172For E172K variant protein as the maximal emission for wild-type enzyme at 37°C is 334 nm while the maximum emission for the E172F and E172K variant enzymes is 339 nm and 340 nm at 37°C. When wild-type enzyme was added directly into 37°C buffer, the fluorescence spectrum recorded within 2 minutes did not show any red-shift of maximal emission (Fig. 3-21, Fig. 3-22). However, all of the variant enzymes showed a red-shift of maximal

emission within 1 minute once they were added to the 37°C buffer (Fig. 3-22). This observation suggests that the thermodynamic processes are different between wild-type and variant enzymes (Fitter and Haber-Pohlmeier, 2004). The thermal unfolding rate of the wild-type enzyme is slower than that of the variant enzymes indicating that the tertiary structure of the wild-type enzyme is more thermally stable than is the tertiary structure of the variant enzymes. As discussed in section 4.6, the profile of thermal inactivation of the wild-type enzyme is different from that of the variant enzymes. After pre-incubation at the non-permissive temperature for 10 minutes, the activity of the wild-type enzyme at 37°C was the same as the initial activity at 22°C. However, one minute inactivation of the variant enzymes (E172H or E172K) almost completely depleted the activity at 37°C. Coincident with the loss of enzyme activity is the structural change at the higher temperature suggesting that the structural change is the reason for the loss of activity. These data support the hypothesis that the variant enzymes are less thermally stable than the wild-type enzyme and that this loss in thermal stability is linked to the loss of enzyme activity.

4.7.2 Circular Dichroism (CD)

Protein folding and stability can be affected by many factors such as hydrogen and disulfide bonds, Van der Waals, hydrophobic, aromatic–aromatic and electrostatic interactions, as well as changes in loop length, compactness or mobility (Sandgren *et al.*, 2003). Studies on glycoside hydrolase family 12 members show that a wide variation in their thermal stability was caused by the single change of a buried residue from Ala to Ser or Val within the protein (Sandgren *et al.*, 2003). A single mutation leading to the

change in stability also was found in the well-studied T4 lysozyme (Zhang *et al.*, 1995). Furthermore, the effect of specific point mutations on protein thermal stability was cumulative with seven mutations in the same gene, causing the melting temperature of the resulting proteins to increase by 8.3°C at pH 5.4 (Zhang *et al.*, 1995). In the case of tRNA nucleotidyltransferase, the mutations likely affect the organization of an adjacent β-strand and α-helix which ultimately may alter the relative orientations of the head and neck domains.

From the thermal denaturation of the secondary structure monitored by CD spectroscopy, the single amino acid change from glutamate to lysine or phenylalanine in tRNA nculeotidyltransferase led to a drop of 6°C in transitional temperature (Fig. 3-19). This suggests that the stability of the secondary structure of this protein has been decreased by the introduction of these large residues. In contrast, substitution of the glutamate by an amino acid with a similar size such as glutamine or histidine lead to little or no change in thermal stability as measured by far UV-CD (Fig. 3-19, Table 3-2, Table 3-3). It seems that the charge of the altered amino acid is not what affects the stability of the secondary structure. The removal of the negatively charged glutamate alone is not sufficient to destabilize the protein as shown by the substitution of glutamate with glutamine and histidine.

The thermal denaturation is highly cooperative for the wild-type, E172Q and E172H proteins with an obvious pretransitional state (Fig. 3-19). The existence of the pretransitional state suggests that a relatively stable intermediate exists (Stelea *et al.*, 2001). In each case, the initial unraveling of α-helices leads to the collapse of the structure between 38°C and 45°C. As for the E172F and E172K variant proteins, there

are no distinct pretransitional states and the absence of a relatively stable intermediate leads to the loss of the secondary structure quickly. They have lost almost half of their secondary structure at 37°C while the wild-type, E172Q and E172H variant proteins all maintain approximately 90% of their secondary structure at this temperature (Table 3-4). Perhaps the introduction of a large residue at position 172 reduces some interactions among the element structures of the enzyme that function in stabilizing the α-helices secondary structure (Galzitskaya *et al.*, 2002). Based on these studies of the thermal stability as measured by changes in secondary and tertiary structure, the wild-type enzyme is more thermally stable than the other variant enzymes. E172Q and E172H have an intermediate thermal stability and E172F and E172K are the least stable.

4.8 The relationship between enzyme activity and thermal stability

In vitro, thermal denaturation was monitored enzymatically (Fig. 3-11, 3-12) and by recording the changes in the fluorescence spectra (Fig. 3-21). From the time course of activity of the wild-type enzyme, it was found that the wild-type enzyme had lost almost 50% of its activity at 37°C after 5 minutes pre-incubation at 37°C and about 88% of its activity at 37°C after 15 minutes pre-incubation at 37°C (Fig. 3-11). Fluorescence emission spectra of the wild-type enzyme at 37°C were determined at selected time points (Fig. 3-21). As expected with increasing time at the elevated temperature, fluorescence intensity decreases and a red-shift of maximal emission wavelength occurred. The greatest decrease in intensity was within the first 5 minutes. Of greater interest is the shift of the emission maximum to the red by a total of 14 nm over this time course. After 20 minutes continued incubation at 37°C no additional red shift was

apparent indicating that the degree of unfolding had stabilized at this temperature (Fig. 3-22) (Fitter and Haber-Pohlmeier, 2004). The reduction in enzyme activity (Fig. 3-11) correlates well with the change in fluorescence spectra (Fig. 3-21) suggesting that the change in conformation brought about by heating was related to the loss of enzyme activity. In contrast, even after one minute preincubation at 37°C, the lysine and histidine variant enzymes showed no detectible enzyme activity at 37°C (Fig. 3-12) and an immediately significant red shift (Fig. 3-21, Fig. 3-22). The variant enzymes (E172Q, E172H, E172F, E172K) all are less thermal stable than the wild-type enzyme based on the fluorescence data (Fig. 3-21, Fig. 3-22) and the tertiary structural changes happened immediately at the non-permissive temperature for variant enzymes E172H, E172K and E172Q. These changes lead to the decrease in activity for wild-type and elimination of activity for variants suggesting that this single mutation affects the enzyme structure and activity at 22°C and even more so at 37°C.

4.9 Intrinsic Fluorescence quenching by tRNA

While the data so far suggest that a structural change is associated with the loss of enzyme activity, it is not clear if this loss of activity is due to reduced substrate binding efficiency or to a decrease in catalytic activity. Since tRNA represents the largest substrate and it interacts in multiple places on the enzyme it seemed worthwhile to see if tRNA binding was affected by any of these alterations in the protein. From the titration of the wild-type enzyme with tRNA, it is clear that 1 μM tRNA can quench 20% of the intrinsic fluorescence of tRNA nucleotidyltransferase (Fig. 3-25). However, this concentration of tRNA is not sufficient to show any detectable quenching of the

fluorescence spectra of any of the variant enzymes tested (Fig.3-25). These results suggest that the interactions of the variant enzymes with tRNAs are weaker than the interaction of wild-type enzyme with tRNA. Considering that all of the variant enzymes do show activity although lower than that of the wild-type enzyme, the variant enzymes must associate with substrate tRNA. The quenching experiments simply may not be sensitive enough to detect an interaction between 1 μM tRNA and the variant proteins. When the amount of tRNA was doubled in the quenching experiments with variant enzymes E172Q, E172H and E172K quenching of the fluorescence intensity was noted. Combined with the results of the enzyme activity assays, it seems that the lower enzyme activity was due to a weaker interaction of the substrate tRNA with the enzyme as opposed to a reduced reaction rate although without additional kinetic analyses the possibility that the reaction rate is also reduced can not be excluded. As discussed above, the mutation at position 172 seems to alter the overall structure of the enzyme such that this structural change results in weaker binding with tRNA leading to a decrease in enzyme activity.

4.10 Conformational change of wild-type enzyme at 37°C

To probe in more detail the conformational change that the wild-type enzyme undergoes on transfer to 37°C, H/D exchange coupled with MALDI-TOF spectrometry was used. H/D exchange of amide protons followed by mass spectrometric analysis can detect topological information about proteins. Of the hydrogen in a protein, that covalently attached to carbon can not be exchanged while the hydrogens on the side chains and at the N- and C- termini are exchanged too fast to be detected (Smith *et al.*, 1997).

Therefore, H/D exchange studies mainly focus on the isotopic exchange at backbone amide positions of proteins where the exchange rate is within the limit of detection by routine techniques (Smith *et al.*, 1997). The H/D exchange rate depends on many factors including temperature, pH, solvent accessibility, side chains adjacent to the amide hydrogen and the arrangement of amino acid residues to the structure of proteins (Smith *et al.*, 1997; Nazabal *et al.*, 2003; Rist *et al.*, 2003; Shields *et al.*, 2003). Factors such as temperature and pH can be controlled experimentally. The exchange rate can be affected by up to tenfold by adjacent side chains (Smith *et al.*, 1997), but by studying a single protein this is not a source of variability. More importantly, the exchange rate can be affected by up to 10^8 by the secondary and tertiary structure of the protein (Smith *et al.*, 1997). It is this kind of change in the exchange rate that makes H/D exchange a sensitive probe to detect conformational changes in proteins. Generally, exchange-in experiments are performed by incubation of folded proteins in desired pD buffer for a period of time, followed by quenching of the exchange reaction by the addition of ice-cold acid to bring the reaction to low temperature and low pH (Mandell *et al.*, 1998). Under the quenched condition, the isotopic exchange at the amide hydrogens of polypeptides has a half-life of up to 30-120 minutes (Smith *et al.*, 1997). The lowest exchange rates minimize the back-exchange, which makes it possible to fragment folded protein into small peptides by protease digestion (Mandell *et al.*, 1998) so that the peptides carrying structural information of the protein can be analyzed by mass spectrometry.

H/D exchange-in was carried at 22°C for 30 minutes on wild–type protein pre-incubated at 22°C or at 37°C for 30 min. The enzyme treated at 37°C has four peptides that incorporate more deuterium than at 22°C suggesting that there is some increase in

solvent access to these regions of the protein. These yeast peptides map on the human enzyme to regions at the end of helix 2 and part of strand 1 to helix 3 in the head domain and at part of two helices (H14 and H19) in the body domain. A final peptide aligned with the tail domain of the human enzyme, but the tail domain was completely disordered in the structure so the precise location of this peptide cannot be defined. The increase in deuterium incorporation on heating could be due to a loss of secondary or tertiary structure of the protein leading to exposure to solvent. The biggest change in deuterium exchange upon heating happened on peptide 36-44 corresponding to helix 2 in the human enzyme which is at the exterior of the enzyme with the helix exposed to solvent. The increase in deuterium incorporated into this peptides can not be due to increased exposure to solvent since at either temperature this helix is on the exterior of the protein. Therefore, increased deuterium uptake by this helix suggests that the secondary structure of this peptide is lost to some extent during thermal denaturation at the non-permissive temperature. The other peptides which would be buried in the yeast protein (based on their positions in the human enzyme) also incorporated more deuterium and this could be the result of increased exposure to solvent or loss of secondary structure after heat treatment. The more likely explanation is increased exposure to solvent suggesting that the whole structure of the protein has some changes.

How do these observations relate to the Fluorescence studies? The enzyme treated at 37°C showed a 14 nm red-shift of maximal emission as a result of exposure to solvent. This is consistent with an increase in solvent accessibility which would lead to higher deuterium incorporation than in the more compact conformation. Considering the sequence coverage of peptic peptides was just 35% of the sequence of the protein, some

structural information was missing. The H/D exchange results confirm a conformation change in the enzyme after thermal denaturation, but we cannot get more detailed information about the conformational change. More effort is needed to optimize the experimental conditions to improve the sequence coverage. The same experiment should be done on variant enzyme E172F or E172K to compare the exchange-in of deuterium of wild-type with that of those variant enzymes. The time profile of the exchange-in of deuterium reflecting the exchange-in rate will be needed to probe the whole conformation of the enzyme.

5.0 Conclusions

To address the question of how a single mutation in the yeast *CCA1* gene leads to a temperature-sensitive phenotype *in vivo*, the wild-type and four mutant genes were constructed in the pGEX-2T expression system. The over-expressed tRNA nucleotidyltransferases were purified and characterized enzymatically and biophysically. Based on this characterization the following conclusions can be drawn:

1) A carboxylated amino acid is not required at position 172 of the yeast enzyme and neither the original amino acid substitution (E172K) nor any of the other changes (E172Q, E172H, and E172F) altered the overall secondary structure of the enzyme at 22°C. Since amino acid 172 is predicted to be in a small turn or loop located in a region linking the head and neck domains but is itself not involved in the construction of either α-helices or β-sheets this change would not be expected to alter the secondary structure of the enzyme.

2) However, the substitution of the amino acid at position 172 does lead to some change in the tertiary structure of the enzyme (revealed by intrinsic fluorescence) such that the activity of the enzyme is reduced. All of the variant enzymes show some red-shift as compared with wild-type enzyme at room temperature and this change in tertiary structure is correlated with a reduction in enzyme activity.

3) The secondary structures of E172Q and E172H are similarly thermal stable and they are both as thermal stable as the wild-type enzyme while the secondary structures of E172F and E172K are less thermal stable than the wild-type enzyme with a 6°C drop in the transitional temperature suggesting that the size of the amino acid at this position is most responsible for defining the level of thermostability.

4) This loss of thermostability is linked to a loss of enzyme activity at the "non-permissive" temperature and this in turn is responsible for the temperature-sensitive phenotype.

5) Intrinsic fluorescence quenching suggests that a structural change leads to a weaker interaction of the enzyme with substrate tRNA and this reduced association is likely the reason for the change in enzyme activity.

6.0 Future work

For yeast tRNA nucleotidyltransferase, some questions need to be addressed to better understand the structure and function of this enzyme. For example, the data here suggest the possibility of a cooperative mechanism for yeast tRNA nucleotidyltransferase. To further explore this possibility it would be useful to know whether the yeast enzyme exists as a multimer (dimer or larger) either alone or in the presence of its substrates.

Forming multimers is one way that cooperativity could be explained. It is interesting that all of the solved crystal structures of tRNA nucleotidyltransferases are dimers and that the *S. shibitae* enzyme seemed to exist as a dimer but formed a tetramer on tRNA binding. Additional biophysical techniques such as AUC, gel filtration or native PAGE could be applied to address the question. In spite of all of the work that has been carried out on tRNA nucleotidyltransferases it is still not clear exactly how the enzyme associates with substrate tRNA. Again, the apparent cooperativity seen here makes this question interesting. A direct binding study of the enzyme with tRNA could reveal the stoichiometry of the enzyme to tRNA and show whether the binding is cooperative. In the binding study described here, the reaction system was simple (only enzyme and tRNA) not like the kinetic system including ATP, CTP and possible substrate analogues. A uniform substrate tRNA also could be synthesized by *in vitro* transcription using the T7 RNA polymerase and intrinsic fluorescence titration could be used to investigate the binding of enzyme with tRNA. Again, tRNA lacking a CCA terminus or containing –C, -CC, or a complete CCA could be used to define the binding kinetics of each of these intermediates or products.

In addition, a more detailed analysis of the variant enzymes could be carried out. The initial fluorescence quenching study on the wild-type and variant enzymes carried out here suggested that the interaction of tRNA with the variant enzymes is weaker than with the wild-type enzyme. Further experiments need to be done to measure the dissociation constant to compare the interaction quantitatively. It is suggested that the reduced enzyme activity is due to the reduced binding efficiency of tRNA to the variant enzymes, but whether the loss of activity is also due to decreased binding to substrate

ATP, CTP or to reduced catalytic activity is not known. A detailed kinetic study on variant enzymes can be carried out to answer these questions.

Finally, as the crystal structure for the yeast enzyme is not resolved, it might be worthwhile to resolve a crystal structure for the yeast enzyme. In the meantime, more structural information could be determined by additional limited proteolysis and H/D exchange coupled with mass spectrometry experiments.

5. REFERENCES

Aebi, M., Kirchner, G., Chen, J. Y., Vijayraghavan, U., Jacobson, A., Martin, N. C., and Abelson, J. (1990). Isolation of a temperature-sensitive mutant with an altered tRNA nucleotidyltransferase and cloning of the gene encoding tRNA nucleotidyltransferase in the yeast *Saccharomyces cerevisiae*. J Biol Chem *265*, 16216-16220.

Augustin, M. A., Reichert, A. S., Betat, H., Huber, R., Morl, M., and Steegborn, C. (2003). Crystal structure of the human CCA-adding enzyme: insights into template-independent polymerization. J Mol Biol *328*, 985-994.

Barton, G. J. (1993). ALSCRIPT: a tool to format multiple sequence alignments. Protein Eng *6*, 37-40.

Bjork, G. R., Ericson, J. U., Gustafsson, C. E., Hagervall, T. G., Jonsson, Y. H., and Wikstrom, P. M. (1987). Transfer RNA modification. Annu Rev Biochem *56*, 263-287.

Gao, H., and Leary, J. A. (2003). Multiplex inhibitor screening and kinetic constant determinations for yeast hexokinase using mass spectrometry based assays. J Am Soc Mass Spectrom *14*, 173-181.

Capage, M., and Hill, C. W. (1979). Preferential unequal recombination in the glyS region of the Escherichia coli chromosome. J Mol Biol *127*, 73-87.

Chen, J. Y., Kirchner, G., Aebi, M., and Martin, N. C. (1990). Purification and properties of yeast ATP (CTP):tRNA nucleotidyltransferase from wild type and overproducing cells. J Biol Chem *265*, 16221-16224.

Chen, J. Y., and Martin, N. C. (1988). Biosynthesis of tRNA in yeast mitochondria. An endonuclease is responsible for the 3'-processing of tRNA precursors. J Biol Chem *263*, 13677-13682.

Cho, H. D., Oyelere, A. K., Strobel, S. A., and Weiner, A. M. (2003). Use of nucleotide analogs by class I and class II CCA-adding enzymes (tRNA nucleotidyltransferase): deciphering the basis for nucleotide selection. RNA *9*, 970-981.

Cho, H. D., and Weiner, A. M. (2004). A single catalytically active subunit in the multimeric Sulfolobus shibatae CCA-adding enzyme can carry out all three steps of CCA addition. J Biol Chem *279*, 40130-40136.

Copeland, R. A. (1996). *Enzymes*: A Practical Introduction to Structure, Mechanism, and Data Analysis. VCH Publishers, Inc. New York.

Cudny, H,. Pietrzak, M., Kaczkowski, J. (1978) Plant tRNA Nucleotidyltransferase: I. Isolation and Purification of tRNA Nucleotidyltransferase from *Lupinus luteus* Seeds.

Planta *142*, 23-27.

Deutscher, M. P. (1972a). Reactions at the 3' terminus of transfer ribonucleic acid. 3. Catalytic properties of two purified rabbit liver transfer ribonucleic acid nucleotidyl transferases. J Biol Chem *247*, 459-468.

Deutscher, M. P. (1972b). Reactions at the 3' terminus of transfer ribonucleic aid. IV. Extents of normal and anomalous nucleotide incorporation catalyzed by transfer ribonucleic acid nucleotidyltransferase. J Biol Chem *247*, 469-480.

Deutscher, M. P. (1982). The enzymes. *15*, 183-215.

Evans, J. A., and Deutscher, M. P. (1978). Kinetic analysis of rabbit liver tRNA nucleotidyltransferase. J Biol Chem *253*, 7276-7281.

Fiser, A., Do, R. K., and Sali, A. (2000). Modeling of loops in protein structures. Protein Sci *9*, 1753-1773.

Fitter, J., and Haber-Pohlmeier, S. (2004). Structural stability and unfolding properties of thermostable bacterial alpha-amylases: a comparative study of homologous enzymes. Biochemistry *43*, 9589-9599.

Fushinobu, S., Ohta, T., and Matsuzawa, H. (1998). Homotropic activation via the subunit interaction and allosteric symmetry revealed on analysis of hybrid enzymes of L-lactate dehydrogenase. J Biol Chem *273*, 2971-2976.

Galzitskaya, O. V., Higo, J., and Finkelstein, A. V. (2002). Alpha-helix and beta-hairpin folding from experiment, analytical theory and molecular dynamics simulations. Curr Protein Pept Sci *3*, 191-200.

Gao, H., and Leary, J. A. (2003). Multiplex inhibitor screening and kinetic constant determinations for yeast hexokinase using mass spectrometry based assays. J Am Soc Mass Spectrom *14*, 173-181.

Greenfield, N. J. (1996). Methods to estimate the conformation of proteins and polypeptides from circular dichroism data. Anal Biochem *235*, 1-10.

Harper, S., Speicher, D. W. *Current protocols in protein science* (1997). John Wiley & Sons, Inc. New York.

Hammamieh, R., and Yang, D. C. (2001). Magnesium ion-mediated binding to tRNA by an amino-terminal peptide of a class II tRNA synthetase. J Biol Chem *276*, 428-433.

Hingerty, B., Brown, R. S., and Jack, A. (1978). Further refinement of the structure of yeast $tRNA^{Phe}$. J Mol Biol *124*, 523-534.

Holm, L., and Sander,C (1995). DNA polymerase beta belongs to an ancient nucleotidyltransferase superfamily. Trends Biochem Sci *20*, 345-347.

Lakowics, J. (1999). *Principles of Fluorescence Spectroscopy*, Kluwer Academic and Plenum Publishers, New York, USA.

Lederberg, E. M., and Cohen, S. N. (1974). Transformation of *Salmonella typhimurium* by plasmid deoxyribonucleic acid. J Bacteriol *119*, 1072-1074.

Li, F., Wang, J., and Steitz, T. A. (2000). *Sulfolobus shibatae* CCA-adding enzyme forms a tetramer upon binding two tRNA molecules: A scrunching-shuttling model of CCA specificity. J Mol Biol *304*, 483-492.

Li, F., Xiong, Y., Wang, J., Cho, H. D., Tomita, K., Weiner, A. M., and Steitz, T. A. (2002). Crystal structures of the *Bacillus stearothermophilus* CCA-adding enzyme and its complexes with ATP or CTP. Cell *111*, 815-824.

Lin, S. X., Wang, Q., and Wang, Y. L. (1988). Interactions between *Escherichia coli* arginyl-tRNA synthetase and its substrates. Biochemistry *27*, 6348-6353.

Li, Z., Gillis, K. A., Hegg, L. A., Zhang, J., and Thurlow, D. L. (1996). Effects of nucleotide substitutions within the T-loop of precursor tRNAs on interaction with ATP/CTP:tRNA nucleotidyltransferases from *Escherichia coli* and yeast. Biochem J *314 (Pt 1)*, 49-53.

Maizels, N., Weiner, A. M., Yue, D., and Shi, P. Y. (1999). New evidence for the genomic tag hypothesis: archaeal CCA-adding enzymes and tDNA substrates. Biol Bull *196*, 331-333; discussion 333-334.

Mandell, J. G., Falick, A. M., and Komives, E. A. (1998). Measurement of amide hydrogen exchange by MALDI-TOF mass spectrometry. Anal Chem *70*, 3987-3995.

Moran, L. A., Scrimgeour, K. G.; Horton H .R., Ochs, R. S.; Rawn, J. D.(1994) *Biochemistry*, Neil Patterson Publishers. Englewood Cliffs, NJ: p.28.5

Nazabal, A., Laguerre, M., Schmitter, J. M., Vaillier, J., Chaignepain, S., and Velours, J. (2003). Hydrogen/deuterium exchange on yeast ATPase supramolecular protein complex analyzed at high sensitivity by MALDI mass spectrometry. J Am Soc Mass Spectrom *14*, 471-481.

Okabe, M., Tomita, K., Ishitani, R., Ishii, R., Takeuchi, N., Arisaka, F., Nureki, O., and Yokoyama, S. (2003). Divergent evolutions of trinucleotide polymerization revealed by an archaeal CCA-adding enzyme structure. EMBO J *22*, 5918-5927.

Peltz, S. W., Donahue, J. L., and Jacobson, A. (1992). A mutation in the tRNA nucleotidyltransferase gene promotes stabilization of mRNAs in *Saccharomyces cerevisiae*. Mol Cell Biol *12*, 5778-5784.

Piszkiewicz, D. (1977). *Kinetics of chemical and enzyme-catalyzed reactions*, New York Oxford University Press.

Rether, B., Bonnet, J., and Ebel, J. P. (1974). Studies on tRNA nucleotidyltransferase from baker's yeast. 1. Purification of the enzyme. Protection against thermal inactivation and inhibition by several substrates. Eur J Biochem *50*, 281-288.

Richards, F. M. (1974). The interpretation of protein structures: total volume, group volume distributions and packing density. J Mol Biol *82*, 1-14.

Rist, W., Jorgensen, T. J., Roepstorff, P., Bukau, B., and Mayer, M. P. (2003). Mapping temperature-induced conformational changes in the *Escherichia coli* heat shock transcription factor sigma 32 by amide hydrogen exchange. J Biol Chem *278*, 51415-51421.

Sambrook, J., E. F. Fritsch and T. Maniatis (1989). *Molecular Cloning*, a labroatory manual, Cold Spring Harbor Press, New York.

Sandgren, M., Gualfetti, P. J., Shaw, A., Gross, L. S., Saldajeno, M., Day, A. G., Jones, T. A., and Mitchinson, C. (2003). Comparison of family 12 glycoside hydrolases and recruited substitutions important for thermal stability. Protein Sci *12*, 848-860.

Seth, M., Thurlow, D. L., and Hou, Y. M. (2002). Poly(C) synthesis by class I and class II CCA-adding enzymes. Biochemistry *41*, 4521-4532.

Shanmugam, K., Hanic-Joyce, P. J., and Joyce, P. B.M. (1996). Purification and characterization of a tRNA nucleotidyltransferase from *Lupinus albus* and functional complementation of a yeast mutation by the corresponding cDNA. Plant Mol Biol *30*, 281-295.

Shi, P. Y., Maizels, N., and Weiner, A. M. (1998). CCA addition by tRNA nucleotidyltransferase: polymerization without translocation? EMBO J *17*, 3197-3206.

Shields, S. J., Oyeyemi, O., Lightstone, F. C., and Balhorn, R. (2003). Mass spectrometry and non-covalent protein-ligand complexes: confirmation of binding sites and changes in tertiary structure. J Am Soc Mass Spectrom *14*, 460-470.

Smith, D. L., Deng, Y., and Zhang, Z. (1997). Probing the non-covalent structure of proteins by amide hydrogen exchange and mass spectrometry. J Mass Spectrom *32*, 135-146.

Stelea, S. D., Pancoska, P., Benight, A. S., and Keiderling, T. A. (2001). Thermal unfolding of ribonuclease A in phosphate at neutral pH: deviations from the two-state model. Protein Sci *10*, 970-978.

Sternbach, H., Sprinzl, M., Hobbs, J. B., and Cramer, F. (1976). Affinity labelling of tRNA nucleotidyltransferase from baker's yeast with $tRNA^{Phe}$ modified on the 3'-terminus. Eur J Biochem *67*, 215-221.

Thrall, S. H., Reinstein, J., Wohrl, B. M., and Goody, R. S. (1996). Evaluation of human immunodeficiency virus type 1 reverse transcriptase primer tRNA binding by fluorescence spectroscopy: specificity and comparison to primer/template binding. Biochemistry *35*, 4609-4618.

Tomari, Y., Suzuki, T., Watanabe, K., and Ueda, T. (2000). The role of tightly bound ATP in *Escherichia coli* tRNA nucleotidyltransferase. Genes Cells *5*, 689-698.

Tomita, K., Fukai, S., Ishitani, R., Ueda, T., Takeuchi, N., Vassylyev, D. G., and Nureki, O. (2004). Structural basis for template-independent RNA polymerization. Nature *430*, 700-704.

Tomita, K., and Weiner, A. M. (2002). Closely related CC- and A-adding enzymes collaborate to construct and repair the 3'-terminal CCA of tRNA in *Synechocystis* sp. and *Deinococcus radiodurans*. J Biol Chem *277*, 48192-48198.

Tsaprailis, G., Chan, D. W., and English, A. M. (1998). Conformational states in denaturants of cytochrome c and horseradish peroxidases examined by fluorescence and circular dichroism. Biochemistry *37*, 2004-2016.

Voet.D., and Voet. J.G. (1995). *Biochemistry*, John Wiley & Sons, Inc, New York.

Wang, G. H., McLaughlin, L. W., Sternbach, H., and Cramer, F. (1984). Preparation of oligonucleotides corresponding to the acceptor stem of yeast $tRNA^{Phe}$ and their interaction with yeast ATP(CTP):tRNA nucleotidyltransferase. Nucleic Acids Res *12*, 6909-6922.

Williams, K. R., and Schofield, P. (1977). Kinetic mechanism of tRNA nucleotidyltransferase from *Escherichia coli*. J Biol Chem *252*, 5589-5597.

Wu, M. X., Filley, S. J., and Hill, K. A. (1994). Cooperative binding of zinc to an aminoacyl-tRNA synthetase. Biochem Biophys Res Commun *201*, 1079-1083.

Xiong, Y., Li, F., Wang, J., Weiner, A. M., and Steitz, T. A. (2003). Crystal structures of an archaeal class I CCA-adding enzyme and its nucleotide complexes. Mol Cell *12*, 1165-1172.

Xiong, Y., and Steitz, T. A. (2004). Mechanism of transfer RNA maturation by CCA-adding enzyme without using an oligonucleotide template. Nature *430*, 640-645.

Yue, D., Maizels, N., and Weiner, A. M. (1996). CCA-adding enzymes and poly(A) polymerases are all members of the same nucleotidyltransferase superfamily: characterization of the CCA-adding enzyme from the archaeal hyperthermophile *Sulfolobus shibatae*. RNA 9(2), 895-908.

Yue, D., Weiner, A. M., and Maizels, N. (1998). The CCA-adding enzyme has a single active site. J Biol Chem *273*, 29693-29700.

Zhang, X. J., Baase, W. A., Shoichet, B. K., Wilson, K. P., and Matthews, B. W. (1995). Enhancement of protein stability by the combination of point mutations in T4 lysozyme is additive. Protein Eng *8*, 1017-1022.

6. APPDNDIX A

Sample calculation to convert CPMs of precipitated tRNA-CCA* in the CCA adding reaction to moles of final product tRNA-CCA.

- Initially, the number of CPMs in an aliquot of [α-^{32}P]-ATP was determined by scintillation counting.
- This number was multiplied by a factor to account for radioactive decay from the reference date to determine the number of counts in this sample expected on the reference date.
- Knowing the volume of [α-^{32}P]-ATP, the number of moles of [α-^{32}P]-ATP is determined based on the concentration (10 μCi/μl) and specific activity (3 000 Ci/mmol) of [α-^{32}P]-ATP provided by the supplier. From this, the number of CPMs/mole of [α-^{32}P]-ATP can be calculated.
- By determining the number of CPMs in the tRNA precipitated after a reaction and accounting for radioactive decay the number of CPMs can be converted into the number of moles of radiolabelled tRNA.
- This number must then be multiplied by the ratio of ATP to [α-^{32}P]-ATP in the reaction to determine the total amount of precipitated tRNA during the course of the reaction.
- This number can then be divided by the time of the reaction to determine a velocity or divided by the enzyme amount in the reaction to determine a specific activity.

For example, 2 μl [α-^{32}P]-ATP was diluted into 1 ml buffer and 1 μl, 2 μl, 4 μl, and 6 μl aliquots out of 1 ml were counted giving 13 454, 44 764, 62 753 and 85 628 CPMs,

respectively. To account for radioactive decay, those numbers were divided by 0.245 derived from the ^{32}P decay chart to get the number of CPMs expected on the reference date, which were 54 914, 182 710, 256 134 and 349 502, respectively. The volume of [α-^{32}P]-ATP in an aliquot to be counted (in this case 2 μl) was calculated as in equation 1

$$\frac{2 \text{ ul}}{1000 \text{ ul}} = \frac{y \text{ ul}}{2 \text{ ul}} \qquad y = \frac{4}{1000} \text{ ul} \qquad \text{(equation 1)}$$

Similarly, the volume of [α-^{32}P]-ATP contained in 1 μl, 4 μl, 6 μl of diluted sample was calculated to be 0.002 μl, 0.008 μl and 0.012 μl, which corresponds to 0.02 μCi, 0.08 μCi, and 0.12 μCi since the concentration of [α-^{32}P]-ATP was 10 μCi/μl from the supplier.

Knowing the number of Ci of [α-^{32}P]-ATP in any aliquot, the number of moles of [α-^{32}P]-ATP in that aliquot can be calculated based on the known specific activity (3000 Ci/mmol) provided by the supplier using the following equation:

Moles of [α-^{32}P]-ATP (mol) = amount of [α-^{32}P]-ATP (Ci)/specific activity (3000 Ci/10^{-3} mol)

Specifically,

$0.02*10^{-6}$ Ci / 3000 Ci/mmol = $6.67*10^{-12}$ mmol = $6.67*10^{-15}$ mol

$0.04*10^{-6}$ Ci /3000 Ci/mmol = $13.33*10^{-12}$ mmol = $13.33*10^{-15}$ mol

$0.08*10^{-6}$ Ci /3000 Ci/mmol = $26.67*10^{-12}$ mmol = $26.67*10^{-15}$ mol

$0.12*10^{-6}$ Ci /3000 Ci/mmol = $40*10^{-12}$ mmol = $40*10^{-15}$ mol

From above we know the number of CPMs in each sample so for each sample we can determine the CPMs/mol.

For 1 μl: 54 914 CPM/6.67×10^{-15} mol = 8.23×10^{18} CPM/mol

For 2 μl: 182 710 cpm/13.33 $\times$ 10^{-15} mol = 13.7 $\times$ 10^{18} CPM/mol

For 4 μl: 256 134 CPM/26.27 $\times$ 10^{-15} mol = 9.8 $\times$ 10^{18} CPM/mol

For 6 μl: 349 502 CPM/40 $\times 10^{-15}$ mol = 8.7 $\times$ 10^{18} CPM/mol

Averaging the number of CPMs/mol in each sample gives 10.1 $\times$ 10^{18} CPM/mol. This number was used to convert the CPMs of precipitated tRNA containing [α-^{32}P]-ATP to moles of tRNA. In this example, the CPMs of the tRNA-CCA* product at different tRNA substrate concentration were divided by 0.908 (three days after the reference date) to get the CPMs on the reference date. Finally, this number was multiplied the ratio of ATP to [α-^{32}P]-ATP in the reaction mixture to get the final total moles of the tRNA-CCA produced in the reaction. Under the reaction condition used, CCA addition was in the linear reaction range and the initial velocity could be obtained by dividing the total moles of tRNA-CCA by the reaction time.

In this experiment, 10 μl of [α-^{32}P]-ATP or 3.3 $\times$ 10^{-11} mol (see equation 2) and 2.6 $\times$ 10^{-6} moles ATP were used to prepare the reaction mixture.

Number of moles of [α-^{32}P]-ATP = Volume of [α-^{32}P]-ATP (μl) $\times$ concentration of [α-^{32}P]-ATP (Ci/μl)/specific activity [α-^{32}P]-ATP (Ci/mol) (equation 2)

= 10 μl $\times$ (10 $\times$ 10^{-6} Ci/ μl)/3000 Ci/10^{-3}mol = 3.33 $\times$ 10^{-11} mol

Based on this the ratio of ATP to [α-^{32}P]-ATP was determined to be 7.8 $\times 10^{4}$ and the calculated data were listed in the following table.

[tRNA] μM	0.5	5	25	50	100	250
CPMs (on experiment date)	3585	9950	41552	45444	44654	47268
CPMs (on reference date)	4144	11502	48036	52536	51623	54645
tRNA-CCA* (10^{-18}mol)	0.0418	0.116	0.484	0.529	0.521	0.541
Total tRNA-CCA (10^{-10}mol)	0.326	0.905	3.775	4.126	4.064	4.219
Velocity (10^{-10}mol/min)	0.163	0.452	1.887	2.066	2.030	2.149
Specific Velocity (×0.1 μmol/min.mg)	1.63	4.52	18.87	20.66	20.30	21.49

In another kinetics study with 10~60 μM tRNA concentration, the number of CPMs/mol determined was 272 193×10^{14}CPM/mol on the reference date. The experiment was four days ahead of the reference date, the number of CPMs of the precipitated tRNA-CCA* was multiply a factor (0.865) to account for radioactive decay to get the CPMs value on the reference date. The ratio of ATP to [α-^{32}P]-ATP in the experiment was 9×10^4. The big difference between the velocities of the two experiments was caused by the large difference of the two number of CPMs/mol, which was 2.72-fold difference (272193×10^{14}/(10.1×10^{18})=2.72). If the same number of 10.1 × 10^{18} CPM/mol were used, the two experiment results would match well. The last row in the below table was the specific velocity calculated using 10.1 × 10^{18} CPM/mol.

[tRNA] μM	10	15	20	25	30	60
CPMs (on experiment date)	16748	27722	43058	53209	61704	66373
CPMs (on reference date)	14152	23425	36384	44961	52139	56085
TRNA-CCA* (10^{-14}mol)	0.0520	0.0861	0.134	0.165	0.192	0.206
Total tRNA-CCA (10^{-10}mol)	0.468	0.775	1.203	1.487	1.724	1.854
Velocity (10^{-10}mol/min)	0.234	0.388	0.615	0.744	0.862	0.927
Specific Velocity (×0.1 μmol/min.mg)	2.34	3.88	6.15	7.44	8.62	9.27
Specific Velocity (×0.1 μmol/min.mg)	6.42	10.65	16.88	20.42	23.66	25.45